The Molecular Mechanism of Mitophagy

by

Ke Wang

A dissertation submitted in partial fulfillment
of the requirements for the degree of
Doctor of Philosophy
(Molecular, Cellular and Developmental Biology)
in the University of Michigan
2014

Doctoral Committee:

Professor Daniel J. Klionsky, Chair
Associate Professor Anuj Kumar
Professor Lois Weisman
Associate Professor Haoxing Xu

To my wife Xin and my son Ancen

ACKNOWLEDGEMENTS

I am very grateful to many people that have helped me with both my projects and my life all the way along the years of my graduate study. It is hard to put into words within this limited space to express my appreciation of all the support and encouragement I have received, together with the happiness and joy these interactions have brought to me. It would be an impossible mission to complete this thesis without the help from my mentors, my family and all of my dear friends.

First of all, I would like to sincerely express my extreme gratitude to my mentor Dr. Daniel J. Klionsky, for not only being an excellent example of a great scientist, but also as a model of living a fulfilling life and of course, being a marvelous mentor. Dan has been tremendously supportive to every aspect of my study and life, every detail I can possibly imagine. I actually decided to apply to the University of Michigan for the purpose of joining his lab – and that is apparently one of the wisest decisions I have ever made.

I would like to thank the members of my thesis committee, Dr. Lois Weisman, Dr. Anuj Kumar and Dr. Haoxing Xu, for all their insightful advice and suggestions during the progression of my thesis work. Dr. Xu has given impressive suggestions to my projects starting with the first we talked. Dr. Kumar, as the Chair of Graduate Study, has also helped me a lot outside of my projects. Working almost side by side with the Weisman lab, I greatly appreciate the discussions I have had with Dr. Weisman and all her lab members.

Additionally, I would also like to thank the members of my prelim committee, Dr. Amy Chang, Dr. Matt Chapman and Dr. Laura Olsen. It was a tough time, but it is through your critical comments and insightful advice that I became a qualified Ph.D. candidate. I am always grateful for your suggestions, which have become treasures that I can carry on to the

next journey in my life.

Very special thanks to Dr. Tomotake Kanki, a former post-doc in the Klionsky lab and now a Professor at Niigata University. I learned from Tomotake almost every technique related with autophagy and mitophagy. He also initiated the mitophagy screen, which directly led to my thesis and several other important projects of the lab. Along with that, I would also like to thank all former members from the Klionsky lab, especially Dr. Zhifen Yang, Dr. Wen-lien Yen, Dr. Usha Nair, Dr. Congcong He, Dr. Yang Cao and Dr. Jiefei Geng. They have not only tremendously helped with my lab projects, but also made my first days in Ann Arbor much easier and enjoyable.

To all the dear members of the Klionsky lab, thank you! It is hard to imagine a journey without you guys! Dr. Backues, Xu and Meiyan, I would like to specially thank you all for sitting close to me in our bay, which is always full of laughter.

To all my dear friends in Ann Arbor, especially Ting Han and Tao Xu, thank you! Thank you for always being there whenever I need help and support. The friendship that you share with me is such an important part of my graduate life that I would not be graduating without it.

Thank you to many labs in both the MCDB department and LSI, especially the Weisman lab, Kumar lab, Kim lab and Southworth lab for generous sharing of their reagents and equipment. I also would like to thank Dr. Yanzhuang Wang for providing the wonderful opportunity of a rotation. Thank you to Mary Carr and Diane Durfy for their hard administrative works all these years. I hope my oral defense would be the last time that I keep you busy.

My parents have always been very encouraging of my decisions and choices. Although I am oceans away from home, I can easily feel their support. They are the reason I can even be here, and for that I would like to express my deepest appreciation. Whenever cheerful,

whenever sad, my wife Xin has always been the greatest companion and sincerest friend. She is a constant of happiness in my life. Without her, I have nowhere to go and nothing to accomplish. We met here in Ann Arbor and she is the most important discovery of my life. For that, I owe my deepest appreciation and gratitude. My son Ancen squared the happiness I received from his mother. He is an angel that brings me all the fortune I needed for graduation and will need for the future. With him, the best has yet to come.

TABLE OF CONTENTS

LIST OF FIGURES

LIST OF TABLES

ABSTRACT

Autophagy is the major cellular degradative pathway that is evolutionarily conserved from yeast to mammalian cells. The hallmark of this process is the formation of the double-membrane structures called autophagosomes. This unique feature of autophagy—the formation of a sequestering compartment that can encompass a wide range of cargos—enables the degradation of large organelles such as mitochondria. Selective autophagic degradation of mitochondria, termed mitophagy, has long been documented and has attracted extensive attention during recent years, in part because of the connection between defects in this process and various human diseases. Studies in both yeast and mammalian systems have greatly expanded our knowledge of both the molecular mechanism and physiological significance of this process.

This thesis is devoted to the characterization of the molecular mechanism of mitophagy using the yeast *Saccharomyces cerevisiae* as the model system. To achieve this goal, we carried out a genome-wide yeast mutant screen for mitophagy-defective strains and identified 32 mutants with a block in mitophagy, in addition to the known autophagy-related (*ATG*) gene mutants. These new mutants will provide a useful foundation for researchers interested in the study of mitochondrial homeostasis and quality control.

The activity of mitophagy in vivo must be tightly regulated considering that mitochondria are essential organelles that not only produce most of the cellular energy, but also generate reactive oxygen species that can be harmful to cell physiology. We found that Atg32 is proteolytically processed at its C terminus upon mitophagy induction, and this modification is required for efficient mitophagy. The mitochondrial i-AAA protease Yme1 mediates Atg32 processing and is required for mitophagy. This study demonstrated that the processing of Atg32 by Yme1 acts as an important regulatory mechanism of cellular mitophagy activity.

In addition, we also studied the roles of PtdIns 4-kinases and PtdIns4P 5-kinases in the regulation of selective and nonselective autophagic pathways. The PtdIns 4-kinase Pik1 is involved in Atg9 trafficking through the Golgi, and is involved in both nonselective and selective types of autophagy, whereas the PtdIns4P 5-kinase Mss4 is specifically involved in mitophagy, but not nonselective autophagy. These data indicate that phosphoinositide kinases have diverse functions in the regulation of autophagic pathways.

Chapter I
GENERAL INTRODUCTION

This chapter is reprinted from the book Autophagy: Cancer, Other Pathologies, Inflammation, Immunity, Infection, and Aging, Volume 4, Chapter 2, Ke Wang and Daniel Klionsky, Molecular Process and Physiological Significance of Mitophagy, in press, with minor modifications.

While mitochondria are essential organelles, their dysfunction could cause severe consequences including aging and the pathogenesis of neurodegenerative diseases. Maintaining a healthy and functional population of mitochondria is critically important for all eukaryotic cells. Despite the fact that several quality control systems within mitochondria have been well characterized from previous research, recent studies have established an important link between mitochondria maintenance and macroautophagy, which is a highly conserved catabolic process responsible for the degradation of cellular components. Accumulated evidence has demonstrated that autophagy plays an important role in the selective elimination of superfluous and dysfunctional mitochondria. This process is specifically termed mitophagy. At the molecular level, a group of proteins has been identified in various model organisms to mediate the association of the degrading mitochondria with the autophagic machinery. Diverse mechanisms have been reported to ensure the efficient and selective recognition and degradation of unwanted mitochondria through macroautophagy, while simultaneously maintaining tight regulation of these degradative processes. The recent advances in our understanding of mitophagy will provide essential insights into the pathogenesis of a variety of mitochondria dysfunction-related diseases.

Macroautophagy (hereafter referred to as autophagy) is a well conserved cellular degradation mechanism among eukaryotic organisms from yeast to mammals (Yang and Klionsky, 2010). Extensive studies on autophagy in the past decade greatly expanded our understanding of this cellular pathway from both the perspective of molecular mechanism and biological significance. The hallmark of the process of autophagy is the formation of the double-membrane vesicles called autophagosomes (Xie and Klionsky, 2007). Upon autophagy induction, an initial membrane structure termed the phagophore, the precursor to the autophagosome, gradually expands and engulfs a portion of the cytoplasm or specific cargos and delivers them to the vacuole/lysosome for degradation (Xie and Klionsky, 2007 and Figure 1.1). Autophagy occurs constitutively and operates as a homeostatic mechanism. In addition, autophagy can also be activated in response to a variety of physiological and pathological stress stimuli. The mechanism of autophagosome formation, which includes the sequential expansion of the phagophore, provides autophagy with the capacity to sequester essentially any cellular component and deliver it into the vacuole/lysosome for degradation. Indeed, autophagy has been documented to play a role in degrading a wide range of cellular components, such as protein complexes, the endoplasmic reticulum, peroxisomes, ribosomes and mitochondria.

1.1 Autophagy

Our understanding of autophagy at the molecular level has largely benefited from genetic screens for defects in this pathway in the yeast *Saccharomyces cerevisiae*. To date, nearly 40 *ATG* genes have been found to play important roles in this process. At least half of these genes are highly conserved in mammalian systems. Mechanistically, the process of autophagy begins with the activation of the Atg1 protein kinase in yeast, or the ULK1 protein complex in mammals, which integrates the initial inducing signal to counter the negative

inhibition by regulators such as TOR complex 1, which otherwise maintain autophagy at the basal level. The formation of the autophagosome proceeds through the subsequent activation of a class III phosphatidylinositol 3-kinase (PtdIns3K) complex that includes Vps30/Atg6 in yeast or BECN1 in mammals. PtdIns3K-mediated formation of the phosphatidylinositol 3-phosphate (PtdIns3P)-rich membranes is important for the nucleation of the phagophore. Atg9-containing vesicles shuttle between the phagophore assembly site (PAS) and putative membrane sources, including the endoplasmic reticulum, Golgi apparatus, plasma membrane or mitochondria for the delivery of membranes and expansion of the phagophore. Atg8–PE conjugates (or LC3–PE [LC3-II] conjugates in mammals) and the Atg12–Atg5-Atg16 complex (or ATG12–ATG5-ATG16L1 in mammals) contribute to the elongation of the phagophore. Atg8–PE or LC3-II is incorporated into both sides of the phagophore, and is required for the elongation of the membrane for the formation of a mature autophagosome (reviewed in Inoue and Klionsky, 2010; Rubinsztein et al., 2012). These protein complexes function in a specific sequence and form part of the core machinery of autophagy that operates in every different type of general and selective autophagic process.

1.2 Selective autophagy in yeast

Although autophagy is generally considered to be a nonselective bulk degradation pathway, research in this field continues to uncover examples of the importance of selective modes of sequestration. The first identified selective autophagy cargo was the vacuolar aminopeptidase I (Ape1). Ape1 is synthesized in a precursor form (prApe1) and subsequently oligomerizes to form a dodecamer, which continues to assemble into a larger Ape1 complex (Kim et al., 1997). The formation of the mature, and thus functional form, of Ape1 requires the delivery of the Ape1 complex (which is now termed the cytoplasm-to-vacuole targeting [Cvt] complex after binding of the receptor Atg19) to, and processing of prApe1 within, the

vacuole. The biosynthetic Cvt pathway occurs constitutively under nutrient-rich conditions. A genetic screen to identify mutants defective in the maturation of prApe1 revealed that the Cvt pathway shares most of the same machinery with the autophagy pathway (Harding et al., 1995). In addition, electron microscopy studies revealed that the Cvt complex is enclosed in double-membrane vesicles that resemble autophagosomes; however, these Cvt vesicles are smaller and exclude most other cytoplasmic components (Baba et al., 1997), strongly suggesting that the Cvt pathway is a type of autophagy that enables the selective sequestration of cargo.

Among the mutants discovered in the Cvt pathway screen was *atg11*, which encodes a scaffold protein (Yorimitsu and Klionsky, 2005). Subsequent studies demonstrated that Atg11 is a common scaffolding protein for a variety of selective autophagic pathways in yeast. In contrast, Atg19 is specific to the Cvt pathway (Shintani et al., 2002b). Atg19 binds prApe1, and this interaction is required for association with Atg11, via the latter's binding to the receptor. This association between Atg19 and Atg11 therefore mediates the recognition of the Cvt complex by the core autophagic machinery; Atg19 subsequently binds Atg8–PE, initiating the sequestration of the Cvt complex (Shintani et al., 2002b). Neither Atg11 nor Atg19 are required for the progression of nonselective autophagy (and therefore are not considered to be part of the "core" autophagy machinery); thus, these proteins are considered as specific adaptations of the core machinery to allow the sequestration of particular cargos, in this case the Cvt complex.

In addition to the Cvt pathway, Atg11 also mediates other types of selective autophagy through its interaction with different receptor proteins. For example, peroxisome degradation by selective autophagy, termed pexophagy, requires the receptor protein Atg36 in *Saccharomyces cerevisiae* (Motley et al., 2012) or PpAtg30 in the case of *Pichia pastoris* (Farre et al., 2008). Mitochondria are another organelle that can be the cargo of selective

autophagy, and Atg32, a mitochondrial outer membrane protein, is the receptor that is required for this process; similar to Atg19 (and Atg36 or PpAtg30), Atg32 binds both Atg11 and Atg8–PE (Kanki et al., 2009; Okamoto et al., 2009). In general, this type of ligand-receptor-scaffold system represents a common model for the mechanism of selective autophagy in yeast cells (although in the case of yeast mitophagy a separate ligand is not required since Atg32 is a resident mitochondrial protein).

As indicated above, the various receptor proteins also interact with Atg8–PE. These receptor proteins contain a well-conserved WXXL sequence that functions as the Atg8-family interacting motif, which is equivalent to the LC3-interacting region (LIR) in mammalian cells. The interactions of the receptor proteins with Atg8 may play auxiliary roles (Kondo-Okamoto et al., 2012), but are not essential for the progression of selective autophagy.

Not all types of selective autophagy are mediated through Atg11. Ald6, a soluble cytoplasmic enzyme, is preferentially degraded by autophagy after nitrogen starvation for an extended time (Onodera and Ohsumi, 2004). The degradation of Ald6 requires the core autophagic machinery, but not Atg11; however, the mechanism used to selectively target Ald6 is not known.

Ribophagy, the selective degradation of ribosomes upon prolonged nutrient deprivation, is another type of selective autophagy. Ribophagy involves the ubiquitination of the ribosomal subunit Rpl25 (Kraft et al., 2008). In this case, a receptor protein has not been identified. Although ubiquitin interacts with the Atg8 homolog LC3 in mammalian cells via non-ATG adaptor proteins (for example, SQSTM1/p62), a clear link between ubiquitination and cargo recognition is yet to be established in yeast.

1.3 Selective autophagy in higher eukaryotes

Selective types of autophagy have also been well documented in higher eukaryotes. In

contrast to yeast cells, there is no apparent homolog of Atg11 in mammalian cells, although analogous scaffolding proteins such as WDFY3/ALFY play a role in some types of autophagy (Filimonenko et al., 2010). Furthermore, various mechanisms have emerged to confer selectivity for the autophagic degradation of different cargos, likely representing the increased complexity and diversity of mammalian cells.

In *C. elegans*, the selective degradation of PGL granules occurs through a mechanism that is comparable to the receptor-scaffold system in yeast. PGL granules are maternally-derived protein aggregates that carry the germ cell determinant. PGL granules are retained in germ cells, whereas they are removed by selective autophagic degradation in somatic cells. SEPA-1, a receptor protein, directly binds the PGL granule through its interaction with the protein PGL-3 (the ligand). SEPA-1 also associates with the autophagy protein LGG-1/Atg8 via its interaction with the scaffold EPG-2 (Tian et al., 2010; Zhang et al., 2009). Therefore, the PGL-3-SEPA-1-EPG-2-LGG-1 protein complex forms the ligand-receptor-scaffold system for the selective autophagic degradation of the PGL granules in *C. elegans*.

In mammalian systems, the selectivity of autophagy may be mediated through ubiquitin-dependent or -independent mechanisms. In the first case, SQSTM1 (Pankiv et al., 2007), CALCOCO2/NDP52 (Thurston et al., 2009), OPTN (Wild et al., 2011) and NBR1 (Kirkin et al., 2009) have been proposed to be autophagic receptors that can link ubiquitinated cargos with the autophagy protein LC3. These proteins play important roles in the degradation of protein aggregates (aggrephagy), invading pathogens (xenophagy) and mitochondria (mitophagy), all of which have connections with pathophysiologies. For example, protein aggregates are commonly seen in various human diseases. Lewy bodies in Parkinson disease contain aggregates of DJ1 or SNCA/α-synuclein. The ubiqutination of these protein aggregates recruits SQSTM1 and leads to their subsequent autophagic

degradation, although not all protein aggregates can be degraded by autophagy. During xenophagy, the autophagic degradation of invasive microbes, SQSTM1 (and other receptors), followed by LC3 (and other LC3-like proteins including members of the GABARAP subfamily), are recruited to the surface of ubiquitin-labeled bacteria (Zheng et al., 2009). In PARK2/PARKIN-mediated mitophagy, ubiquitination of several mitochondrial proteins by the E3 ubiquitin ligase PARK2 has been suggested to be important for the subsequent recognition of damaged mitochondria by the autophagic machinery. The mechanism of mitophagy is discussed in more detail below.

Ubiquitin-independent mechanisms also exist to mediate selective autophagy. For example, two mitochondria outer membrane proteins, BNIP3L/NIX and FUNDC1, can interact with LC3, thus providing a direct association between the degrading mitochondria and the core autophagy machinery. In addition, in some cases SQSTM1 can also directly associate with cargo proteins. For example, a mutant of SOD1 (superoxide dismutase 1) that is associated with amyotrophic lateral sclerosis is targeted for autophagic degradation in a ubiquitin-independent manner through a direct interaction with SQSTM1 (Gal et al., 2009). Autophagy has also been demonstrated to control lipid metabolism through the selective degradation of lipid droplet triglycerides and cholesterol (Singh et al., 2009), although the molecular mechanism in regard to the selectivity of this process is yet to be characterized.

In summary, a variety of different mechanisms exist to mediate the selective autophagic degradation of a range of cargos in different organisms. These selective autophagic pathways share a common theme in that they all require a receptor and scaffold protein that can specifically link the degrading cargo to the autophagic machinery. The receptor proteins can interact both with autophagy proteins (Atg11 and Atg8 in yeast cells, LC3 in higher eukaryotes), and they can associate with the cargo. These receptors can either bind the cargo directly through interaction with a ligand (such as occurs with Atg19, Atg36,

PpAtg30, SEPA-1, BNIP3L, and FUNDC1) or they can interact with cargo that has been ubiquitinated (such as occurs with SQSTM1 and NBR1).

As mentioned above, mitochondria have been well documented to be a major target of autophagy. Recent research has greatly advanced our knowledge on both the molecular process and physiological significance of mitophagy from yeast to mammalian cells. Mitophagy has attracted extensive interest in the autophagy field, which is largely because of the important functions of this organelle and the well-established link between mitochondria dysfunction and the pathogenesis of a range of diseases.

1.4 Mitochondria dysfunction in age-related diseases

Mitochondria are essential organelles for all eukaryotes. Long known as the powerhouse of the cell, modern studies have established a central role of mitochondria in a range of different cellular activities such as calcium and iron metabolism, and apoptosis (Wallace, 2005). Conversely, reactive oxygen species (ROS), the inevitable toxic by-product of mitochondrial oxidative phosphorylation may cause severe damage to mitochondrial components and other parts of the cell (Wallace, 2005). Furthermore, oxidative damage caused by ROS can make mitochondria prone to additional ROS production leading to a downward spiral that may eventually result in cell death (Miquel et al., 1980).

Mitochondrial dysfunction is associated with aging, diabetes and neurodegenerative diseases. The mitochondrial theory of aging proposes that oxidative damage resulting from oxidative phosphorylation is an important contributor to the process of aging (Miquel et al., 1980). In addition, mitochondrial dysfunction is linked with the pathogenesis of several age-related neurodegenerative diseases, such as Alzheimer, Parkinson, and Huntington diseases.

Alzheimer disease (AD) is characterized by neurodegenerative changes such as

cerebral atrophy. Mitochondria mass is significantly reduced in affected cells obtained from patients with AD. Cytochrome c oxidase deficiency is often present in AD patients, which leads to an increase in ROS production and disruption of energy metabolism (Mutisya et al., 1994; Zhu et al., 2006). Parkinson disease (PD) is the second most common progressive disorder in the central nervous system, which is characterized primarily by the selective loss of dopaminergic neurons in the substania nigra and the formation of intraneuronal protein aggregates (Dauer and Przedborski, 2003). Mitochondrial dysfunction plays a prevalent role in the pathogenesis of PD; a significant decrease in the activity of complex I of the electron transport chain is observed in the substania nigra from PD patients (Mann et al., 1994). In familial PD, which accounts for about 10% of all cases, several genes have been linked with the pathogenesis of PD (Dodson and Guo, 2007). Autosomal recessive mutations in PINK1 and PARK2 are associated with juvenile parkinsonism (Kitada et al., 1998). Studies in Drosophila and primary fibroblasts derived from PD patients revealed the role of PINK1 and PARK2 in the maintenance of normal mitochondrial morphology (Yang et al., 2006a), suggesting that mitochondrial dynamics and function play an important role in PD pathogenesis. Huntington disease (HD) is caused by an autosomal dominant mutation in the *HTT/HUNTINGTIN* gene that affects muscle coordination and leads to a cognitive defect. Mitochondrial morphological defects and reduced activity are commonly observed in HD patients (Bossy-Wetzel et al., 2008).

Considering the extensive involvement of mitochondrial dysfunction and oxidative stress in human diseases, it is essential for the cell to tightly regulate the quality, number and activity of mitochondria—dysfunctional and superfluous mitochondria need to be eliminated in a timely manner.

1.5 Mitochondrial quality control systems

To preserve a healthy and properly functional population of mitochondria, several quality control systems that operate at different levels have been developed. First of all, mitochondria have their own proteolytic system that is responsible for the degradation of misfolded and dysfunctional mitochondrial proteins. In yeast and higher eukaryotes, ATP-dependent proteases sense the folding status of their substrates and mediate the proteolysis of misfolded proteins (Tatsuta and Langer, 2008).

In addition to proteolytic degradation of mitochondrial proteins, a recent study identified a mitochondria-to-lysosome pathway in which vesicles bud from mitochondrial tubules and sequester selected mitochondrial cargos for delivery to the lysosome for degradation. This pathway operates under normal conditions and is more active when stimulated by oxidative stress (Soubannier et al., 2012).

Mitochondria can also be turned over at the organelle level by bulk degradation through autophagy. In fact, electron microscopy studies often reveal entire mitochondria within the yeast vacuole (Takeshige et al., 1992) or mammalian lysosome (Clark, 1957). Nonselective autophagy can degrade a portion of the mitochondria population, while a selective form of autophagy, termed mitophagy, is the main pathway responsible for the degradation of damaged or superfluous mitochondria.

1.6 Overview of the thesis

In this thesis, I will describe the methods we established to induce and measure mitophagy, the genes we discovered to be involved in mitophagy and the mechanism through which mitophagy is induced and regulated.

Chapter II will focus on the genome-wide screening aimed to identify genes involved in the process of mitophagy. In this chapter, I will describe the methods we used to induce mitophagy and different assays we developed to measure mitophagy activity. The detailed

procedure of the screening and the mitophagy-related genes we finally identified will also be included in detail in this chapter. In addition, the phenotypes related to these genes in regard to general autophagy, the Cvt pathway and pexophagy are also demonstrated to create a general picture. In particular, one of the identified genes is characterized in more detail.

Chapter III will focus on the mechanism of mitophagy regulation. The findings in this chapter are based on the previous screening and the characterization of the mitophagy receptor protein Atg32, which is also a protein identified in the screen. In this part, I will describe the discovery of the proteolytic processing of Atg32 by the mitochondrial i-AAA protease Yme1 and how this processing is related to the proper induction of mitophagy. This work provides a link between mitophagy and the mitochondrial protein quality control system.

Chapter IV will examine the role of the phosphatidylinositol (PtdIns) 4-kinases and PtdIns4P 5-kinases in selective and nonselective types of autophagy in yeast. While the lipid kinase PtdIns 3-kinase Vps34 has been well documented to be involved in the regulation of autophagy, the role of other PtdIns kinases has not been examined. In this chapter, I will describe the autophagy-related functions of three related kinases of the PtdIns4P pathway, Pik1, Stt4 and Mss4. The potential molecular mechanisms of how these kinases may be involved in autophagy are also been explored.

Chapter V will summarize the thesis work and also discuss other related findings to create a big picture of our current understanding of mitophagy. In addition, important discoveries of mitophagy in mammalian cells are also included in this chapter to reflect the rapid growth of the field. I will also discuss potential perspectives and future directions in this chapter.

1.7 Figures

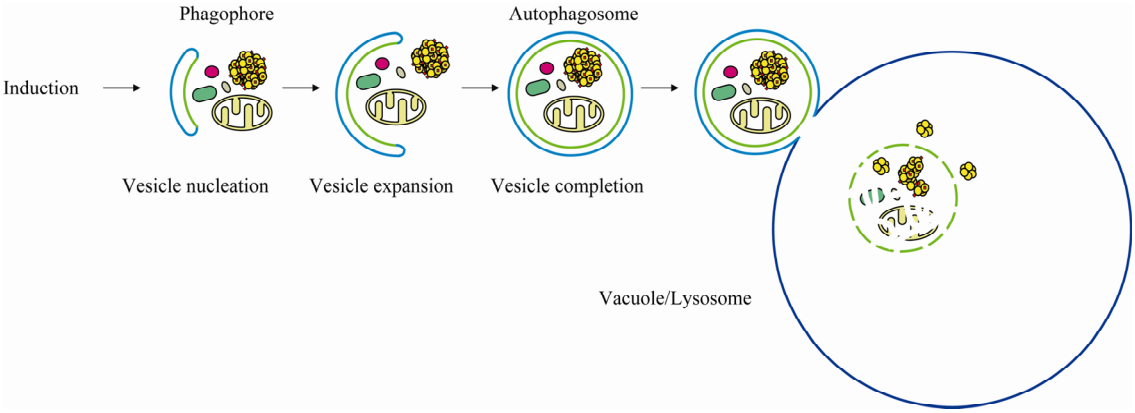

Figure 1.1 The general process of autophagy.

Chapter II
A GENOMIC SCREEN FOR YEAST MUTANTS DEFECTIVE IN SELECTIVE MITOCHONDRIA AUTOPHAGY

This chapter is reprinted from Molecular Biology of the Cell, Volume 20, Tomotake Kanki*, Ke Wang*, Misuzu Baba, Clinton R. Bartholomew, Melinda A. Lynch-Day, Zhou Du, Jiefei Geng, Kai Mao, Zhifen Yang, Wei-Lien Yen, and Daniel J. Klionsky, A Genomic Screen for Yeast Mutants Defective in Selective Mitochondria Autophagy, pg. 4730-4738, 2009, with minor modifications. I was the co-first author with Dr. Tomotake Kanki and I contributed to Figures 2.5, 2.7, 2.9, 2.10 and 2.12.

2.1 Abstract

Mitophagy is the process of selective mitochondrial degradation via autophagy, which has an important role in mitochondrial quality control. Very little is known, however, about the molecular mechanism of mitophagy. A genome-wide yeast mutant screen for mitophagy-defective strains identified 32 mutants with a block in mitophagy, in addition to the known autophagy-related (*ATG*) gene mutants. We further characterized one of these mutants, *ylr356w*Δ that corresponds to a gene whose function has not been identified. *YLR356W* is a mitophagy-specific gene that was not required for other types of selective autophagy or macroautophagy. The deletion of *YLR356W* partially inhibited mitophagy during starvation, whereas there was an almost complete inhibition at post-log phase. Accordingly, we have named this gene *ATG33*. The new mutants identified in this analysis will provide a useful foundation for researchers interested in the study of mitochondrial homeostasis and quality control.

2.2 Introduction

The mitochondrion is an organelle that carries out a number of important metabolic processes such as fatty acid oxidation, the citric acid cycle and oxidative phosphorylation. Mitochondrial oxidative phosphorylation supplies a large amount of energy that contributes to a range of cellular activities. However, this organelle is also the major source of cellular reactive oxygen species (ROS) that cause damage to mitochondrial lipid, DNA and proteins, and the accumulation of these types of damage are related to aging, cancer and neurodegenerative diseases (Wallace, 2005). Thus, intensive analyses of mitochondrial DNA repair and damaged protein degradation mechanisms have been carried out (Bogenhagen, 1999; Larsson and Clayton, 1995; Rep and Grivell, 1996). In addition, it has long been assumed that autophagy is the pathway for mitochondrial recycling, and various theories suggest that a specific targeting of damaged mitochondria to vacuoles or lysosomes occurs by autophagy (Abeliovich and Klionsky, 2001). Very recently, several studies suggest that selective mitochondrial degradation via autophagy (mitophagy) might play an important role for mitochondrial quality control (Mijaljica et al., 2007; Nowikovsky et al., 2007; Priault et al., 2005; Twig et al., 2008; Zhang et al., 2007). However, the molecular mechanism of mitophagy is poorly understood.

Macroautophagy is the bulk (i.e., nonspecific) degradation of cytoplasmic components that allows cells to respond to various types of stress and to adapt to changing nutrient conditions (Klionsky, 2005; Yorimitsu and Klionsky, 2007). In contrast to macroautophagy, the cytoplasm-to-vacuole targeting (Cvt) pathway, pexophagy (specific autophagy of peroxisomes) and mitophagy are categorized as selective types of autophagy. These processes have specific cargos comprised of the Cvt complex (precursor aminopeptidase I [prApe1] and -mannosidase [Ams1], along with receptor and adaptor proteins), peroxisomes and mitochondria, respectively (Dunn et al., 2005; Farre et al., 2008; Kanki and Klionsky, 2008; Shintani et al., 2002a). Studies in the yeast *Saccharomyces cerevisiae* and other fungi have

enabled the identification of several molecular factors essential for autophagy (Yorimitsu and Klionsky, 2005c). At present, there are 32 genes that are primarily involved in autophagy-related (Atg) pathways. Most of the *ATG* genes are required for both macroautophagy and selective autophagy, but some are required only for specific types of autophagy (Kanki and Klionsky, 2008). For example, Atg19, a receptor protein for the Cvt pathway, binds the Cvt complex, then interacts with Atg11, an adaptor protein for selective autophagy, and recruits them to the phagophore assembly site (PAS), where the sequestering cytosolic vesicles are generated (Shintani et al., 2002a). Similarly, during pexophagy in *Pichia pastoris*, Atg30 localizes to peroxisomes, where it is bound by Atg11 allowing recruitment of the peroxisomes to the PAS (Farre et al., 2008). Atg11 is also required for mitochondrial degradation during starvation or in post-log phase, suggesting that mitochondria are selected by Atg11 for autophagic degradation (Kanki and Klionsky, 2008). Recently, we identified Atg32 as a mitochondrial protein that interacts with Atg11 and is required specifically for mitophagy (Kanki et al., 2009; Okamoto et al., 2009); however the detailed mechanism of mitophagy has not been determined.

To figure out the molecular mechanism of selective mitochondria autophagy, we recently established a method to monitor this process (Kanki and Klionsky, 2008). Using this method, we screened a yeast knockout library for strains that are deficient in mitophagy. Among 4,667 strains, we found 32 strains that showed a complete or partial block of mitophagy, in addition to the *ATG* gene knockout strains. We also screened these mutants to ascertain the functionality of macroautophagy and the Cvt pathway. Nine of the strains showed defects in all autophagic pathways, whereas the other 23 strains were normal for the Cvt pathway, but defective to varying extents for macroautophagy and mitophagy. We further characterized the product of one of the genes, *YLR356W*, whose function has not been previously identified. The Ylr356w protein localized to mitochondria, and the deletion of

YLR356W resulted in an almost complete inhibition of mitophagy at post-log phase.

2.3 Materials and methods

Strains and media

The yeast strains used in this study are listed in Table 2.1. Yeast cells were grown in rich medium (YPD; 1% yeast extract, 2% peptone, 2% glucose), lactate medium (YPL; 1% yeast extract, 2% peptone, 2% lactate), synthetic minimal medium with glucose (SMD; 0.67% yeast nitrogen base, 2% glucose, amino acids, and vitamins), synthetic minimal medium with lactate (SML; 0.67% yeast nitrogen base, 2% lactate, amino acids, and vitamins), synthetic minimal medium with oleic acid (YTO; 0.67% yeast nitrogen base without amino acids, 0.1% Tween-40, and 0.1% oleic acid) or synthetic minimal medium with galactose (SMGal; 0.67% yeast nitrogen base, 2% galactose, amino acids, and vitamins). Starvation experiments were performed in synthetic minimal medium lacking nitrogen (SD-N; 0.17% yeast nitrogen base without amino acids, 2% glucose, SL-N; 0.17% yeast nitrogen base without amino acids, 2% lactate).

Table 2.1 Yeast strains used in this study

Strain	Genotype	Source
KWY007	SEY6210 *atg1Δ::HIS5 S.p. ICY2-GFP::TRP1*	This study
KWY20	SEY6210 *pho8Δ::TRP1 pho13Δ::LEU2* pRS406-*ADH1-COX4-pho8Δ60*	This study
KWY21	SEY6210 *pho8Δ::TRP1 pho13Δ::LEU2* pRS406-*ADH1-COX4-pho8Δ60 atg1Δ::ble*	This study
KWY22	SEY6210 *pho8Δ::TRP1 pho13Δ::LEU2* pRS406-*ADH1-COX4-pho8Δ60 atg32Δ::KAN*	This study
KWY23	SEY6210 *pho8Δ::TRP1 pho13Δ::LEU2* pRS406-*ADH1-COX4-pho8Δ60 aim26Δ::KAN*	This study
KWY24	SEY6210 *pho8Δ::TRP1 pho13Δ::LEU2* pRS406-*ADH1-COX4-pho8Δ60 aim28Δ::KAN*	This study
KWY25	SEY6210 *pho8Δ::TRP1 pho13Δ::LEU2* pRS406-*ADH1-COX4-pho8Δ60 dnm1Δ::KAN*	This study
KWY26	SEY6210 *pho8Δ::TRP1 pho13Δ::LEU2*	

	pRS406-*ADH1-COX4-pho8Δ60 fmc1Δ::KAN*	This study
KWY27	SEY6210 *pho8Δ::TRP1 pho13Δ::LEU2*	
	pRS406-*ADH1-COX4-pho8Δ60 lpe10Δ::KAN*	This study
KWY28	SEY6210 *pho8Δ::TRP1 pho13Δ::LEU2*	
	pRS406-*ADH1-COX4-pho8Δ60 ypr146cΔ::KAN*	This study
KWY29	SEY6210 *pho8Δ::TRP1 pho13Δ::LEU2*	
	pRS406-*ADH1-COX4-pho8Δ60 ylr356wΔ::KAN*	This study
KWY30	SEY6210 *pho8Δ::TRP1 pho13Δ::LEU2*	
	pRS406-*ADH1-COX4-pho8Δ60 rpl13bΔ::KAN*	This study
KWY31	SEY6210 *pho8Δ::TRP1 pho13Δ::LEU2*	
	pRS406-*ADH1-COX4-pho8Δ60 rpl15bΔ::KAN*	This study
KWY32	SEY6210 *pho8Δ::TRP1 pho13Δ::LEU2*	
	pRS406-*ADH1-COX4-pho8Δ60 aro2Δ::KAN*	This study
KWY33	SEY6210 *pho8Δ::TRP1 pho13Δ::LEU2*	
	pRS406-*ADH1-COX4-pho8Δ60 bck1Δ::KAN*	This study
KWY34	SEY6210 *pho8Δ::TRP1 pho13Δ::LEU2*	
	pRS406-*ADH1-COX4-pho8Δ60 bub1Δ::KAN*	This study
KWY35	SEY6210 *pho8Δ::TRP1 pho13Δ::LEU2*	
	pRS406-*ADH1-COX4-pho8Δ60 egd1Δ::KAN*	This study
KWY36	SEY6210 *pho8Δ::TRP1 pho13Δ::LEU2*	
	pRS406-*ADH1-COX4-pho8Δ60 icy2Δ::HIS5*	This study
KWY37	SEY6210 *pho8Δ::TRP1 pho13Δ::LEU2*	
	pRS406-*ADH1-COX4-pho8Δ60 mak10Δ::KAN*	This study
KWY38	SEY6210 *pho8Δ::TRP1 pho13Δ::LEU2*	
	pRS406-*ADH1-COX4-pho8Δ60 nft1Δ::KAN*	This study
KWY39	SEY6210 *pho8Δ::TRP1 pho13Δ::LEU2*	
	pRS406-*ADH1-COX4-pho8Δ60 yil165cΔ::KAN*	This study
KWY40	SEY6210 *pho8Δ::TRP1 pho13Δ::LEU2*	
	pRS406-*ADH1-COX4-pho8Δ60 yor019wΔ::KAN*	This study
KWY41	SEY6210 *OM45-GFP::TRP1 aim26Δ::KAN*	This study
KWY42	SEY6210 *OM45-GFP::TRP1 aim28Δ::KAN*	This study
KWY43	SEY6210 *OM45-GFP::TRP1 dnm1Δ::KAN*	This study
KWY44	SEY6210 *OM45-GFP::TRP1 fmc1Δ::KAN*	This study
KWY45	SEY6210 *OM45-GFP::TRP1 lpe10Δ::KAN*	This study
KWY46	SEY6210 *OM45-GFP::TRP1 ypr146cΔ::KAN*	This study
KWY47	SEY6210 *OM45-GFP::TRP1 ylr356wΔ::KAN*	This study
KWY48	SEY6210 *OM45-GFP::TRP1 rpl13bΔ::KAN*	This study
KWY49	SEY6210 *OM45-GFP::TRP1 rpl15bΔ::KAN*	This study
KWY50	SEY6210 *OM45-GFP::TRP1 aro2Δ::KAN*	This study
KWY51	SEY6210 *OM45-GFP::TRP1 bck1ΔΔ::KAN*	This study
KWY52	SEY6210 *OM45-GFP::TRP1 bub1Δ::KAN*	This study
KWY53	SEY6210 *OM45-GFP::TRP1 egd1Δ::KAN*	This study
KWY54	SEY6210 *OM45-GFP::TRP1 icy2Δ::KAN*	This study
KWY55	SEY6210 *OM45-GFP::TRP1 mak10Δ::KAN*	This study
KWY56	SEY6210 *OM45-GFP::TRP1 nft1Δ::KAN*	This study
KWY57	SEY6210 *OM45-GFP::TRP1 pmr1Δ::KAN*	This study
KWY58	SEY6210 *OM45-GFP::TRP1 hur1Δ::KAN*	This study
KWY59	SEY6210 *OM45-GFP::TRP1 yil165cΔ::KAN*	This study
KWY60	SEY6210 *OM45-GFP::TRP1 yor019wΔ::KAN*	This study
KWY61	SEY6210 *AIM26-GFP::TRP1*	This study

KWY62	SEY6210 *AIM28-GFP::TRP1*	This study
KWY63	SEY6210 *DNM1-GFP::TRP1*	This study
KWY64	SEY6210 *FMC1-GFP::TRP1*	This study
KWY65	SEY6210 *LPE10-GFP::TRP1*	This study
KWY66	SEY6210 *YPR146C-GFP::TRP1*	This study
KWY67	SEY6210 *RPL13B-GFP::TRP1*	This study
KWY68	SEY6210 *RPL15B-GFP::TRP1*	This study
KWY69	SEY6210 *ARG82-GFP::TRP1*	This study
KWY70	SEY6210 *ARO2-GFP::TRP1*	This study
KWY71	SEY6210 *BCK1-GFP::TRP1*	This study
KWY72	SEY6210 *BUB1-GFP::TRP1*	This study
KWY73	SEY6210 *EGD1-GFP::TRP1*	This study
SEY6210	MATα *his3-Δ200 leu2-3,112 lys2-801 trp1-Δ901 ura3-52 suc2-Δ9 GAL*	(Robinson et al., 1988)
TKYM22	SEY6210 *OM45-GFP::TRP1*	(Kanki and Klionsky, 2008)
TKYM25	SEY6210 *atg1Δ::KanMX6 OM45-GFP::TRP1*	This study
TKYM28	SEY6210 *pep4Δ::LEU2*	This study
TKYM36	SEY6210 *atg8Δ::HIS5 S.p. OM45-GFP::TRP1*	This study
TKYM37	SEY6210 *atg5Δ::LEU2 OM45-GFP::HIS3MX6*	This study
TKYM38	SEY6210 *atg9Δ::HIS5 S.p. OM45-GFP::TRP1*	This study
TKYM39	SEY6210 *atg11Δ::LEU2 OM45-GFP::TRP1*	This study
TKYM44	SEY6210 *atg27Δ::TRP1 OM45-GFP::HIS3MX6*	This study
TKYM45	SEY6210 *atg31Δ::HIS5 S.p. OM45-GFP::KanMX6*	This study
TKYM47	SEY6210 *atg17Δ::KanMX6 OM45-GFP::HIS3MX6*	This study
TKYM49	SEY6210 *atg29Δ::KanMX6 OM45-GFP::HIS3MX6*	This study
TKYM50	SEY6210 *IDH1-GFP::KanMX6*	(Kanki and Klionsky, 2008)
TKYM53	SEY6210 *atg20Δ::HIS5 S.p. OM45-GFP::KanMX6*	This study
TKYM54	SEY6210 *atg24Δ::HIS5 S.p. OM45-GFP::KanMX6*	This study
TKYM57	SEY6210 *atg23Δ::KanMX6 OM45-GFP::TRP1*	This study
TKYM62	SEY6210 *atg19Δ::HIS5 S.p. OM45-GFP::TRP1*	This study
TKYM67	SEY6210 *PEX14-GFP::KanMX6*	(Kanki and Klionsky, 2008)
TKYM72	SEY6210 *atg1Δ::HIS5 S.p. PEX14-GFP::KanMX6*	(Kanki and Klionsky, 2008)
TKYM80	SEY6210 *atg1Δ::HIS5 S.p. IDH1-GFP::TRP1*	This study
TKYM167	SEY6210 *ylr356wΔ::HIS5 S.p. OM45-GFP::TRP1*	This study

TKYM170	SEY6210 *atg2Δ::HIS5 S.p. OM45-GFP::TRP1*	This study
TKYM171	SEY6210 *atg3Δ::HIS5 S.p. OM45-GFP::KanMX6*	This study
TKYM172	SEY6210 *atg4Δ::LEU2 OM45-GFP::HIS3MX6*	This study
TKYM173	SEY6210 *atg6Δ::LEU2 OM45-GFP::HIS3MX6*	This study
TKYM174	SEY6210 *atg7Δ::HIS5 S.p. OM45-GFP::TRP1*	This study
TKYM175	SEY6210 *atg10Δ::HIS5 S.p. OM45-GFP::TRP1*	This study
TKYM176	SEY6210 *atg12Δ::KanMX6 OM45-GFP::HIS3MX6*	This study
TKYM177	SEY6210 *atg13Δ::KanMX6 OM45-GFP::HIS3MX6*	This study
TKYM178	SEY6210 *atg14Δ::LEU2 OM45-GFP::HIS3MX6*	This study
TKYM179	SEY6210 *atg15Δ::KanMX6 OM45-GFP::HIS3MX6*	This study
TKYM180	SEY6210 *atg16Δ::KanMX6 OM45-GFP::URA3*	This study
TKYM181	SEY6210 *atg18Δ::KanMX6 OM45-GFP::HIS3MX6*	This study
TKYM182	SEY6210 *atg21Δ::HIS5 S.p. OM45-GFP::TRP1*	This study
TKYM183	SEY6210 *atg22Δ::TRP1 OM45-GFP::HIS3MX6*	This study
TKYM184	SEY6210 *atg26Δ::URA3 OM45-GFP::HIS3MX6*	This study
TKYM186	SEY6210 *icy2Δ::HIS5 S.p. OM45-GFP::TRP1*	This study
TKYM187	SEY6210 *icy2Δ::HIS5 S.p. PEX14-GFP::TRP1*	This study
TKYM188	SEY6210 *ylr356wΔ::HIS5 S.p. PEX14-GFP:: TRP1*	This study
TKYM194	SEY6210 *ylr356wΔ::HIS5 S.p. IDH1-GFP::TRP1*	This study
TKYM195	SEY6210 *icy2Δ::HIS5 S.p. IDH1-GFP::TRP1*	This study
TKYM196	SEY6210 *ylr356wΔ::HIS5 S.p.*	This study
TKYM197	SEY6210 *icy2Δ::HIS5 S.p.*	This study
TKYM199	TN124 *ylr356wΔ::URA3*	This study
TKYM200	TN124 *icy2Δ::URA3*	This study
TKYM201	SEY6210 *KanMX6::GAL-YLR356W-GFP::TRP1*	This study
TKYM205	SEY6210 *YLR356W-Protein A:: TRP1 OM45-GFP::URA3*	This study
TKYM206	SEY6210 *YLR356W-Protein A:: TRP1 TIM23-13myc:: HIS5 S.p.*	This study
TN124	MATa *leu2-3,112 ura3-52 trp1*	(Noda et al., 1995)

	pho8::pho8Δ60 pho13Δ::LEU2	
WLY176	SEY6210 *pho13Δ pho8Δ60::HIS3*	This study
WLY192	SEY6210 *pho13Δ::KAN pho8Δ60::URA3 atg1Δ::HIS5*	This study
WLY233	SEY6210 *pho13Δ pho8Δ60::HIS3 arg82Δ::KAN*	This study
WLY234	SEY6210 *pho13Δ pho8Δ60::HIS3 aim28Δ::KAN*	This study
WLY235	SEY6210 *pho13Δ pho8Δ60::HIS3 rpl14aΔ::KAN*	This study
WLY236	SEY6210 *pho13Δ pho8Δ60::HIS3 yor019wΔ::KAN*	This study
WLY237	SEY6210 *pho13Δ pho8Δ60::HIS3 icy2Δ::KAN*	This study
WLY238	SEY6210 *pho13Δ pho8Δ60::HIS3 hur1Δ::LEU2*	This study
WLY239	SEY6210 *pho13Δ pho8Δ60::HIS3 fmc1Δ::KAN*	This study
WLY240	SEY6210 *pho13Δ pho8Δ60::HIS3 yil165cΔ::KAN*	This study
WLY241	SEY6210 *pho13Δ pho8Δ60::HIS3 rpl15bΔ::KAN*	This study
WLY242	SEY6210 *pho13Δ pho8Δ60::HIS3 ylr356wΔ::KAN*	This study
WLY243	SEY6210 *pho13Δ pho8Δ60::HIS3 atg32Δ::KAN*	This study
WLY244	SEY6210 *pho13Δ pho8Δ60::HIS3 bck1Δ::KAN*	This study
WLY245	SEY6210 *pho13Δ pho8Δ60::HIS3 aim26Δ::KAN*	This study
WLY246	SEY6210 *pho13Δ pho8Δ60::HIS3 nft1Δ::KAN*	This study
WLY247	SEY6210 *pho13Δ pho8Δ60::HIS3 ypr146cΔ::KAN*	This study
WLY248	SEY6210 *pho13Δ pho8Δ60::HIS3 mak10Δ::KAN*	This study
WLY249	SEY6210 *pho13Δ pho8Δ60::HIS3 egd1Δ::KAN*	This study
WLY250	SEY6210 *pho13Δ pho8Δ60::HIS3 dnm1Δ::KAN*	This study
WLY251	SEY6210 *pho13Δ pho8Δ60::HIS3 aro2Δ::KAN*	This study
WLY252	SEY6210 *pho13Δ pho8Δ60::HIS3 bub1Δ::KAN*	This study
WLY253	SEY6210 *pho13Δ pho8Δ60::HIS3 lpe10Δ::KAN*	This study
WLY254	SEY6210 *pho13Δ pho8Δ60::HIS3 pmr1Δ::KAN*	This study

Mitophagy screening

For the first round of screening, a yeast knockout strain library (BY4739 or BY4742 background) was analyzed. To express Om45-GFP, a DNA fragment encoding GFP was integrated at the 3' end of *OM45* by a PCR-based integration method (Longtine et al., 1998). Cells grown on SMD plates were shifted to YPL medium and cultured for 3 days (50 +/- 5 h), and the vacuolar GFP fluorescence was observed by fluorescence microscopy. If there was no vacuolar GFP signal, or a weak signal, the mitochondrial GFP signal and the cell growth were also recorded.

For the secondary screening, the Om45-GFP-expressing strains that showed a weak or absent vacuolar GFP signal were cultured in YPL medium for 12 h and then shifted to SD-N medium. The cells were collected after 6 h and the cell lysates equivalent to A_{600} = 0.2 units

of cells were subjected to immunoblotting analysis.

Plasmids and antibodies

The mitoPho8Δ60 expressing plasmid (ADH1-COXIV- PHO8Δ60(406)) was derived from ADH1-COXIV- PHO8Δ60(313) described previously (Campbell and Thorsness, 1998) by digesting with Pvu1 and inserting the *ADH1-COXIV-PHO8Δ60* fragment into the pRS406 vector.

Monoclonal anti-YFP antibody clone JL-8 (Clontech, Mountain View, CA) and anti-Ape1 antiserum (Shintani et al., 2002a) were used for immunoblotting. Monoclonal anti-myc and anti-porin antibodies were from Molecular Probes/Invitrogen (Eugene, OR), and anti-Pgk1 antiserum was a kind gift of Dr. Jeremy Thorner (University of California, Berkeley).

Assays for autophagy and pexophagy

For monitoring bulk autophagy, the alkaline phosphatase activity of Pho8Δ60 was carried out as described previously (Noda et al., 1995). The Pex14-GFP processing assay to monitor pexophagy has been described previously (Reggiori et al., 2005).

MitoPho8Δ60 assay

For monitoring mitophagy, the mitochondrially-targeted Pho8Δ60-expressing strains were cultured in YPL medium for 12 h and then shifted to SD-N or SL-N medium. The cells were collected after 4 h and the alkaline phosphatase activity of Pho8Δ60 was carried out as described previously (Noda et al., 1995).

Cell fractionation and sub-mitochondrial localization

Cells expressing Tim23-myc and Ylr356w tagged with protein A (PA) were converted to spheroplasts with Zymolyase, suspended in homogenization buffer (0.6 M mannitol, 20 mM HEPES, pH 7.4, and proteinase inhibitors) and homogenized in a potter homogenizer on ice. The cell homogenate was centrifuged at 600 x g for 10 min at 4°C to remove the nucleus and unbroken cells. The supernatant fraction was then centrifuged at 6,500 x g for 10 min at 4°C. The pellet was collected as the mitochondrial fraction. Isolated mitochondria was suspended in ice-cold suspension medium (0.6 M mannitol, 20 mM HEPES, pH 7.4) or hypotonic buffer (10 mM Tris-HCl, pH 7.4, 1 mM EDTA) and treated with proteinase K (200 μg/ml) for 30 min on ice with or without 0.5% Triton X-100. The proteinase K reaction was stopped by adding 10% trichloroacetic acid (TCA). TCA precipitated proteins were washed with acetone and subjected to immunoblotting.

Fluorescence microscopy

Yeast cells expressing fluorescent protein-fused chimeras were grown to mid-log phase or starved in the indicated media. To label the vacuolar membrane or mitochondria, cells were incubated in medium containing 20 μg/ml N-(3-triethylammoniumpropyl)-4-(p-diethylaminophenylhexatrienyl) pyridinium dibromide (FM 4-64; Molecular Probes, Eugene, OR) or 1 μM MitoFluor Red 589 (Molecular Probes, Eugene, OR) at 30°C for 30 min, respectively. After being washed with medium, the cells were incubated in medium at 30°C for 30 to 60 min. Fluorescence microscopy observation was carried out as described previously (Monastyrska et al., 2008).

Electron microscopy

The *pep4*Δ strain (TKY28) was cultured in YPL medium to mid-log phase, then shifted to SD-N and cultured for 6 h or was cultured in YPL medium to stationary phase (for

50 h). Cells were frozen in a KF80 freezing device (Reichert-Jung, Vienna, Austria). Transmission electron microscopy was performed according to the procedures described previously (Baba, 2008).

2.4 Results

A genome-wide screen for yeast mitophagy mutants

Mitophagy can be induced by culturing yeast strains in a medium with a non-fermentable carbon source such as lactate (YPL) (Kanki and Klionsky, 2008; Tal et al., 2007) or ethanol and glycerol to post-log phase. The green fluorescent protein (GFP) tagged on the C terminus of the mitochondrial outer membrane protein Om45 (Om45-GFP) accumulates in the vacuole, when mitophagy is induced (Kanki and Klionsky, 2008). To identify mitochondrial autophagy-related genes, we used a *MATα* yeast knockout library and chromosomally tagged the C terminus of Om45 with GFP in each strain. After the strains were cultured in YPL medium for three days to allow growth to the post-log phase, they were observed for vacuolar GFP fluorescence. Among 4,667 strains examined (Figure 2.1), 4,142 strains showed a clear level of vacuolar GFP, and 400 strains showed either no, or a very weak, vacuolar GFP signal (some examples are shown in Figure 2.2.A). We could not examine 125 strains due to their displaying a growth defect in YPD medium (some of the library strains grew poorly even in YPD) or because of a difficulty in the Om45-GFP tagging.

The vacuolar GFP-negative or weak strains included 19 AuTophaGy-related (*ATG*) gene knockout strains. We screened all *ATG* gene knockout strains for mitophagy separately (see below); these strains were examined apart from the other mutants uncovered in the present screen. In addition to post-logarithmic phase growth in lactate medium, mitophagy can be induced when cells are shifted from YPL to nitrogen starvation medium (SD-N), and the level of mitophagy can be semi-quantitatively monitored by measuring the amount of

GFP processed from Om45-GFP in the vacuole using immunoblotting (Kanki and Klionsky, 2008). For this GFP processing analysis, we required a certain volume of cells and an adequate level of Om45-GFP expression; we excluded 91 strains that showed very slow growth in YPL or very low Om45-GFP expression based on fluorescence microscopy. Among the remaining 290 strains that we screened by GFP processing, 32 strains showed a complete or partial block of mitophagy (Figure 2.3), 30 strains showed lower, but substantial, GFP processing compared with the wild-type strain, 85 strains showed the same level of GFP processing as the wild type, and 140 strains showed lower Om45-GFP expression; in these latter strains we could not determine from this analysis whether the lower amount of GFP processing was a result of a block in mitophagy or was due to a low level of Om45-GFP (an example is shown in Figure 2.2.B). Three strains, with deletions of *VMA13*, *TFP1* (*VMA1*) or *YOR331C* (which overlaps with *VMA4*) showed more than a two-fold increase in GFP processing compared with the wild type (our unpublished results). The results for all 4,667 strains are available on line at http://www.molbiolcell.org/content/20/22/4730/suppl/DC1 and summarized in Figure 2.1.

Analysis for defects in macroautophagy and the Cvt pathway

To further characterize the 32 newly identified mutant strains that showed a clear defect in mitochondrial degradation, we decided to monitor the nonspecific macroautophagy activity using the Pho8Δ60 alkaline phosphatase assay (Noda et al., 1995). Pho8Δ60 is a truncated form of the vacuolar alkaline phosphatase. Deletion of the native signal sequence causes the precursor protein to remain in the cytosol, and it is only delivered to the vacuole by an autophagic mechanism. Upon delivery, the C-terminal propeptide is removed, resulting in activation of the zymogen, which can be measured enzymatically. We introduced Pho8Δ60 into these 32 knockout strains and measured the Pho8Δ60-dependent alkaline phosphatase

activity in both growing and 4 h starvation conditions (Figure 2.4.A). For the initial analysis, to simplify the strain construction, we did not delete the *PHO13* gene, which encodes a cytosolic alkaline phosphatase. This resulted in a higher level of background activity during growing conditions; however, after 4 h starvation the alkaline phosphatase activity was significantly increased in wild-type cells relative to growing conditions, so there was an adequate signal:noise ratio. We found eight strains that showed a complete block of nonspecific autophagy and four strains that showed a partial block. We also screened these mutants for defects in the biosynthetic Cvt pathway, a selective type of autophagy used for delivery of the resident hydrolase Ape1 to the vacuole (Klionsky and Emr, 2000), by monitoring the processing of prApe1 (Figure 2.4.B). Eight strains showed a complete block of the Cvt pathway and one strain showed a partial block. We summarized the results for macroautophagy, the Cvt pathway and mitophagy, which is available on line at http://www.molbiolcell.org/content/20/22/4730/suppl/DC1.

Analysis of 23 novel mutants

Among these 32 mitophagy-related genes identified from the screen, 9 of them are related with vacuolar protein sorting, membrane fusion machinery or normal vacuolar function. As expected based on published data, deletion of these genes resulted in a partial or complete block in all autophagy-related pathways, and we did not pursue a further analysis of the associated gene products. The remaining 23 gene products are involved in diverse cellular processes. In particular, Atg32 is a mitochondrially-localized receptor required for starvation-dependent and post-log phase growth mitophagy (Kanki et al., 2009; Okamoto et al., 2009). In addition, eight of these 23 genes encode mitochondrially-related proteins. Accordingly, we decided to extend our analysis of these 23 mutants.

First, to verify the screen results, we decided to delete these 23 genes in another yeast

strain background to eliminate potential strain-dependent phenotypes, and to verify that the mitophagy defect was due to the correct gene deletion. We used the SEY6210 strain that had the integrated Om45-GFP tag, and conducted the same processing assay (Figure 2.5). Two mutants, *rpl15b*Δ and *yil165c*Δ, showed comparable GFP processing with the wild type, while other mutants showed partial or no GFP processing, consistent with the previous screen result. In two cases, for *rpl14a* and *arg82*, we were unable to generate the appropriate strains.

To provide a second method of mitophagy analysis, we also integrated GFP at the 3' end of the *IDH1* locus of the corresponding deletion strains and carried out an Idh1-GFP processing assay; Idh1 is a mitochondrial matrix protein, and its delivery to the vacuole should mirror that of Om45-GFP (Figure 2.6). We found that the *rpl5b*Δ and *aim28*Δ mutant strains showed normal GFP-processing compared with the wild type, while the other mutant strains displayed reduced or no GFP-processing. In two cases, for *ypr146c*Δ and *lpe10*Δ, we were unable to generate the appropriate strains.

In some cases, we noted discrepancies between the results for the Om45-GFP and Idh1-GFP processing assays. In addition, neither of these assays is quantitative. Therefore, we modified a previously described alkaline phosphatase assay that uses a mitochondrially-targeted Pho8Δ60 (mitoPho8Δ60) construct (Campbell and Thorsness, 1998) and assayed the deletion mutants for mitophagy activity. The mitoPho8Δ60 can only be delivered into the vacuole following the autophagic degradation of mitochondria. Cells expressing mitoPho8Δ60 were cultured in YPL to mid-log phase and shifted to SD-N or SL-N for 4 h, and mitoPho8Δ60-dependent alkaline phosphatase activity was measured. The YPL to SD-N shift will induce selective autophagic mitochondria degradation as well as nonselective autophagy, whereas the YPL to SL-N shift will only induce bulk autophagy (Kanki and Klionsky, 2008); thus, the SD-N minus SL-N value represents the activity of selective autophagic mitochondrial degradation. For the wild-type strain, we observed 36%

higher alkaline phosphatase activity during the SD-N shift than was seen following the shift to SL-N (Figure 2.7). In the *atg1*Δ strain, the alkaline phosphatase activities during both starvation conditions represent the background level. In the *atg32*Δ strain, we observed a significant decrease (75%) of mitoPho8Δ60 activity during the SD-N shift compared to the wild type, which showed that Atg32 is required for efficient selective autophagic mitochondria degradation. We also observed a 63% decrease of alkaline phosphatase activity during the SL-N shift compared to the wild type, possibly due to the absence of Atg32-dependent mitochondrial degradation that occurs through nonspecific autophagy (which is likely to still require Atg32 to be efficient). We were unable to generate the mitoPho8Δ60 strains for deletions of *ARG82*, *RPL14A*, *PMR1* and *HUR1*. For the remaining nineteen mutants, eight strains (*icy2*Δ, *rpl15b*Δ, *nft1*Δ, *yil165c*Δ, *lpe10*Δ, *egd1*Δ, *aim28*Δ and *ypr146c*Δ) showed comparable mitophagy activity with the wild type, whereas the eleven other strains displayed a significant to complete mitophagy defect (Figure 2.7). The potential reasons for the differences between the Om45-GFP processing assay results and those of the mitoPho8Δ60 assay are considered in the Discussion.

Next, to examine potential effects on nonspecific macroautophagy we used the GFP-Atg8 processing assay. This assay relies on the same principle as the Om45-GFP processing assay, but the marker protein is a component of the autophagosome; substantial generation of free GFP from GFP-Atg8 is only seen during nonspecific autophagy. All 23 mutant strains essentially showed normal GFP-Atg8 processing (Figure 2.8), demonstrating they do not have substantial defects in non-specific macroautophagy. To extend the analysis, we generated *pho8::pho8*Δ*60 pho13*Δ strains in the SEY6210 background for each mutant and monitored them using the more quantitative Pho8Δ60 activity assay as a second method for analyzing potential macroautophagy defects (Figure 2.9); we were unable to generate the Pho8Δ60 strain for *rpl13b*Δ. Two strains (*rpl14a*Δ *and icy2*Δ) displayed a more than 40%

decrease of Pho8Δ60 activity, seven strains (*aim26*Δ, *fmc1*Δ, *bck1*Δ, *bub1*Δ, *egd1*Δ, *nft1*Δ and *yil165c*Δ) showed a slightly reduced Pho8Δ60 activity (less than 30% decrease), and the other strains were essentially normal.

Finally, we determined the subcellular localization of these proteins by chromosomally tagging them with GFP and observed them with fluorescence microscopy (Figure 2.10). Atg32 has already been reported as being localized to the mitochondria. For the other 22 proteins, eight of them (Aim26, Aim28, Dnm1, Fmc1, Lpe10, Ypr146c and Ylr356w) displayed a mitochondrial localization pattern. The localization of Ylr356w was further studied as described below. The subcellular localization of most proteins under nitrogen starvation condition was basically the same as during vegetative growth (data not show). The localization information is summarized and available on line at http://www.molbiolcell.org/content/20/22/4730/suppl/DC1.

Characterization of *ylr356w*Δ

The mitophagy-related genes that we found from the screen include eight genes of unknown function. Among them, we initially focused on *YLR356W*. The Ylr356w protein is reported to localize to mitochondria (Huh et al., 2003) and we obtained consistent data between our different detection methods for both mitophagy and autophagy. Thus, we decided to characterize this gene as a candidate for a novel *ATG* gene. In agreement with the previous report, we found that Ylr356w tagged with GFP is mitochondrially-localized (Figure 2.10, Figure 2.11.A); however, the overexpressed chimera is not fully functional. We detected a similar mitochondrial localization using a chromosomally tagged GFP construct, but the fluorescence signal was extremely weak (our unpublished data). Accordingly, we further examined the mitochondrial localization of Ylr356w using a biochemical approach. A strain expressing protein A-tagged Ylr356w (Ylr356w-PA) and Myc-tagged Tim23 (inner

membrane marker) was fractionated by differential centrifugation. Mitochondrial porin and Tim23-myc were enriched in the mitochondrial (6,500 x g) fraction, along with Ylr356w-PA (Figure 2.11.B), whereas the cytosolic marker Pgk1 was mostly in the supernatant fraction. Next, the isolated mitochondria were treated with proteinase K before or after hypotonic treatment or in the presence of Triton X-100. Although Tim23-myc was protected from proteinase K before hypotonic treatment or in the absence of detergent, Ylr356w-PA was degraded, suggesting that this protein localizes on the mitochondrial outer membrane (Figure 2.11.C). As our data showed, macroautophagy and the Cvt pathway were essentially normal in *ylr356w*Δ strains in both the BY4742 and SEY6210 backgrounds (Figure 2.9, Figure 2.4, 2.8, 2.12.A). There was a substantial decrease of Om45-GFP processing for starvation-induced mitophagy (Figure 2.5), and the mitoPho8Δ60 assay revealed a 36% decrease of mitophagy activity (Figure 2.7) in the *ylr356w*Δ strain. We also monitored pexophagy, another type of selective autophagy, using the Pex14-GFP processing assay. Pex14 is a peroxisomal membrane protein, and processing of Pex14-GFP to release free GFP can be used for monitoring peroxisome degradation in the vacuole (Reggiori et al., 2005). The *ylr356w*Δ strain displayed processing of Pex14-GFP at a similar level to the wild-type strain after shifting cells from oleic acid medium to starvation medium, whereas the *atg1*Δ mutant showed a complete block (Figure 2.12.B). From these findings, we conclude that *YLR356W* is a mitophagy-specific gene that is not required for macroautophagy or other types of selective autophagy.

Considering that we observed relatively minor vacuolar GFP fluorescence from the *ylr356w*Δ (BY4742 background) strain expressing Om45-GFP at the post-log phase (day 3 in YPL medium) in our initial screen, while we obtained a relatively slight decrease (36% based on the mitoPho8Δ60 assay (Figure 2.7) and 33% based on the Om45-GFP processing assay (Figure 2.11.D)) of mitophagy activity during starvation, we considered the possibility that

Ylr356w might play different roles in these two mitophagy inducing conditions. Thus, we repeated the analysis of Om45-GFP fluorescence of the *ylr356w*Δ strain in the SEY6210 background. After 45 h in YPL medium, the *ylr356w*Δ strain again showed only faint vacuolar GFP fluorescence (Figure 2.12.C), and Om45-GFP processing was mostly blocked (93% and 80% decrease compared with the wild type at 32 and 50 h in YPL, respectively; Figure 2.11.E). One possibility to explain the mitophagy defect in the *ylr356w*Δ strain in the post-log phase was that the severe block in Om45-GFP processing was due to a growth defect in YPL medium that prevented the cells from reaching the mitophagy-inducing post-log phase. Accordingly, we checked the growth of the *ylr356w*Δ strain. This strain showed the same growth both on YPD and YPL plates and was similar to the wild-type strain (Figure 2.12.D). Thus, we concluded that Ylr356w was required primarily for mitophagy induced at the post-log phase, and played a less significant role during starvation-induced mitophagy. Based on the cumulative analyses of the phenotypes of the *ylr356w*Δ strain, we named this gene *ATG33*.

Screen of *ATG* knockout strains for mitophagy defects

Several *ATG* genes are required for mitophagy (Kanki and Klionsky, 2008; Kissova et al., 2004; Kissova et al., 2007; Tal et al., 2007; Zhang et al., 2007) and our first mitophagy screen revealed eighteen *ATG* genes that may be required for this process (one of the additional strains with a mitophagy defect is deleted for *YMR158W-A*, a gene that overlaps with *ATG16*, thus implicating 19 *ATG* genes in total). Thus, we decided to screen all 28 *ATG* knockout strains that play a role in autophagy-related processes in *S. cerevisiae* using the Om45-GFP processing analysis. *ATG* genes that play a fundamental role in autophagy such as that encoding the protein kinase Atg1 and its binding partner Atg13, the genes for the ubiquitin-like protein modification systems (*ATG3*, *4*, *5*, *7*, *8*, *10*, *12* and *16*) and those that

encode components that are involved in supplying membrane to the phagophore (*ATG2* and *ATG9*) were essential for mitophagy (Figure 2.13). Genes that are required for the Cvt pathway but not macroautophagy (*ATG20*, *21* and *24*), or for macroautophagy but not the Cvt pathway (*ATG17*, *29* and *31*) were also required for efficient mitophagy. Finally, the gene encoding *ATG11*, which is a common adaptor for selective types of autophagy was required for mitophagy as shown previously (Kanki and Klionsky, 2008), whereas the genes for the Cvt cargo-specific receptor, *ATG19* (Shintani et al., 2002a), a vacuolar permease, *ATG22* (Yang et al., 2006), and an autophagy gene that is not required in *S. cerevisiae*, *ATG26* (Cao and Klionsky, 2007), were not required for mitophagy.

2.5 Discussion

A mitochondria degradation screen identified 32 mitophagy-related genes

The initial screen for mitophagy was carried out in 96-well plates. Thus, the screen was performed in a blind manner as the gene names of each strain were hidden during the screen. Among 25 *ATG* genes that are required for mitophagy (Figure 2.13), our knockout library included 21 *ATG* knockout strains (*atg2*Δ, *4*Δ and *10*Δ were not included in our BY4739 or BY4742 background library, and *atg14*Δ was incorrect). Based on our initial screen, 17 of them (18 if we include the strain where the deletion overlaps with *ATG16*) were identified as positive for a defect in mitophagy, and 3 of them were negative (*atg17*Δ, *24*Δ and *31*Δ). If it is assumed that these *ATG* knockout strains serve as positive controls, our initial screen sensitivity was 81 to 86% (17 or 18/21). In other words, we may have missed 14 to 19% of the positive strains during our initial screen; however, considering that *atg17*Δ and *atg31*Δ have only partial defects, our detection rate may have been closer to 95%. We cannot calculate the sensitivity of the secondary screen, because the *ATG* genes were screened by the Om45-GFP processing assay (the secondary screen for the other mutants). The fact that at

least one novel *ATG* gene, *YLR356W/ATG33*, was identified from our screen further supports its utility.

Our screen identified eight membrane trafficking-related genes (*CCZ1*, *MON1*, *PEP12*, *TRS85*, *VAM7*, *VPS36, VPS41* and *VPT7*) that are required for mitophagy. All of them are also required for both macroautophagy and the Cvt pathway. The requirement of some of these genes for autophagy has been reported previously (Meiling-Wesse et al., 2002; Meiling-Wesse et al., 2005; Nazarko et al., 2005; Sato et al., 1998; Wang et al., 2003; Wichmann et al., 1992; Wurmser et al., 2000), and the requirement of membrane trafficking pathways for autophagy has also been reported (Ishihara et al., 2001; Reggiori et al., 2004). It is widely believed that defects in membrane trafficking pathways affect the lipid supply that is needed for extension of the phagophore, the initial sequestering compartment that generates the autophagosome. The two genes identified here that are involved in membrane trafficking that have not been reported previously as affecting autophagy, *PEP12* and *VPS36*, presumably do so for the same reason.

We identified nine mitophagy-related genes whose functions were not previously known (*AIM26*, *AIM28*, *ATG32*, *HUR1*, *ICY2*, *YIL165C*, *YLR356W*, *YOR019W* and *YPR146C*). *HUR1* overlaps with *PMR1*, which encodes a cation P-type ATPase in the Golgi complex. Thus, the phenotype of the *hur1*Δ strain may result from a knockout of the *PMR1* gene. The further characterization of the other eight gene products may provide substantial insight into the mechanism of mitophagy. In particular, Ylr356w localized to mitochondria and may play an important role in determining whether a particular mitochondrial segment is destined for degradation by autophagy. Thus, we initially focused on the *YLR356W* gene and the corresponding protein.

DNM1 encodes mitochondrial dynamin-related GTPase that is required for mitochondrial fission. The fragmentation of mitochondria is a prerequisite for mitophagy in

mammalian cells (Twig *et al.*, 2008) and the *dnm1*Δ strain inhibits the mitophagy induced by *mdm38* conditional knockout in yeast (Nowikovsky *et al.*, 2007). The identification of the *dnm1*Δ strain from our screen further confirmed the importance of mitochondrial fission for mitophagy.

Different methods to monitor mitophagy

In this paper, we used the Om45-GFP processing and mitoPho8Δ60 assays to measure mitophagy activity. Importantly, with the mitoPho8Δ60 assay, we can measure mitophagy in a quantitative manner. Both assays showed the expected results for the wild-type, *atg1*Δ and *atg32*Δ strains, demonstrating they are adequate for measuring mitophagy. In some cases, however, we obtained different results between these two methods. One potential problem with the mitoPho8Δ60 assay is that the marker protein may not be properly targeted to the mitochondria in each mutant strain, especially in mutants that may have a defect in the mitochondrial protein import system. This would cause an apparent mitophagy defect, and correct localization should be confirmed in each case.

YLR356W/ATG33 is required primarily for mitophagy induced at the post-log phase

Although a genome-wide screen for protein localization revealed that Ylr356w localizes to mitochondria (Huh et al., 2003), there have not been any other reports about this protein. Ylr356w is composed of 197 amino acids and is predicted to have four transmembrane domains. This protein is conserved within fungi, but not in higher eukaryotes. *YLR356W* is a mitophagy-specific gene that is not required for macroautophagy or other types of selective autophagy (Figures 2.4.B, 2.8, 2.9, 2.11, and 2.12). Although *ylr356w*Δ blocked mitophagy to half the level of the wild type during starvation, it blocked mitophagy almost completely at the post-log phase (Figure 2.11.D E). This finding suggests that

Ylr356w may be required to detect or present aged mitochondria for mitophagy when cells have reached the post-log phase.

The induction of mitophagy during starvation and at the post-log phase in yeast

Although mitochondria depolarized by an uncoupler such as carbonyl cyanide m-chlorophenylhydrazone (CCCP) are degraded by autophagy in mammalian cells (Narendra et al., 2008b; Sandoval et al., 2008), we did not observe mitochondrial degradation in wild-type yeast under similar conditions (our unpublished results). Thus, in our experience, nitrogen starvation or culturing cells to the post-log phase in a non-fermentable carbon source medium are the only reliable methods that can induce mitophagy efficiently in a wild-type yeast strain. A previous study suggests that mitophagy in *S. cerevisiae* occurs by a microautophagic process when cells are grown under nonfermentable conditions (Kissova et al., 2007). Thus, we considered the possibility that mitophagy might happen by different mechanisms depending on the inducing conditions. We attempted to examine the mode of autophagic sequestration occurring in SD-N versus post-log phase growth through electron microscopy (Figure 2.14). In both conditions we could detect mitochondria within double-membrane vesicles, suggesting a macroautophagic mechanism; however, we cannot rule out the possibility of a microautophagic process.

It is thought that mitophagy is induced to adapt the cell to conditions where the cell energy requirement is decreased, and accordingly the cell needs to reduce the amount of mitochondria when reaching the post-log phase in non-fermentable medium (Kanki and Klionsky, 2008), although there is little direct evidence for this hypothesis. On the other hand, macroautophagy is induced at the post-log phase (Wang et al., 2001), presumably because cells are starved at this growing phase. Thus, it has been unclear whether mitophagy is induced at the post-log phase through some specific mechanism or simply as a result of

cellular starvation. The specific requirement of Ylr356w for mitophagy primarily at the post-log phase suggests that there are some differences between the pathways of mitophagy induced during starvation versus post-log phase growth. Because only a fraction of the total mitochondrial pool is degraded by mitophagy at the post-log phase (compare full-length Om45-GFP and the processed GFP band in Figure 2.11.E, WT), it is reasonable to propose that aged or damaged mitochondria are selected for degradation. We propose that Ylr356w may contribute to this selection process, although future experiments will be needed to confirm this hypothesis.

2.6 Figures

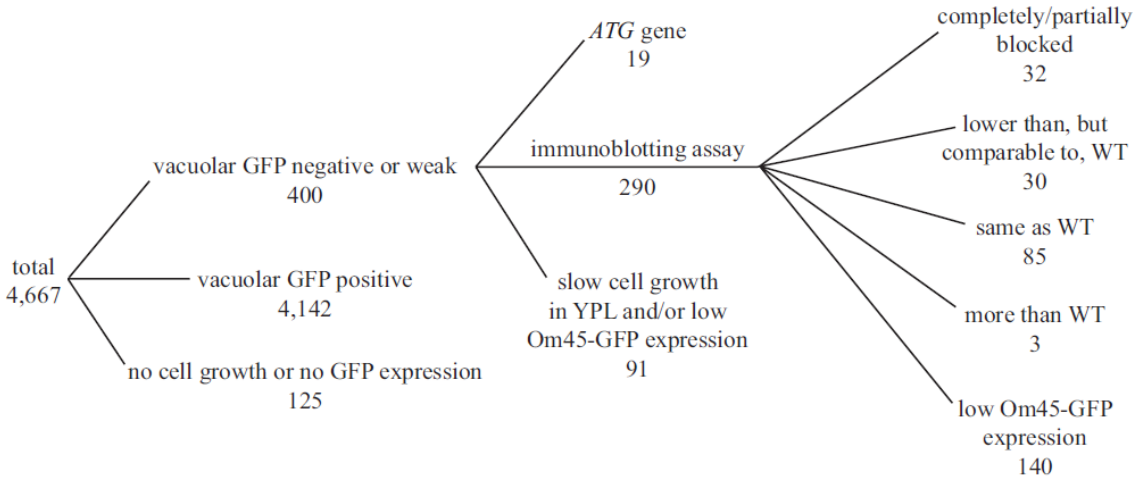

Figure 2.1 Schematic diagram of the mitophagy screen and the resulting number of mutants

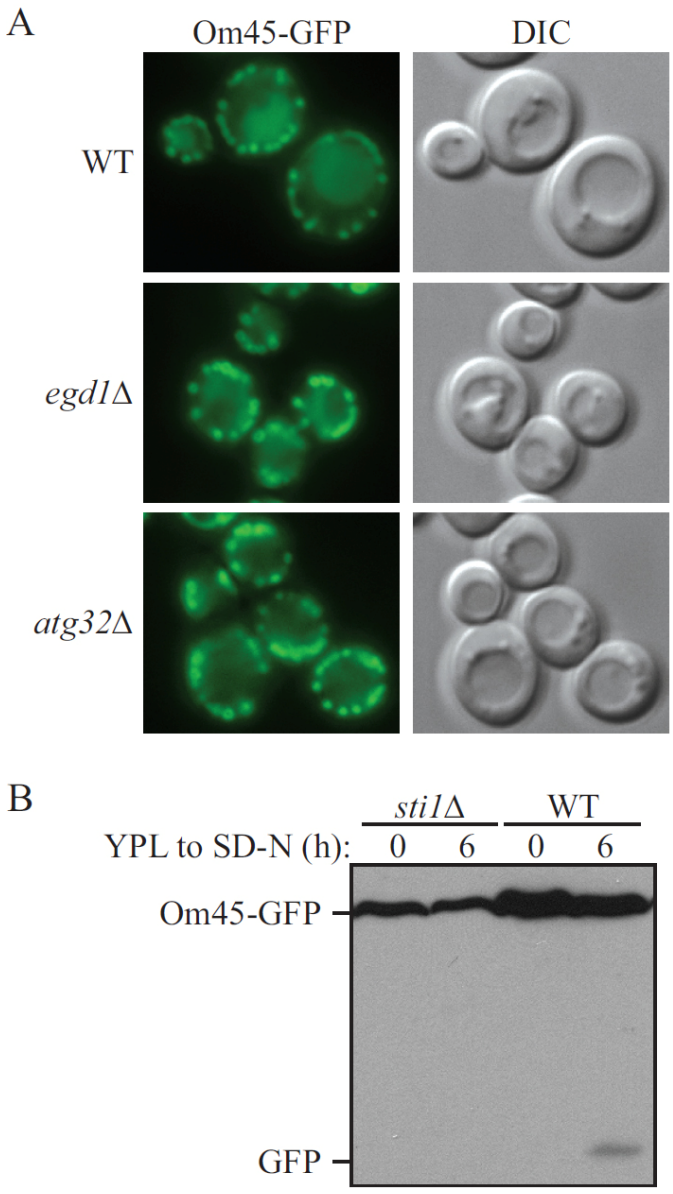

Figure 2.2 Examples of fluorescence microscopy and Om45-GFP processing from the mitophagy screen

(A) Wild-type (WT; BY4742) and knockout strains expressing Om45-GFP were cultured in YPL medium for three days to allow growth to the post-log phase, and were then observed for vacuolar GFP fluorescence. The wild-type strain showed a clear level of vacuolar GFP, *egd1*Δ showed a very weak vacuolar GFP signal and *atg32*Δ showed no vacuolar GFP signal. (B) Wild-type and *sti1*Δ strains expressing Om45-GFP were cultured in YPL medium for 12 h and then starved in SD-N for 6 h. The cell lysates equivalent to A_{600} = 0.2 units of cells were subjected to immunoblot analysis with anti-YFP antibody. Although no processed GFP was observed in the *sti1*Δ strain after 6 h starvation, we cannot conclude whether it is the result of a defect in mitophagy or a low level of Om45-GFP expression.

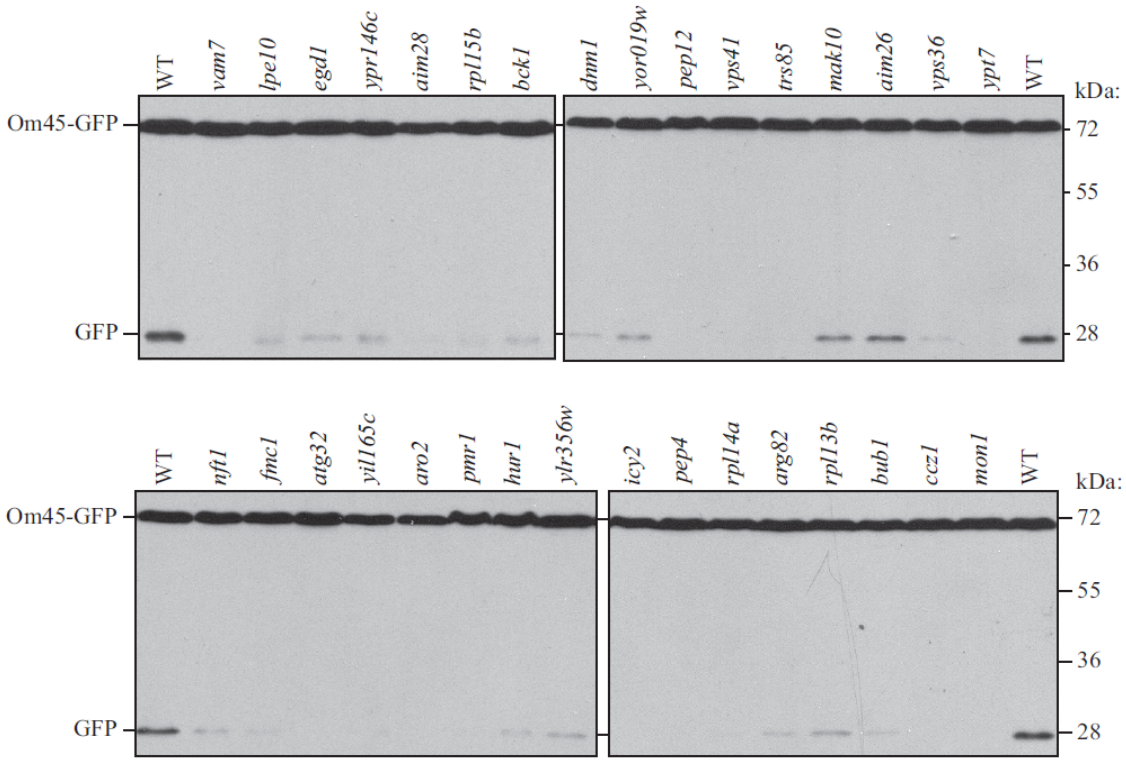

Figure 2.3 Screen for defects in mitophagy
Wild-type (WT; BY4742) and the indicated mutant strains expressing Om45-GFP were cultured in YPL medium for 12 h and then starved in SD-N for 6 h. The cell lysates equivalent to A_{600} = 0.2 units of cells were subjected to immunoblot analysis with anti-YFP antibody. The position of full-length Om45-GFP and free GFP are indicated.

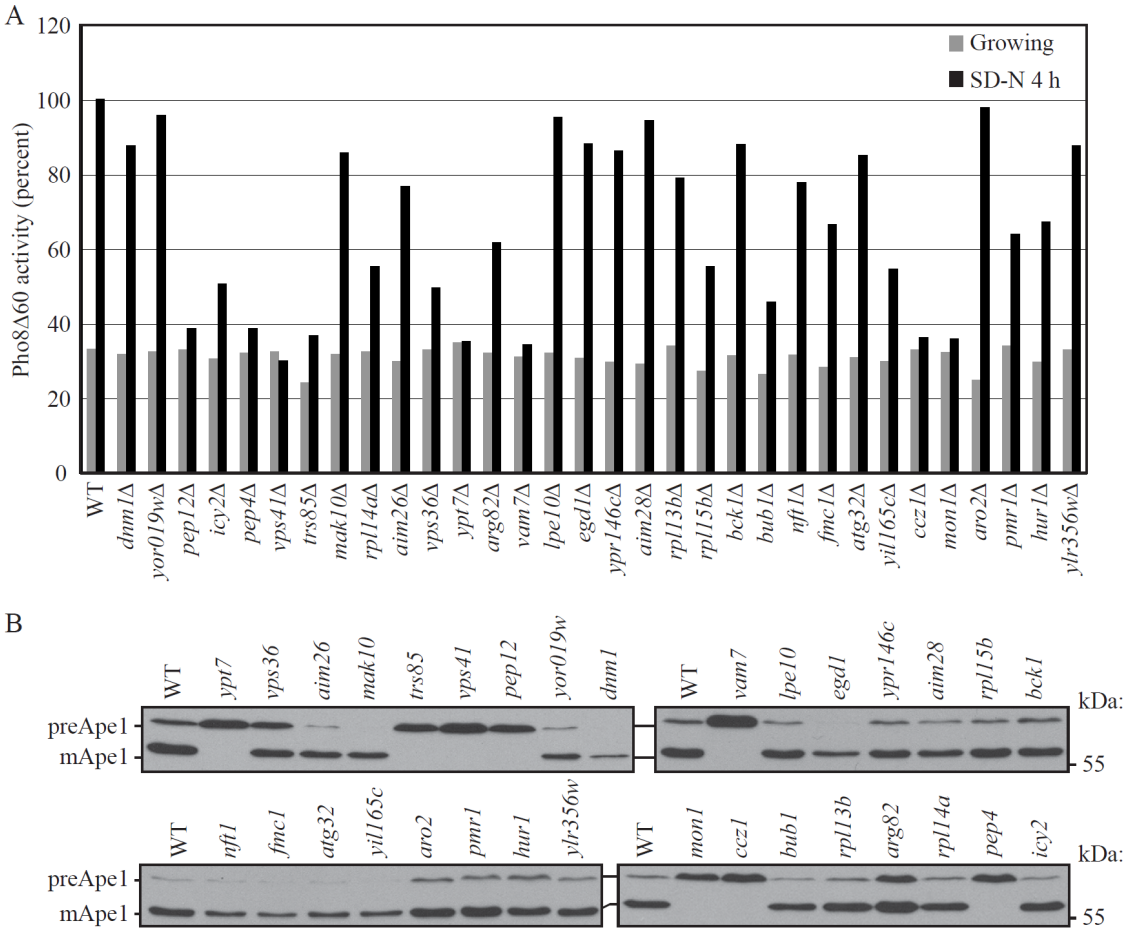

Figure 2.4 Screen for defects in macroautophagy and the Cvt pathway
(A) Wild-type (WT; BY4742) and the indicated mutant strains expressing Pho8Δ60 were grown in YPD and shifted to SD-N for 4 h. Samples were collected and protein extracts assayed for Pho8Δ60 activity. The value for the wild-type strain was set to 100% and the other values were normalized.
(B) Wild-type and the indicated mutant strains were cultured in YPD medium and analyzed for prApe1 maturation by immunoblotting to monitor the Cvt pathway during vegetative growth. The positions of precursor and mature Ape1 are indicated.

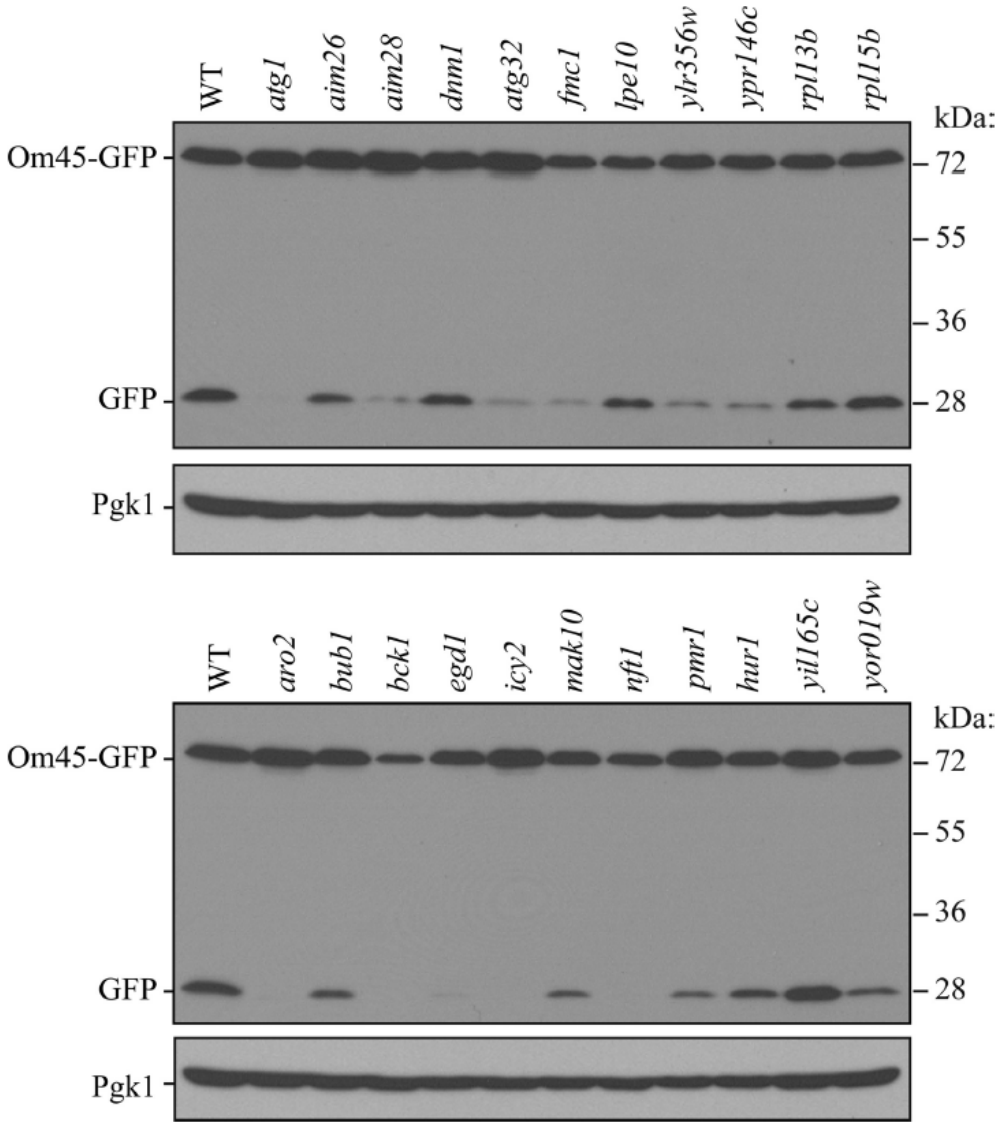

Figure 2.5 Om45-GFP processing analysis of novel mutants
Wild-type (WT; TKYM22) and the indicated mutant strains expressing Om45-GFP were cultured in YPL medium for 12 h and then starved in SD-N for 6 h. The cell lysates equivalent to A_{600} = 0.2 units of cells were subjected to immunoblot analysis with anti-YFP or anti-Pgk1 (loading control) antibodies or antiserum, respectively.

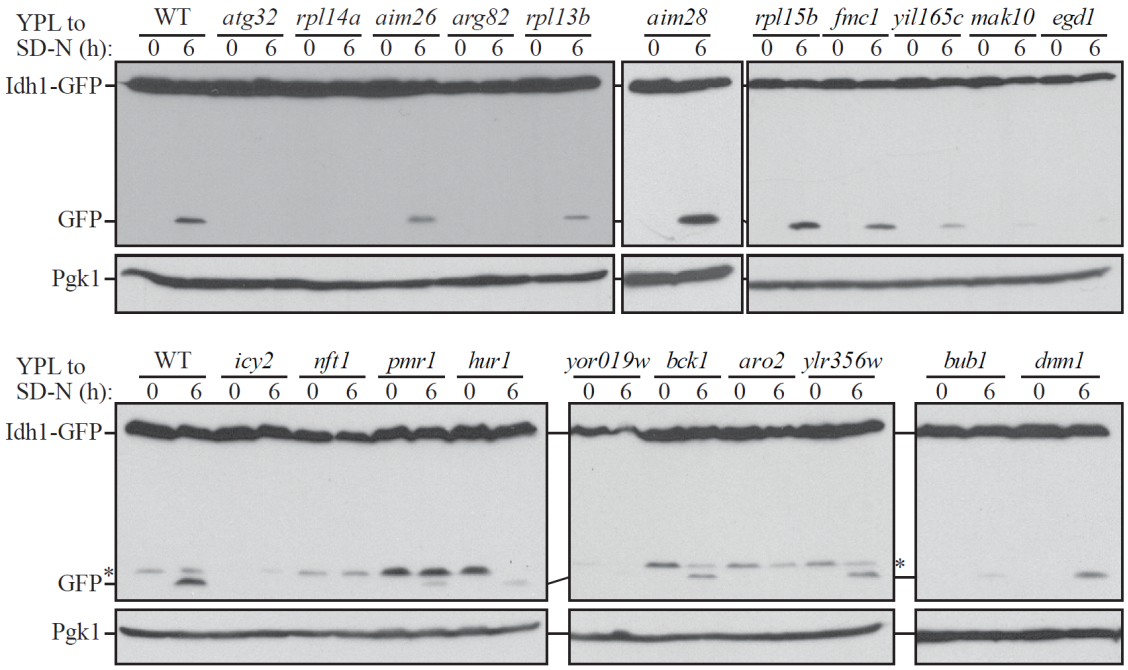

Figure 2.6 Idh1-GFP processing analysis for novel mutants
Wild-type (WT; BY4742) and the indicated mutant strains expressing Idh1-GFP were cultured in YPL medium for 12 h and then starved in SD-N for 6 h. The cell lysates equivalent to A_{600} = 0.2 units of cells were subjected to immunoblot analysis with anti-YFP antibody and anti-Pgk1 antiserum as a loading control. The asterisks indicate non-specific bands that result from repeated use of the anti-YFP antibody.

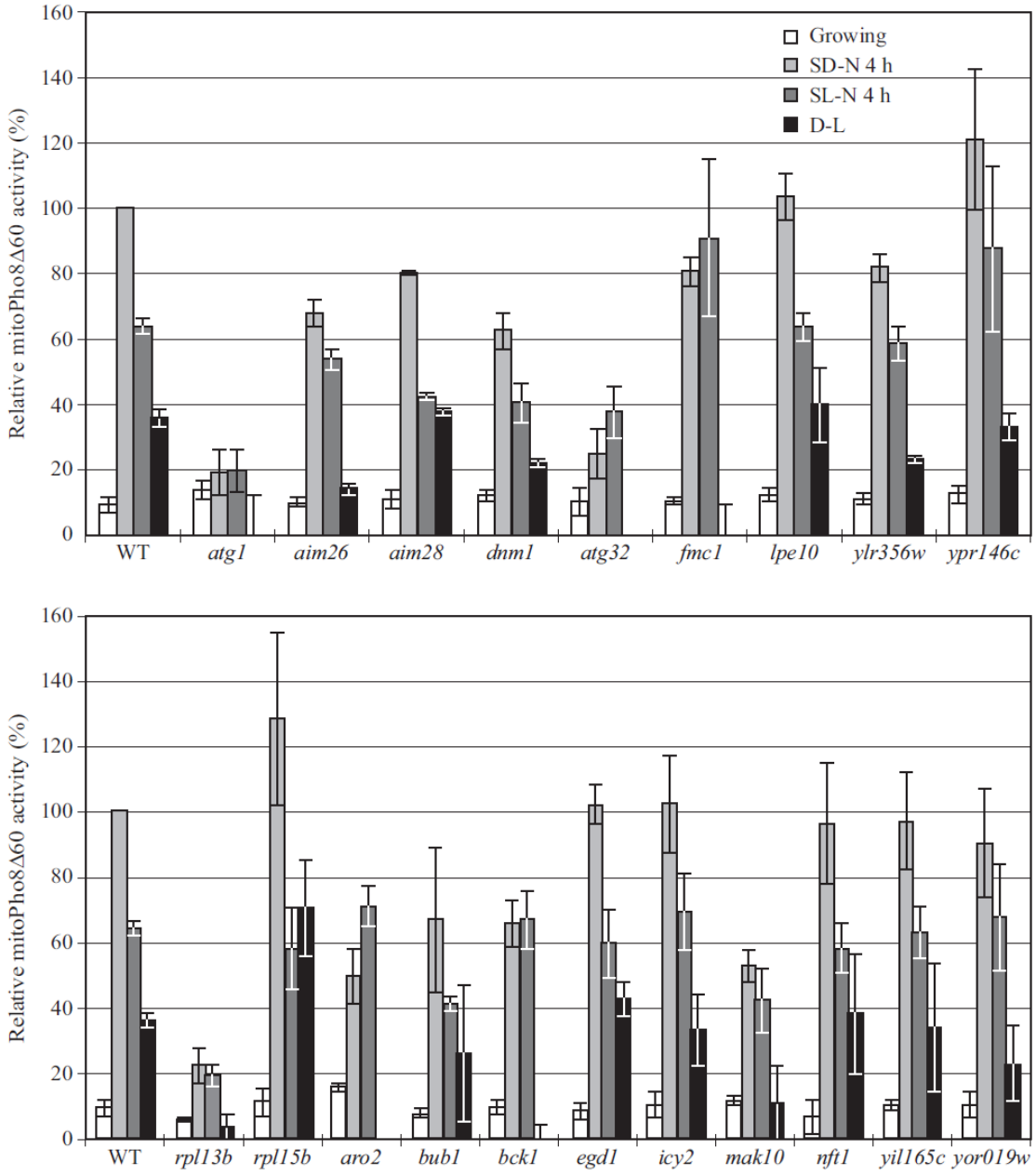

Figure 2.7 MitoPho8Δ60 analysis of novel mutants
Wild-type (WT; KWY20) and the indicated mutant strains expressing mitoPho8Δ60 were grown in YPL and shifted to SD-N and SL-N for 4 h. Samples were collected and protein extracts assayed for mitoPho8Δ60 activity. The value for the wild-type strain was set to 100% and the other values were normalized. Values lower than zero are depicted as zero.

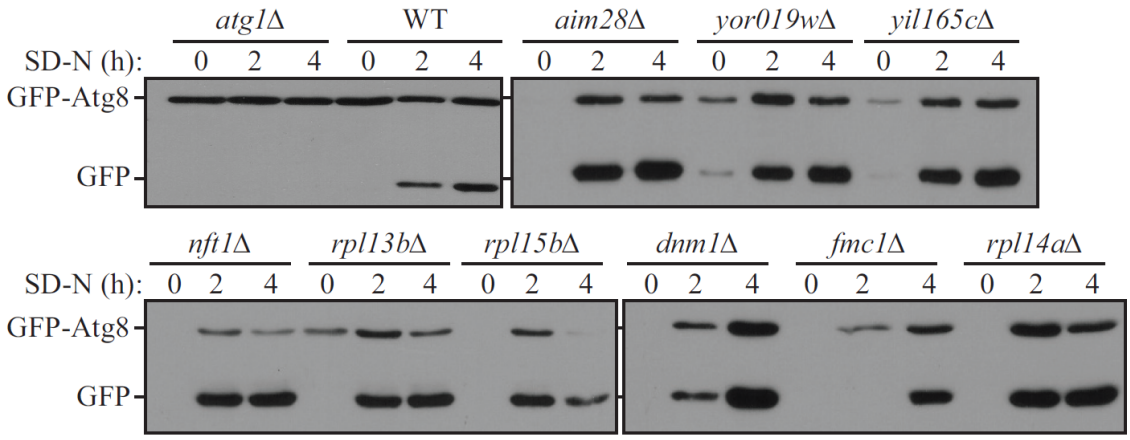

Figure 2.8 GFP-Atg8 processing analysis for novel mutants
Wild-type (WT, BY4742) and the indicated mutant strains expressing GFP-Atg8 were cultured in YPD medium to mid-log phase and then starved in SD-N for 2 and 4 h. The cell lysates equivalent to A_{600} = 0.2 units of cells were subjected to immunoblot analysis with anti-YFP antibody.

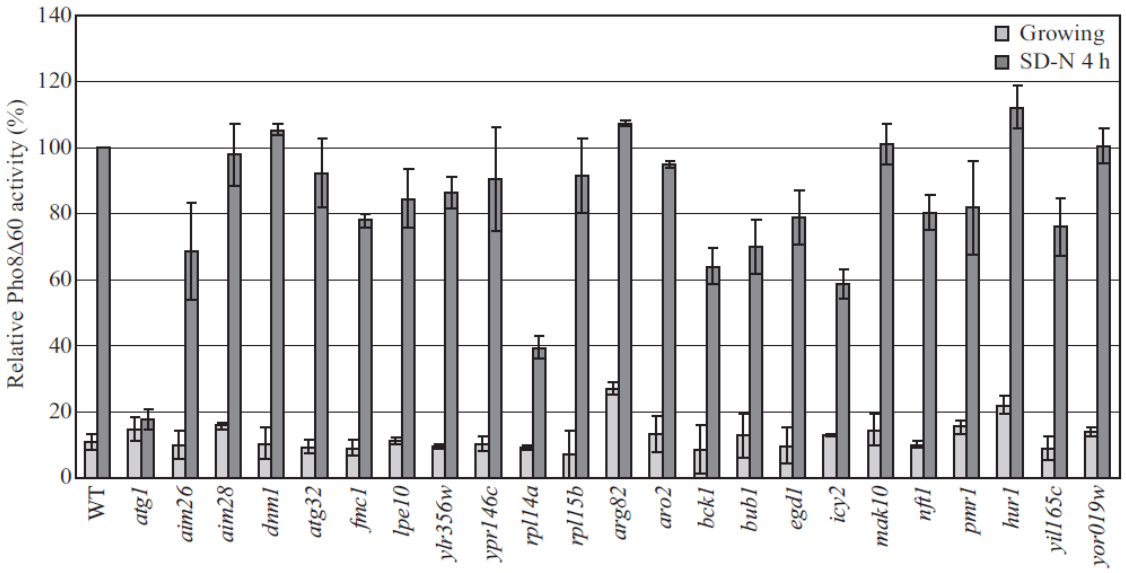

Figure 2.9 Pho8Δ60 analysis for novel mutants
Wild-type (WT; WLY176) and the indicated mutant strains expressing Pho8Δ60 were grown in YPD and shifted to SD-N for 4 h. Samples were collected and protein extracts assayed for Pho8Δ60 activity. The value for the wild-type strain was set to 100% and the other values were normalized.

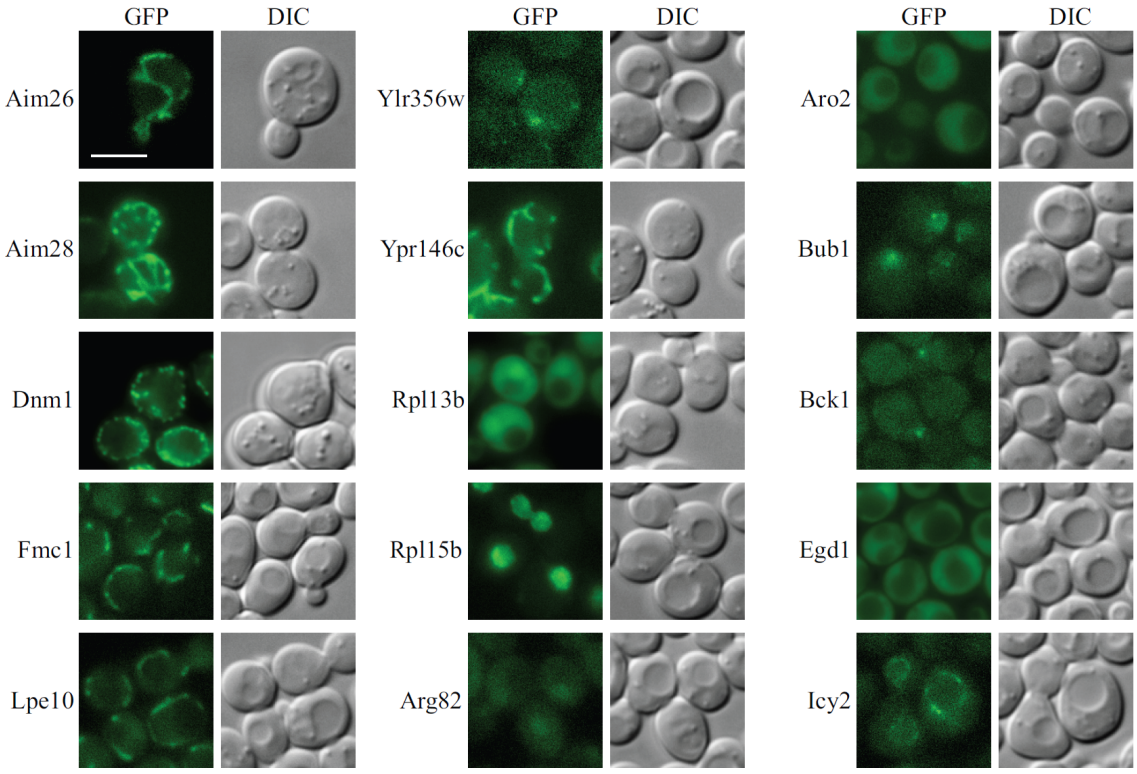

Figure 2.10 Subcellular localization of the mitophagy-related proteins identified from the screen

Each protein was chromosomally tagged with GFP and observed with fluorescence microscopy as described in Materials and Methods. DIC, differential interference contrast.

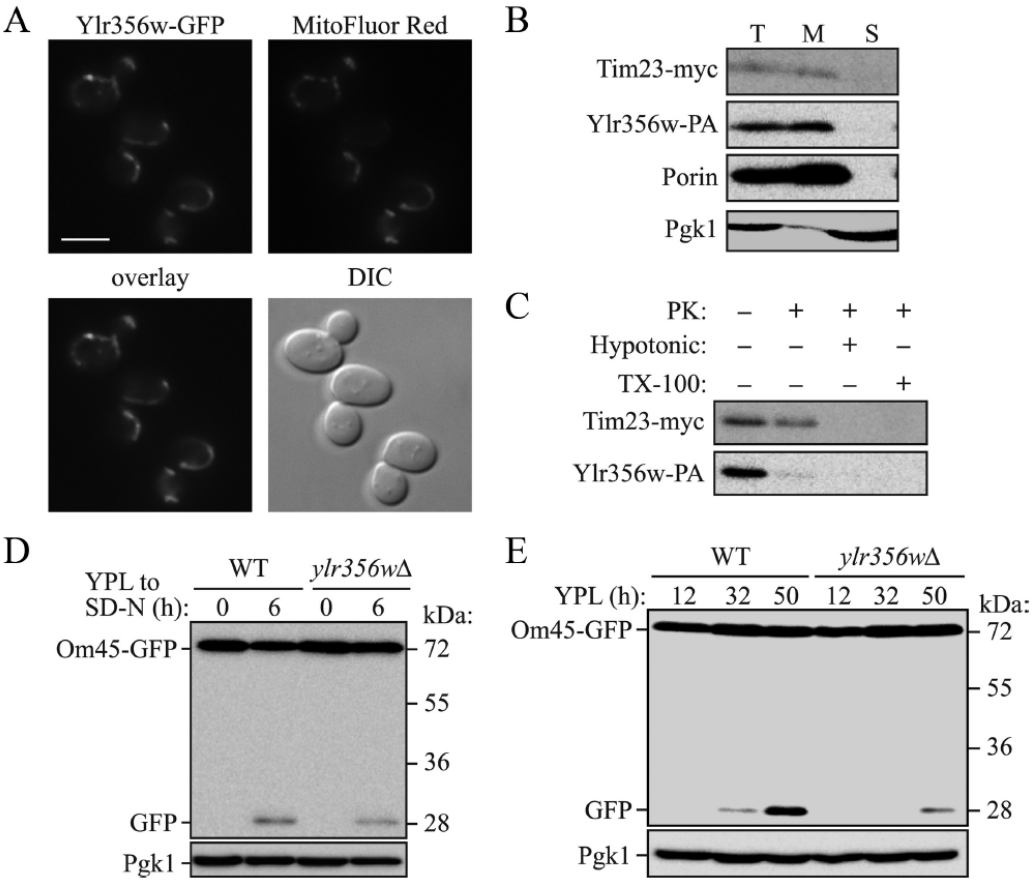

Figure 2.11 Characterization of Ylr356w

(A) A strain expressing Ylr356w-GFP under the control of the *GAL1* promoter (TKYM201) was cultured in YPD medium to mid-log phase and shifted to YPGal medium for 4 h. Cells were labeled with the mitochondrial marker MitoFluor Red 589. The localization of GFP and MitoFluor Red were visualized by fluorescence microscopy. DIC, differential interference contrast. Bar, 5 μm.

(B) Mitochondria were purified from a strain expressing chromosomally tagged Tim23-myc and Ylr356w-PA as described in Materials and Methods. Equal amounts of the total cell homogenate (T), mitochondrial (M) and supernatant (S) fractions were loaded and detected with antibodies to myc and porin, a purified antibody that recognizes PA, or antiserum to Pgk1.

(C) Isolated mitochondria were treated with proteinase K (PK) with or without hypotonic or Triton X-100 treatment. Samples were TCA precipitated and subjected to immunoblotting using the appropriate antibodies.

(D) Wild-type (WT; TKYM22) and *ylr356w*Δ strains expressing Om45-GFP were cultured in YPL medium for 12 h and then starved in SD-N for 6 h. The cell lysates equivalent to A_{600} = 0.2 units of cells were subjected to immunoblot analysis with anti-YFP and anti-Pgk1 (loading control) antibody or antiserum, respectively.

(E) Wild-type (WT; TKYM22) and *ylr356w*Δ strains expressing Om45-GFP were cultured in YPL medium for the indicated times. Cell lysates equivalent to A_{600} = 0.2 units of cells were subjected to immunoblot analysis with anti-YFP antibodies and anti-Pgk1 antiserum.

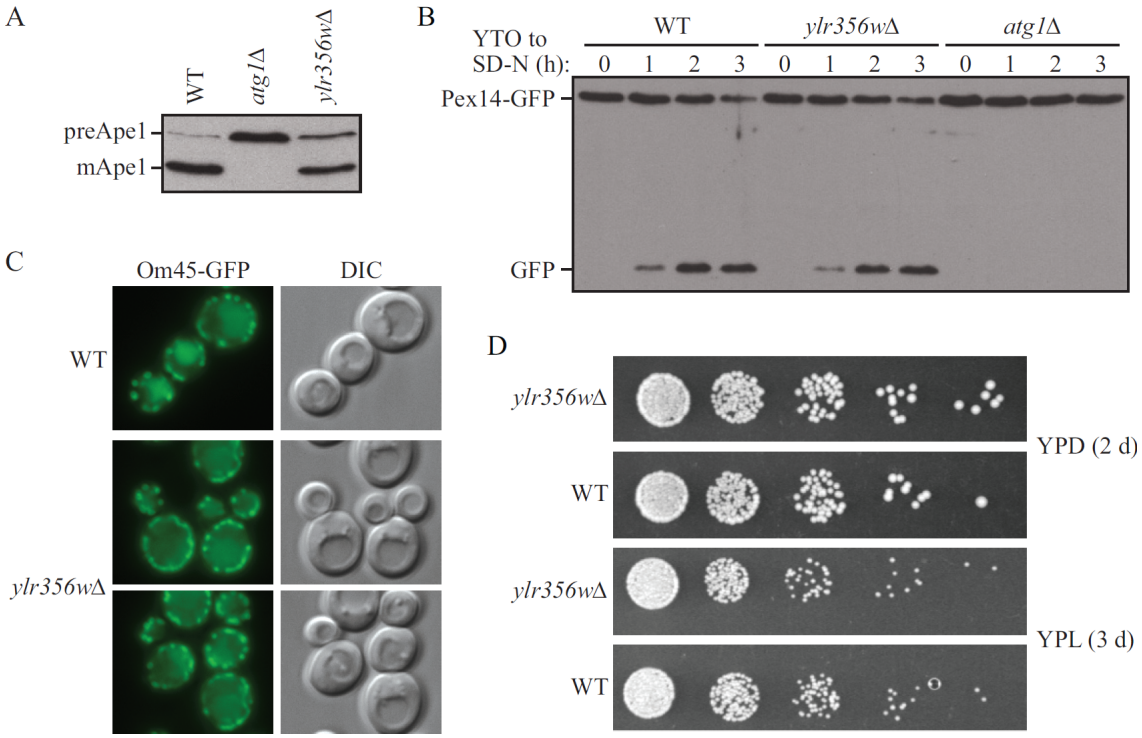

Figure 2.12 The Cvt pathway, pexophagy and cell growth are normal in the *ylr356w*Δ strain

(A) Wild-type (WT; SEY6210), *atg1*Δ, and *ylr356w*Δ strains were cultured in YPD medium and analyzed for prApe1 maturation by immunoblotting to monitor the Cvt pathway during vegetative growth. The positions of precursor and mature Ape1 are indicated.

(B) GFP was integrated at the *PEX14* locus in wild-type (SEY6210), *atg1*Δ, and *ylr356w*Δ strains. Cells were grown in oleic acid-containing medium (YTO) for 19 h, then shifted to SD-N for the indicated times. Samples were collected and analyzed by immunoblot with antibody to YFP.

(C) Wild-type (SEY6210) and *ylr356w*Δ strains expressing Om45-GFP were cultured in YPL medium for three days. The localization of GFP was visualized by fluorescence microscopy. DIC, differential interference contrast.

(D) Wild-type (WT; SEY6210), *ylr356w*Δ and *icy2*Δ strains were cultured in YPD medium to mid-log phase and washed in sterile water. Equal numbers of cells suspended in sterile water were inoculated on YPD and YPL plates. Cells were diluted 1:5 in each step from left to right.

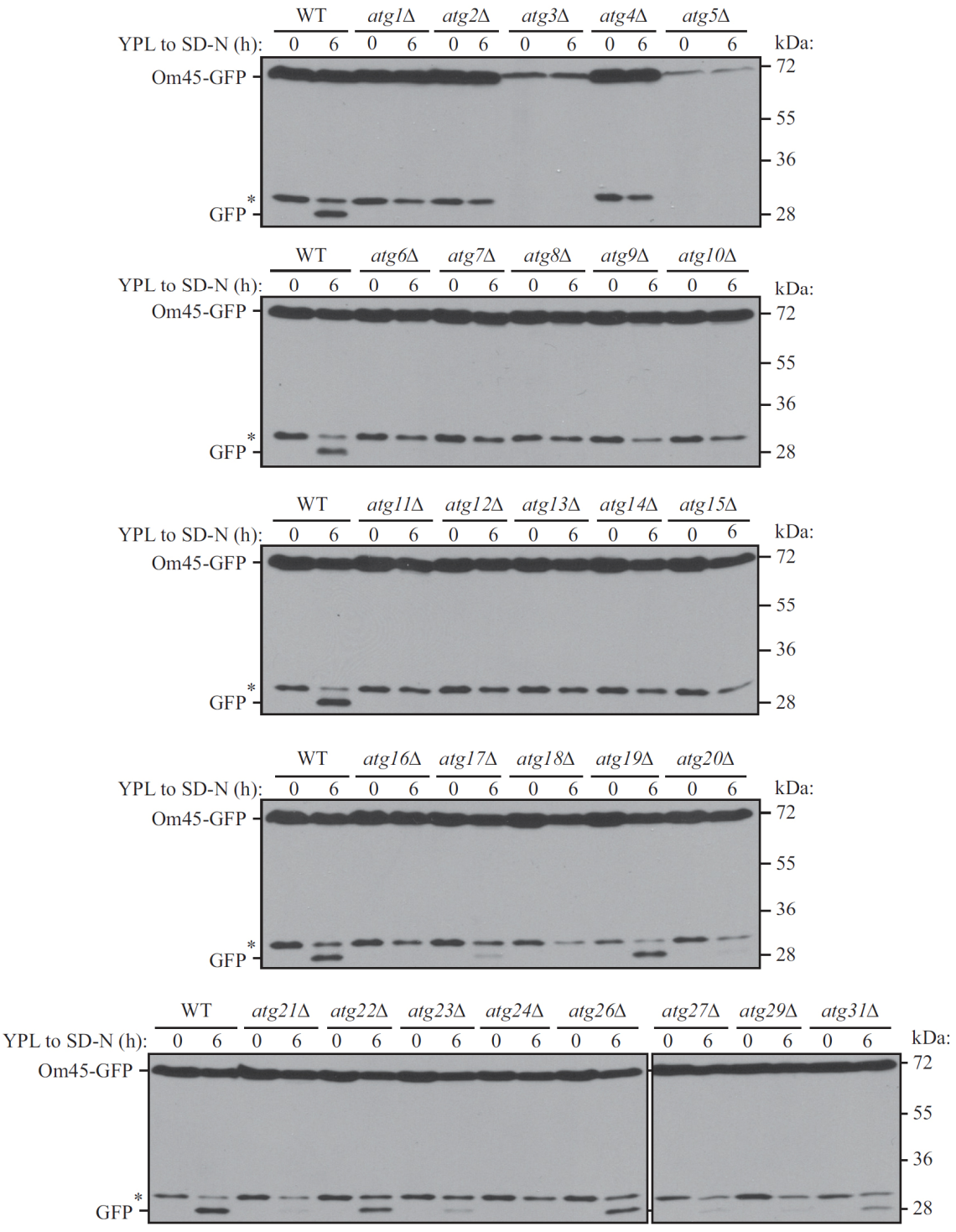

Figure 2.13 Analysis of mitophagy in the *atg* mutant strains
The wild type (WT; TKYM22) and the indicated *atg* mutant strains expressing Om45-GFP were cultured in YPL medium for 12 h and then starved in SD-N for 6 h. The cell lysates equivalent to A_{600} = 0.2 units of cells were subjected to immunoblot analysis with anti-YFP antibodies.

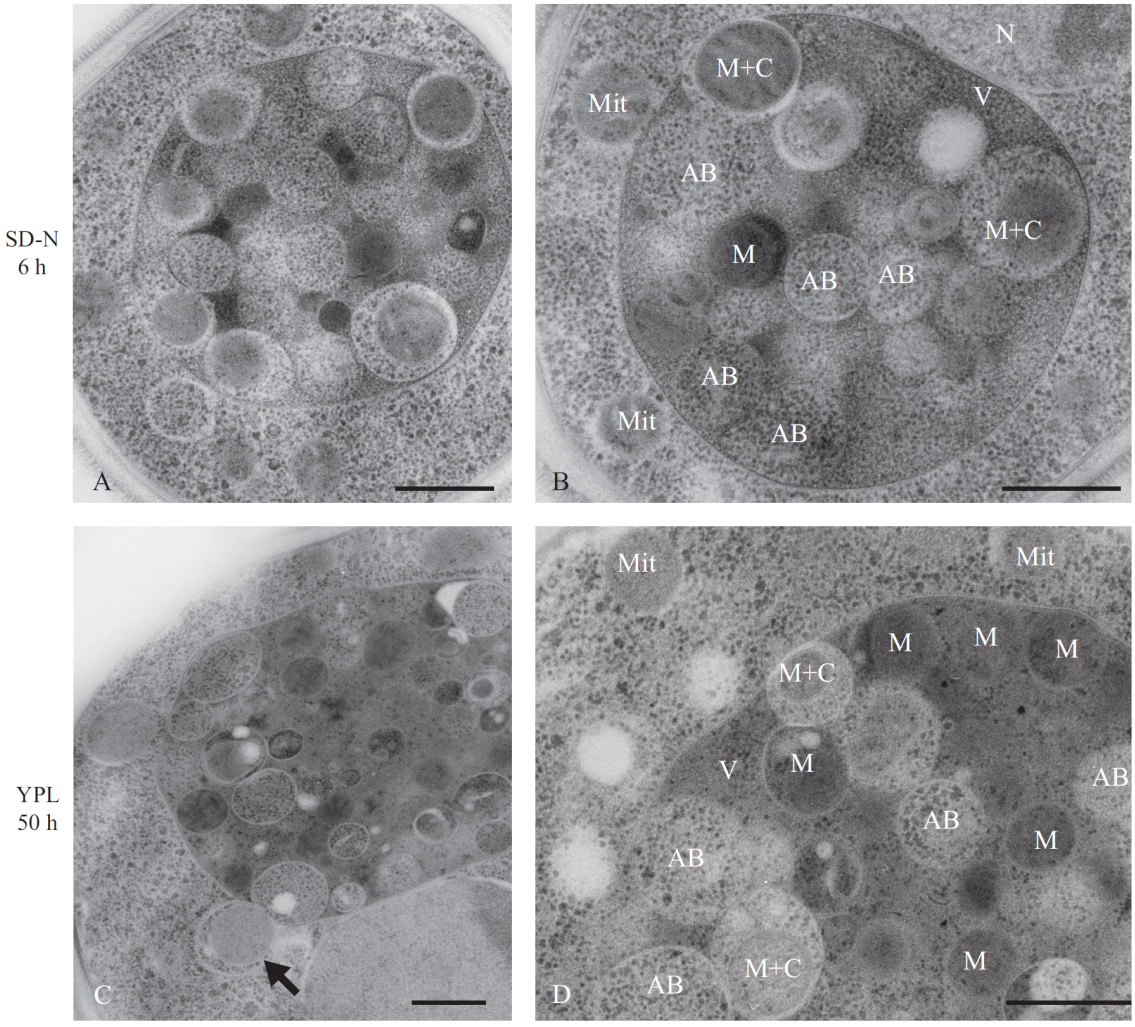

Figure 2.14 Electron microscopy of mitophagy during starvation and at post-log phase
The *pep4*Δ strain was cultured in YPL medium to growing phase, then shifted to SD-N and cultured for 6 h (A and B) or was cultured in YPL medium to stationary phase (for 50 h; C and D). Cells were prepared for electron microscopy using freeze substitution. The arrow marks an example of autophagosome containing a mitochondria and cytosolic components. AB, autophagic body including cytosolic components; M, autophagic body including mitochondria only; M+C, autophagic body including mitochondria and cytosolic components; Mit, mitochondria in cytosol; V, vacuole; N, nucleus. Scale bar, 500 nm.

Chapter III
PROTEOLYTIC PROCESSING OF ATG32 BY THE MITOCHONDRIAL I-AAA PROTEASE YME1 REGULATES MITOPHAGY

This chapter is reprinted from Autophagy, Volume 9, Issue 11, Ke Wang, Meiyan Jin, Xu Liu and Daniel J. Klionsky, Proteolytic Processing of Atg32 by the Mitochondrial i-AAA Protease Yme1 Regulates Mitophagy, pg. 1828-1836, 2013, with minor modifications.

3.1 Abstract

Mitophagy, the autophagic removal of mitochondria, occurs through a highly selective mechanism. In the yeast *Saccharomyces cerevisiae*, the mitochondrial outer membrane protein Atg32 confers selectivity for mitochondria sequestration as a cargo by the autophagic machinery through its interaction with Atg11, a scaffold protein for selective types of autophagy. The activity of mitophagy in vivo must be tightly regulated considering that mitochondria are essential organelles that produce most of the cellular energy, but also generate reactive oxygen species that can be harmful to cell physiology. We found that Atg32 was proteolytically processed at its C terminus upon mitophagy induction. Adding an epitope tag to the C terminus of Atg32 interfered with its processing and caused a mitophagy defect, suggesting the processing is required for efficient mitophagy. Furthermore, we determined that the mitochondrial i-AAA protease Yme1 mediated Atg32 processing and was required for mitophagy. Finally, we found that the interaction between Atg32 and Atg11 was significantly weakened in *yme1*Δ cells. We propose that the processing of Atg32 by Yme1 acts as an important regulatory mechanism of cellular mitophagy activity.

3.2 Introduction

Mitophagy is the cellular process of autophagic degradation of mitochondria (Wang et al., 2011). The molecular mechanism and physiological significance of mitophagy have been extensively studied in recent years in both yeast and mammalian cells. And the importance of mitophagy as a primary mitochondrial quality control system has been gradually revealed.

Mitochondria are essential organelles, but they are costly to maintain. Oxidative phosphorylation inside mitochondria provides the cells with energy to support a variety of cellular activities, while reactive oxygen species, the inevitable byproduct of oxidative respiration, has the potential to cause severe damage to cellular components, with mitochondria themselves as the most vulnerable targets (Wallace, 2005). Mitochondrial damage and dysfunction have severe cellular consequences and are linked with neurodegenerative diseases and aging (Yen and Klionsky, 2008). Therefore, the amount and activity of mitochondria need to be tightly controlled, and excessive or damaged mitochondria need to be removed in a timely manner.

In fact, mitochondria have their own quality control systems including a protein degradation system (Tatsuta and Langer, 2008), a DNA repair system (Larsson and Clayton, 1995) and phospholipid hydroperoxide glutathione peroxidase that is protective against membrane-damaging lipid peroxidation (Arai et al., 1999). In particular, the highly conserved, intraorganellar proteolytic system conducts the surveillance of protein quality control within mitochondria. Molecular chaperones and energy-dependent proteases monitor the folding status of mitochondrial proteins and remove excess and damaged proteins (Tatsuta and Langer, 2008). A variety of ATP-dependent proteases are present in different subcompartments of the mitochondria, recognizing non-native polypeptides and triggering their proteolysis to peptides that are further degraded by oligopeptidases (Koppen and Langer, 2007).

Despite these mitochondrial quality control systems, autophagy has been recently demonstrated to play important roles in mitochondrial maintenance by delivering excess and damaged mitochondria to the vacuole/lysosome for degradation (Ashrafi and Schwarz, 2013). Autophagy is a conserved cellular pathway in which double-membrane phagophores that form in the cytosol have the capacity to sequester essentially any cellular component (Yorimitsu and Klionsky, 2005c). In fact, mitochondria were one of the first documented autophagic cargos (Clark, 1957). Recent studies in both yeast and mammals have greatly expanded our knowledge on the selective autophagic degradation of mitochondria, or mitophagy (Kanki and Klionsky, 2008; Kanki et al., 2009; Kurihara et al., 2012; Narendra et al., 2008; Narendra et al., 2010; Okamoto et al., 2009).

In mammalian cells, damaged mitochondria with disrupted membrane potential are selectively recognized and degraded by autophagy (Narendra et al., 2008). During this process, the E3 ubiquitin ligase PARK2/PARKIN is selectively recruited to damaged mitochondria to facilitate recognition by the autophagic machinery. In addition, during erythroid cell maturation, mitochondria are eliminated by autophagy when BNIP3L/Nix-dependent loss of membrane potential is induced (Sandoval et al., 2008). Mitochondria elimination is also observed during spermatogenesis to prevent paternal mitochondrial DNA transmission (Al Rawi et al., 2011). These studies demonstrated that mitophagy plays important roles in both cellular homeostasis and development.

In yeast, mitophagy has been characterized as a type of selective autophagy, similar to the cytoplasm-to-vacuole targeting (Cvt) pathway and pexophagy (Kanki and Klionsky, 2008). Mitophagy in yeast requires the scaffold protein Atg11 (Kanki and Klionsky, 2008; Mijaljica et al., 2012) and the receptor protein Atg32 (Kanki et al., 2009; Okamoto et al., 2009). Atg11 is the common scaffold protein for selective types of autophagy that links the cargo to the core autophagic machinery (Yorimitsu and Klionsky, 2005). In contrast, Atg32 is

specific for mitophagy; it is a mitochondrial outer membrane protein that confers selectivity for mitophagy through its interaction with Atg11 under mitophagy-inducing conditions (Kanki et al., 2009; Okamoto et al., 2009). Atg32 contains a single transmembrane domain with its N terminus facing the cytosol and the C terminus in the intermembrane space (IMS).

The N-terminal cytosolic domain of Atg32 mediates the interaction with Atg11 and is critical for mitophagy (Aoki et al., 2011). In contrast, two recent studies suggested that the C-terminal 117 amino acids in the IMS are dispensable for mitophagy (Aoki et al., 2011; Kondo-Okamoto et al., 2012). Kondo-Okamoto et al. reported that an Atg32 mutant engineered such that the N terminus is targeted to mitochondria is sufficient to promote mitophagy. Similarly, Aoki et al. (Aoki et al., 2011) reported that deletion of up to 100 amino acids of the C terminus of Atg32 caused no defect in mitophagy activity. These results demonstrated that the C-terminal 20 amino acids next to the transmembrane domain are important for the mitochondrial targeting of Atg32, while the majority of the C-terminal domain in the IMS is not needed for mitophagy.

Atg32 is phosphorylated at its N-terminal domain by an unknown kinase.(Aoki et al., 2011) This phosphorylation is required for mitophagy and is affected by Hog1 and Pbs2, which are involved in the osmoregulatory signal transduction cascade, suggesting that cytosolic factors contributes to the regulation of mitophagy by modifying Atg32. Considering that the IMS domain of Atg32 could be a potential module that can communicate with other proteins or sense physiological changes inside the organelle, we decided to explore the function of this domain.

We found that the C-terminal IMS domain of Atg32 needs to be removed for proper mitophagy activity. We observed that Atg32 undergoes a molecular mass shift upon mitophagy induction, caused by the processing of its C terminus. Blocking this processing caused a significant defect in mitophagy. We determined that the mitochondrial i-AAA

protease Yme1 is responsible for the proteolytic processing of Atg32, and that Yme1 activity is required for mitophagy. Our results suggest that mitophagy is regulated in part by factors inside mitochondria. In addition, since Yme1 is responsible for degradation of unfolded or misfolded mitochondrial gene products (Leonhard et al., 1999), these findings establish a link between mitophagy and other mitochondrial quality control systems.

3.3 Materials and methods

Strains and growth conditions

The yeast strains used in this study are listed in Table 3.1. Yeast cells were grown in rich medium (YPD; 1% yeast extract, 2% peptone, 2% glucose), lactate medium (YPL; 1% yeast extract, 2% peptone, 2% lactate), galactose medium (YPG; 1% yeast extract, 2% peptone, 2% galactose), synthetic minimal medium with glucose (SMD; 0.67% yeast nitrogen base, 2% glucose, amino acids, and vitamins), synthetic minimal medium with lactate (SML; 0.67% yeast nitrogen base, 2% lactate, amino acids, and vitamins) or synthetic minimal medium with galactose (SMG; 0.67% yeast nitrogen base, 2% galactose, amino acids, and vitamins). Starvation experiments were performed in synthetic minimal medium lacking nitrogen (SD-N; 0.17% yeast nitrogen base without amino acids, 2% glucose).

Table 3.1 Strains used in this study

Strain	Genotype	Source
KWY20	SEY6210 *pho8Δ::TRP1 pho13Δ::LEU2* pRS406-*ADH1-COX4-pho8Δ60*	*(Kanki et al., 2009a)*
KWY22	SEY6210 *pho8Δ::TRP1 pho13Δ::LEU2* pRS406-*ADH1-COX4-pho8Δ60 atg32Δ::KAN*	(Kanki et al., 2009a)
KWY90	SEY6210 *pho8Δ::KAN pho13Δ::Ble* pRS406-*ADH1-COX4-pho8Δ60*	This study
KWY100	SEY6210 *GAL1-TAP-ATG32::TRP1*	This study
KWY101	KWY100 *atg1Δ::HIS5 S.p.*	This study
KWY104	KWY100 *atg11Δ::LEU2*	This study
KWY110	KWY100 *ATG32-GFP::HIS3MX6*	This study

KWY111	SEY6210 *GAL1-GFP-ATG32::His3MX6*	This study
KWY113	KWY104 *oma1Δ::HIS5 S.p.*	This study
KWY114	KWY104 *yme1Δ::URA3*	This study
KWY115	KWY104 *pcp1Δ::HIS5 S.p.*	This study
KWY117	KWY104 *yta12Δ::URA3*	This study
KWY118	KWY100 *yme1Δ::HIS5 S.p.*	This study
KWY121	KWY90 *ATG32-GFP::HIS3MX6*	This study
KWY129	KWY100 *atg32Δ90::HIS5 S.p.*	This study
KWY134	KWY100 *YME1-GFP::HIS3MX6*	This study
KWY136	KWY20 *yme1Δ::HIS5 S.p.*	This study
KWY138	KWY20 *YME1-E541Q-GFP::HIS3MX6*	This study
KWY139	*ATG32p-TAP-ATG32*	This study
KWY140	*ATG32p-TAP-ATG32, yme1Δ::HIS5 S.p.*	This study
KWY141	KWY100 *YME1-E541Q-GFP::HIS3MX6*	This study
KWY142	SEY6210 *yme1Δ::HIS5 S.p.*	This study
KWY143	WLY176 *yme1Δ::HIS5 S.p.*	This study
KWY144	KWY100 *atg32Δ100::HIS5 S.p.*	This study
KWY145	KWY100 *atg32Δ117::HIS5 S.p.*	This study
KWY146	KWY100 *mgr1Δ::HIS5 S.p.*	This study
KWY147	KWY100 *mgr3Δ::HIS5 S.p*	This study
KWY148	KWY146 *mgr3Δ::LEU2*	This study
SEY6210	MATα *his3-Δ200 leu2-3,112 lys2-801 trp1-Δ901 ura3-52 suc2-Δ9 GAL*	(Robinson et al., 1988)
WLY176	SEY6210 *pho13Δ pho8Δ60*	(Kanki et al., 2009a)
WLY192	SEY6210 *pho13Δ pho8Δ60 atg1Δ::HIS5*	(Kanki et al., 2009a)

Plasmids and antibodies

The plasmids used to express PA-tagged Atg32 [pCuPA-Atg32(416)] and HA-tagged Atg11 [pCuHA-Atg11(414)] have been described previously (Kanki et al., 2009). Monoclonal anti-YFP antibody clone JL-8 (Clontech, 632381), monoclonal anti-HA antibody clone-HA7 (Sigma-Aldrich, H3663), an antibody that binds to protein A with high affinity (no longer commercially available) and anti-Ape1 antiserum (Klionsky et al., 1992), were used for immunoblotting. Anti-Pgk1 antiserum was a kind gift of Dr. Jeremy Thorner (University of California, Berkeley).

Assays for non-specific autophagy and mitophagy

For monitoring nonspecific autophagy, the alkaline phosphatase activity of Pho8Δ60

was carried out as described previously (Noda and Klionsky, 2008). To monitor mitophagy, the alkaline phosphatase activity of mitoPho8Δ60 was carried out as described previously (Kanki et al., 2009).

Fluorescence microscopy

Yeast cells expressing fluorescent protein-fused chimeras were grown to mid-log phase or starved in the indicated media. To label mitochondria, cells were incubated in medium containing 1 μM MitoTracker Red CMXRos (Molecular Probes/Invitrogen, M7512) at 30°C for 30 min. After being washed with medium, the cells were incubated in medium at 30°C for 30 to 60 min. Fluorescence microscopy observations were carried out as described previously (Monastyrska et al., 2008).

3.4 Results

Atg32 undergoes a starvation-dependent molecular mass shift

Mitophagy is induced when cells are cultured in medium using non-fermentable substrates such as lactate as the sole carbon source and then shifted to nitrogen starvation medium supplemented with glucose (Kanki and Klionsky, 2008). The mitochondrial outer membrane protein Atg32 is essential for this process, acting as the receptor protein that confers selectivity for mitophagy (Kanki et al., 2009; Okamoto et al., 2009). The protein level of endogenous Atg32 is low and therefore it is difficult to detect. Accordingly, we generated strains expressing N-terminal TAP tagged Atg32 under the control of the *GAL1* promoter as described previously (Puig et al., 2001). The protein level of Atg32 in this construct is greatly increased and the TAP tag allows sensitive detection of the protein by western blotting. Overexpression of N-terminal tagged Atg32 has previously been shown to be functional for mitophagy (Kanki et al., 2009). Nonetheless, we confirmed our results by also examining the

endogenous level of Atg32; expression of the Cre recombinase makes it possible to remove the *GAL1* promoter, leaving the N-terminal TAP tagged Atg32 under the control of its native promoter.

With the overexpression strain, we found that TAP-Atg32 generated a second band with faster migration upon mitophagy induction (Figure 3.1.A, arrowhead). The intensity of the upper band, corresponding to full-length Atg32, gradually decreased during starvation, while the lower band gradually increased, suggesting a precursor-product relationship. Considering that the TAP tag was added to the N terminus, we hypothesized that formation of the lower band might be caused by processing of the C-terminal region of Atg32. To test this hypothesis, we decided to make C-terminal truncations of Atg32 and monitor the gel migration of the mutated constructs. A previous study demonstrated that the C-terminal region of Atg32, consisting of 117 amino acids, is in the mitochondrial IMS (Okamoto et al., 2009). Accordingly, we generated Atg32 C-terminal truncations of 90, 100 or 117 amino acids and examined their migration patterns. No lower bands corresponding to a processed form of the truncated mutants was observed, suggesting that cleavage indeed occurs at the C terminus of Atg32 upon mitophagy induction (Figure 3.2).

Atg32 is degraded along with the part of the mitochondria during mitophagy (Kanki et al., 2009; Okamoto et al., 2009). Therefore, we decided to examine the two forms of Atg32 during mitophagy. In wild-type cells, both forms of Atg32 were undetectable by 4 h after mitophagy induction (Figure 3.1.B). However, in *atg1*Δ and *atg11*Δ cells, which are defective for mitophagy, the lower band accumulated relative to the full-length protein, suggesting the faster-migrating species of Atg32 is the form that participates in mitophagic degradation, whereas the slower-migrating form of Atg32 serves as a precursor that is processed under mitophagy-inducing conditions to generate the faster-migrating form. Both forms of Atg32 were eventually degraded, even in autophagy mutants. This loss of signal could be explained

by the fact that both autophagic and non-autophagic pathways are involved in Atg32 degradation, as previously reported (Okamoto et al., 2009).

Next, we decided to validate our data by examining processing of Atg32 expressed at the endogenous level. To do this, we generated a strain expressing endogenous promoter-driven TAP-tagged Atg32 by removing the *GAL1* promoter using the *cre-loxp* system as described previously (Puig et al., 2001). With this strain, a similar processed band was detected (Figure 3.1.C, arrowhead). The extent of processing was much weaker when Atg32 was expressed at the endogenous level, possibly reflecting a lower level of mitophagy induction (overexpression of Atg32 induces mitophagy; Kanki et al., 2009), and the fact that the level of mitochondrial turnover during mitophagy in a wild-type strain is relatively low, corresponding to a few percent of the total mitochondrial population. The processed band gradually accumulated upon shifting to glucose-containing medium lacking nitrogen, and then gradually degraded as starvation persisted, similar to what was observed with the overexpression strain.

Therefore, we conclude that the C terminus of Atg32 is proteolytically processed upon mitophagy induction, generating a form of the protein that is directly involved in mitophagy. Next, we decided to further explore the physiological meaning of this processing event.

C-terminal tagging of Atg32 blocks its processing and causes a mitophagy defect

A recent study reported that the C-terminal 100 amino acids of Atg32 are dispensable for mitophagy (Aoki et al., 2011). This agrees with our data, which indicate that the C terminus is processed under mitophagy-inducing conditions. Accordingly, we hypothesized that the C terminus of Atg32 may play a negative, regulatory role in mitophagy, and that this part of the protein needs to be removed for proper mitophagy activity.

Previously, we had noted that the addition of a GFP tag to the C terminus of Atg32

resulted in a mitophagy defect (our unpublished data). Therefore, we decided to examine the effect of C-terminal tagging on processing of Atg32. When GFP was fused at the C terminus, there was a complete block in processing (Figure 3.3.A). When TAP-Atg32 was chromosomally tagged with a GFP tag at its C terminus, it remained as a single band upon mitophagy induction, in contrast to the C-terminal untagged TAP-Atg32 that generated the processed band (Figure 3.3.A, arrowhead).

Therefore, we next tested whether mitophagy was affected by C-terminal tagging of Atg32. We used the mitoPho8Δ60 assay to detect mitophagy activity. *PHO8* encodes a vacuolar alkaline phosphatase, and its delivery into the vacuole through the secretory pathway is dependent on its N-terminal transmembrane domain (Klionsky and Emr, 1989). Pho8Δ60 is a truncated form that lacks the 60 N-terminal amino acid residues including the transmembrane domain; this altered protein is unable to enter the endoplasmic reticulum, remains in the cytosol and is delivered into the vacuole only through bulk autophagy (Noda et al., 1995). The mitoPho8Δ60 construct is a modified version of Pho8Δ60 that allows the quantitative measurement of mitophagy activity. If *PHO8Δ60* is fused with a mitochondrial targeting sequence, the encoded protein is specifically localized to mitochondria, and the ensuing alkaline phosphatase activity becomes an indicator of mitophagy (Kanki et al., 2009).

During a shift from rich medium containing lactate (YPL) to glucose-containing medium lacking nitrogen (SD-N) for 2, 4 and 6 h, wild-type cells showed a time-dependent increase of mitoPho8Δ60-dependent alkaline phosphatase activity, indicating a robust induction of mitophagy (Figure 3.3.B, white bars). The mitophagy level in the *atg32*Δ strain showed a minor increase over time, and represented the background level (Figure 3.3.B, gray bars). Notably, there was not a complete block of mitophagy in the *atg32*Δ strain because non-specific autophagy can also target a small portion of mitochondria for degradation (Kanki et al., 2009). In cells harboring Atg32 that was C-terminally tagged with GFP, the

mitoPho8Δ60 activity was significantly reduced, being only slightly above the background level of the *atg32*Δ strain (Figure 3.3.B, black bars), suggesting a strong defect in mitophagy. Therefore, C-terminal tagging of Atg32 interferes with its function in mitophagy.

To exclude the possibility that C-terminally tagged Atg32 was not properly targeted to mitochondria, we checked the localization of Atg32-GFP by fluorescence microscopy. Since the protein level of endogenous Atg32 is too low to be observed by microscopy, we carried out this experiment with overexpressed Atg32 under the control of the *GAL1* promoter. With 8 h culturing in rich medium containing galactose (YPG), both N-terminally tagged and C-terminally tagged Atg32 were localized to mitochondria as determined by colocalization with the mitochondrial marker MitoTracker Red (Figure 3.3.C). This finding agrees with a previous report studying the topology of Atg32, which used both N-terminal 3HA- and C-terminal 2HA-tagged Atg32. In that case, both forms of Atg32 showed the expected localization and topology on mitochondria (Okamoto et al., 2009), suggesting that a C-terminal tag does not interfere with localization.

Taken together, these results support the conclusion that C-terminal tagging blocks Atg32 processing and affects its function in mitophagy, thus suggesting that the C-terminal region of Atg32 needs to be processed for proper mitophagy activity.

The mitochondrial i-AAA protease Yme1 mediates the processing of Atg32

To extend our analysis, we decided to investigate the mechanism of Atg32 processing. Considering the location of the C terminus in the IMS, we hypothesized that the processing could be mediated by a mitochondrial protease, and clearly one that had access to this subcompartment (i.e., not one present within the matrix). Therefore, we initially tested the effect of four mitochondrial proteases of the inner membrane, Oma1, Yta12, Pcp1 and Yme1 (Koppen and Langer, 2007) on Atg32 processing by deleting each corresponding gene. We

found that the deletion of *YME1*, but not the genes encoding the other proteases caused a complete block in Atg32 processing (Figure 3.4), suggesting that Yme1 is the protease that mediates the proteolytic cleavage of Atg32.

To confirm the role of Yme1 in Atg32 processing, we further compared the processing of TAP-Atg32 in a *yme1*Δ strain with that in an isogenic wild-type strain over time (Figure 3.5.A). Although we could observe the processed form of Atg32 increase over the time course of mitophagy induction in wild-type cells, it was completely missing in the *yme1*Δ strain. In addition, the unprocessed Atg32 accumulated at a much higher level in the *yme1*Δ strain compared with the wild type, further suggesting a defect in processing, similar to the results with the *atg1*Δ and *atg11*Δ mutants (Figure 3.1.B).

Yme1 is a mitochondrial i-AAA protease that functions in mitochondrial quality control by degrading unfolded or misfolded mitochondrial proteins (Gerdes et al., 2012). Yme1 has been reported to be the catalytic subunit of a protease complex with two other components, Mgr1 and Mgr3 (Dunn et al., 2008). Next, we tested whether these two other components are also required for Atg32 processing (Figure 3.6). Compared with the *yme1*Δ strain, no apparent defect of Atg32 processing was observed in *mgr1*Δ, *mgr3*Δ or *mgr1*Δ *mgr3*Δ strains. Mgr1 and Mgr3 function as adaptors that facilitate substrate binding to Yme1, but are not critical for its function (Dunn et al., 2008).

To further test whether the processing is dependent on the protease activity of Yme1, we generated a strain expressing a protease inactive mutant version harboring a point mutation, E541Q, in the proteolytic center (Graef et al., 2007). This version of Yme1 was also tagged with GFP at its C terminus so that the protein level could be detected by western blotting. In cells expressing chromosomally GFP tagged wild-type Yme1, Atg32 was properly processed in response to a shift to mitophagy-inducing conditions (Figure 3.5.B). This result also demonstrated that in the case of Yme1, C-terminal tagging had no affect on

its function. However, in cells expressing chromosomally GFP-tagged Yme1^{E541Q}, the processing of Atg32 was completely blocked, comparable to *yme1*Δ cells, while the protein level of Yme1^{E541Q} was comparable to the wild-type Yme1.

This result suggests that the processing of Atg32 by Yme1 depends on Yme1 protease activity, and implies that Atg32 could be a direct substrate of Yme1. Accordingly, we examined whether Atg32 directly interacts with Yme1. To test this possibility, we expressed PA-Atg32 in strains with Yme1 chromosomally tagged with GFP and performed protein A (PA) affinity isolation with immunoglobin G (IgG)-Sepharose (Figure 3.5.C). PA-Atg32 coprecipitated Yme1-GFP in both growing conditions (minimal medium with lactate, SML) and in SD-N, suggesting that Atg32 interacts with Yme1 in vivo.

Next, to test whether Yme1 is required for Atg32 processing at the endogenous level, we compared the processing of endogenous promoter-driven TAP-tagged Atg32 in wild-type and *yme1*Δ strains (Figure 3.5.D). Similar to the results with overexpressed Atg32, the *yme1*Δ strain displayed a complete block of Atg32 processing, suggesting that Yme1 is required for Atg32 processing at its physiological level. Taken together, these results demonstrated that the mitochondrial i-AAA protease Yme1 directly mediates Atg32 processing in response to mitophagy-inducing conditions.

Yme1 is specifically required for mitophagy

As C-terminal processing is required for mitophagy, and Yme1 mediates the processing, we next tested whether Yme1 is involved in mitophagy. We used the previously described mitoPho8Δ60 assay to monitor mitophagy activity. As expected, the wild-type strain showed a gradual increase in mitoPho8Δ60 activity in response to a shift to SD-N (Figure 3.7.A). In contrast, the *yme1*Δ strain displayed a significant block in mitophagy activity (~50% decrease at 6 h compared to wild type; however, if we account for the

background level of activity represented by the *atg32*Δ strain, the absence of Yme1 caused an ~70% reduction).

Since the protease activity of Yme1 is critical in its function of Atg32 processing, we further tested whether the mitophagy defect seen in the *yme1*Δ strain is dependent on its protease activity (Figure 3.7.B). The Yme1 protease inactive mutant (E541Q) displayed a mitophagy defect comparable to that of *yme1*Δ as determined by the mitoPho8Δ60 assay. Therefore, these results demonstrated that proteolytically active Yme1 is required for mitophagy.

Next, we decided to test whether Yme1 is involved in other autophagic pathways, or is confined to a role in mitophagy. The Pho8Δ60 assay is used to monitor the activity of non-specific autophagy. This assay is similar to that used for monitoring mitophagy. In this case, Pho8Δ60 remains cytosolic so that the Pho8Δ60-dependent alkaline phosphatase activity represents the level of non-specific autophagy.(Klionsky, 2007) The wild-type strain showed increased Pho8Δ60-dependent alkaline phosphatase activity following a shift from rich medium to SD-N, whereas the *atg1*Δ strain maintained a background level of activity (**Figure 3.7.C**). The *yme1*Δ strain displayed a level of autophagy activity comparable to wild type, demonstrating that Yme1 is not required for nonspecific autophagy.

The Cvt pathway is a type of selective autophagy that has been extensively characterized. This pathway is used for the delivery of the precursor form of the resident hydrolase Ape1 (prApe1) to the vacuole (Lynch-Day and Klionsky, 2010). We monitored the maturation of prApe1 in wild-type, *atg1*Δ and *yme1*Δ strains. The wild-type strain showed a substantial degree of maturation of prApe1 under vegetative growing conditions, while the *atg1*Δ strain was completely defective for prApe1 maturation (Figure 3.7.D). The *yme1*Δ strain displayed normal prApe1 maturation comparable to that of wild type, suggesting that Yme1 is not required for the Cvt pathway. Therefore, these results indicate that Yme1 is

specifically required for mitophagy, but not nonspecific autophagy or the Cvt pathway.

Yme1 is required for Atg32 processing and mitophagy in a post-log phase culture

In addition to nitrogen starvation in a glucose-containing medium, mitophagy can also be induced in a post-log phase culture (Kanki and Klionsky, 2008; Okamoto et al., 2009). To test whether Atg32 processing is also occurring during post-log phase growth, we examined processing in the TAP-Atg32 overexpression strain cultured in YPG to post-log phase (Figure 3.8.A). In the wild-type strain a processed form of Atg32 was observed when cells were cultured for more than 12 h. Similar to the results in SD-N, Yme1 was required for this process since the *yme1*Δ strain showed a complete block in processing. Next, to test whether Yme1 and its protease activity are required for mitophagy induced at post-log phase, we used the mitoPho8Δ60 assay to monitor mitophagy activity (Figure 3.8.B). The wild-type control strain displayed an increase in mitoPho8Δ60-dependent alkaline phosphatase activity when cultured to post-log phase. In contrast, the *yme1*Δ strain and the $Yme1^{E541Q}$-expressing strain showed a significant defect in mitophagy that was comparable to that observed during starvation-induced mitophagy. Therefore, Yme1 is also required for Atg32 processing and mitophagy during post-log phase growth-induced mitophagy.

Yme1 regulates the Atg32-Atg11 interaction

Atg32 interacts with Atg11 upon mitophagy induction (Kanki et al., 2009; Okamoto et al., 2009), and this interaction is critical for mitophagy activity (Aoki et al., 2011; Kondo-Okamoto et al., 2012). To provide a more mechanistic insight of how Yme1 regulates mitophagy, we decided to examine whether Atg32 and Atg11 interaction was affected in the *yme1*Δ strain. To do this, we expressed PA-Atg32 and HA-Atg11 in the wild-type and *yme1*Δ strains and carried out PA affinity isolation with immunoglobin G (IgG)-Sepharose (Figure

3.9). In wild-type cells, PA-Atg32 coprecipitated a significant amount of HA-Atg11 following a 1 h shift to mitophagy-inducing conditions (Figure 3.9, lane 2). However, in the *yme1*Δ strain, the amount of HA-Atg11 coprecipitated by PA-Atg32 was significantly decreased (Figure 3.9, lane 4), suggesting a strong block in the Atg32-Atg11 interaction. Therefore, Yme1 is required for the efficient interaction between Atg32 and Atg11.

3.5 Discussion

In the past few years there has been a steady increase in our knowledge about the process of mitophagy, in particular at the molecular level. The identification of the receptor protein Atg32 provided an important breakthrough regarding the mechanism of mitophagy in yeast (Kanki et al., 2009; Okamoto et al., 2009); however, the identification of this protein also raised important questions as to how mitophagy is regulated. Considering that mitochondria are essential organelles, the proper regulation of mitophagy is critically important for mitochondrial and cellular homeostasis.

In this study, we characterized one aspect of mitophagy regulation. We demonstrated that Atg32 undergoes proteolytic processing of its C terminus upon mitophagy induction (Figure 3.1), which is mediated by the mitochondrial i-AAA protease Yme1 (Figure 3.5). This processing is important for mitophagy, as blocking the processing by C-terminal tagging of Atg32 caused a significant mitophagy defect (Figure 3.3). In addition, Yme1 protease activity is required for efficient mitophagy (Figure 3.7). Our results also suggest that the unprocessed Atg32 has lower binding affinity to Atg11, since the interaction between Atg32 and Atg11 was significantly reduced in a *yme1*Δ strain (Figure 3.9). Therefore, our results suggest a model of mitophagy regulation where, upon induction, Yme1 processes Atg32 to allow its tight association with Atg11 and subsequent interaction with the core macroautophagic machinery (Figure 3.10).

This model of regulation is reminiscent of PINK1-PARK2-mediated mitophagy in mammalian cells. In steady-state cells, PINK1 is imported into the mitochondrial inner membrane in a membrane potential-dependent manner. The mitochondrial inner membrane protein PARL (presenilin associated, rhomboid-like) mediates the cleavage and destabilization of PINK1 (Jin et al., 2010). Upon mitochondria depolarization, PINK1 import into the inner membrane is impaired, leading to a rapid PINK1 accumulation on the outer membrane of damaged mitochondria. Accumulated PINK1 recruits PARK2 to the mitochondria, resulting in the ubiquitination of outer membrane proteins, which is required for the recognition of damaged mitochondria by the autophagic machinery. In this case, however, proteolytic processing of PINK1 leads to its destabilization and an inhibition of mitophagy. In addition, Pcp1, which is the yeast homolog of PARL, is not required for Atg32 processing (Figure 3.4); however, Yme1 is well conserved in mammalian cells, and the function of YME1L, the homolog of Yme1, is largely unknown (Koppen and Langer, 2007). It will be interesting to see whether YME1L plays a role in mitophagy in mammalian cells.

Through this study, we established a link between mitophagy and the mitochondrial protein quality control system. Yme1 is responsible for the degradation of unfolded or misfolded mitochondrial proteins (Weber et al., 1996), and is thus an important component of the mitochondrial protein quality control system. A recent study provided evidence that disruption of mitochondrial protein quality control promotes mitophagy (Heo et al., 2010), suggesting a crosstalk between these two types of mitochondrial quality control systems. Our study provided a molecular link for this crosstalk by showing that Yme1 recognizes the mitophagy receptor protein Atg32 as a substrate. If Atg32 was the only target of Yme1 that is relevant to mitophagy, expression of a truncated form of Atg32 lacking its C terminus should suppress the mitophagy defect of the *yme1*Δ strain; however, we found that a C-terminally truncated Atg32 did not complement the mitophagy defect seen in *yme1*Δ cells (our

unpublished data). Therefore, we speculate that Yme1 has an additional target(s) and another role(s) during mitophagy besides the processing of Atg32. Furthermore, in our study, we monitored the role of Yme1 in removing superfluous mitochondria following a shift from a non-fermentable carbon source to glucose. It is reasonable to speculate that under other mitochondrial stress conditions, Yme1 actively degrades unfolded or misfolded mitochondrial proteins and at the same time activates Atg32 to trigger mitophagy to prevent the accumulation of damaged mitochondria.

Yme1 was first discovered to be involved in mitochondrial DNA transfer to the nucleus (Thorsness et al., 1993). Inactivation of Yme1 causes increased escape of DNA from mitochondria, which is dependent on vacuole function (Campbell and Thorsness, 1998). However, based on our analyis, mitochondrial DNA transfer to the nucleus seemed to be an autophagy-independent process (our unpublished data). Thus, the involvement of Yme1 in mitophagy regulation may be distinct from its potential role in mitochondrial DNA escape.

What regulates Yme1 activity remains a mystery. Our results showed that Atg32 could be a direct substrate of Yme1, and the interaction between Atg32 and Yme1 is independent of culture conditions. Therefore, we speculate Yme1 is associated with Atg32 constitutively, but the processing only occurs upon mitophagy induction. What activates Yme1 to process Atg32 remains an interesting question for future study.

Why unprocessed Atg32 has a decreased affinity for Atg11 also needs to be further characterized. We speculate that the processing of Atg32 at its C terminus may cause a conformational change at its N terminus that favors its interaction with Atg11. If demonstrated, this will provide an example of how the status of the mitochondria, such as the potential across the inner membrane, can be transmitted to factors in the cytosol to initiate mitophagy. Such a mechanism has been characterized for various cell surface receptors (Lemmon and Schlessinger, 2010). Upon binding to extracellular ligands, a conformational

change is induced and the catalytic domain in the cytosol is activated. Structural studies of Atg32 are needed to explore this intriguing possibility that proteolytic processing can also play a role in signal transduction across the membrane.

Atg32 is phosphorylated by a still unknown kinase (Aoki et al., 2011). This phosphorylation is required for mitophagy and the interaction between Atg32 and Atg11. We tried to explore the relationship between Atg32 processing and phosphorylation, but we were not able to detect a clear band shift corresponding to Atg32 phosphorylation. Nonetheless, it is clear that cellular mitophagy is a tightly controlled process and is regulated by multiple factors. So far, the regulation of mitophagy in yeast has largely focused on the receptor protein Atg32 and its interaction with Atg11. Apparently more experiments of a broader scope are needed to further elucidate the details of mitophagy regulation.

3.6 Figures

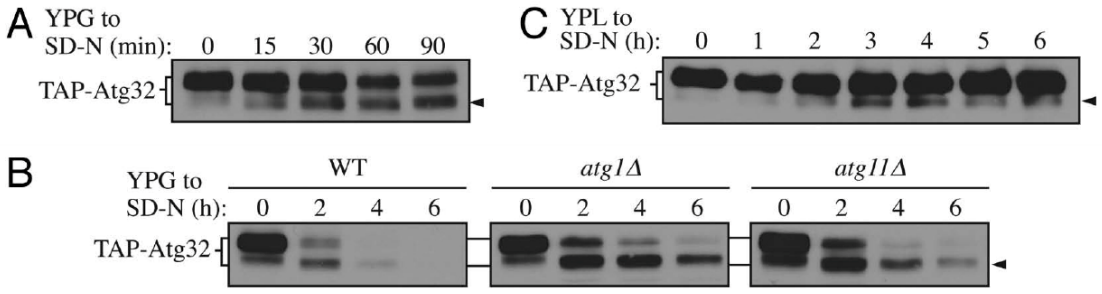

Figure 3.1 Atg32 undergoes starvation-dependent processing
(A) Cells expressing TAP tagged Atg32 under the control of the *GAL1* promoter (KWY100) were cultured in YPG to mid-log phase and shifted to SD-N for the indicated times. TAP-Atg32 was monitored by immunobloting with an antibody that recognizes PA. The arrowhead here and in the following panels indicates the processed band.
(B) Cells expressing *GAL1* promoter-driven TAP-Atg32 in wild-type (WT; KWY100), *atg1*Δ (KWY101), and *atg11*Δ (KWY104) backgrounds were cultured in YPG to mid-log phase and shifted to SD-N for the indicated times.
(C) Cells expressing endogenous promoter-driven TAP-Atg32 in a WT background (KWY139) were cultured in YPL to mid-log phase and shifted to SD-N for the indicated times.

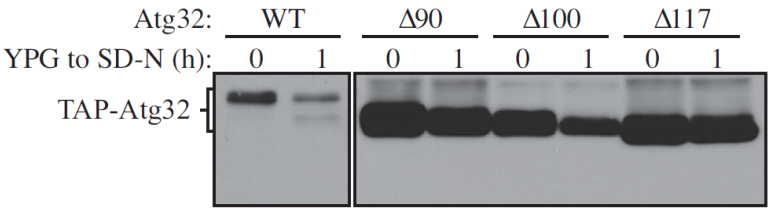

Figure 3.2 Atg32 processing occurs at its C terminus.
Cells expressing *GAL1* promoter-driven TAP-Atg32 (KWY100), TAP-Atg32Δ90 (KWY129), TAP-Atg32Δ100 (KWY144) or TAP-Atg32Δ117 (KWY145) were cultured in YPG to mid-log phase and shifted to SD-N for 1h. TAP-Atg32 was monitored by immunobloting with an antibody that binds to PA.

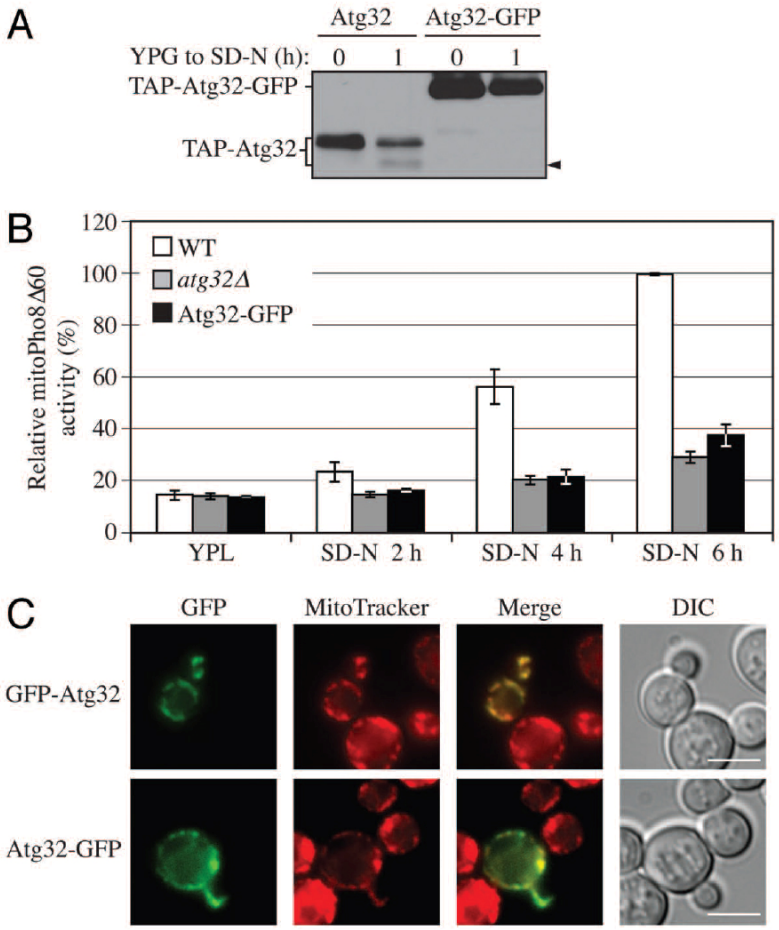

Figure 3.3 C terminal tagging of Atg32 interferes with its processing and mitophagy
(A) Strains expressing *GAL1* promoter-driven TAP-Atg32 (KWY100) and TAP-Atg32-GFP (KWY110) were cultured as in Figure 1A. Proteins were monitored by immunobloting with an antibody that detects PA.
(B) Wild-type (WT; KWY90), *atg32*Δ (KWY22) and Atg32-GFP (KWY121) strains expressing mitoPho8Δ60 were grown in YPL and shifted to SD-N for the indicated times. Samples were collected and protein extracts were assayed for mitoPho8Δ60 activity. The results represent the mean and standard deviation (SD) of three independent experiments.
(C) Strains expressing *GAL1* promoter-driven N terminal GFP-tagged Atg32 (KWY111) and C terminal GFP-tagged Atg32 (KWY121) were cultured in YPGal to mid-log phase and stained with the mitochondrial marker MitoTracker Red. The localization of GFP and MitoTracker Red were visualized by fluorescence microscopy. DIC, differential interference contrast. Scale bar, 5 μm.

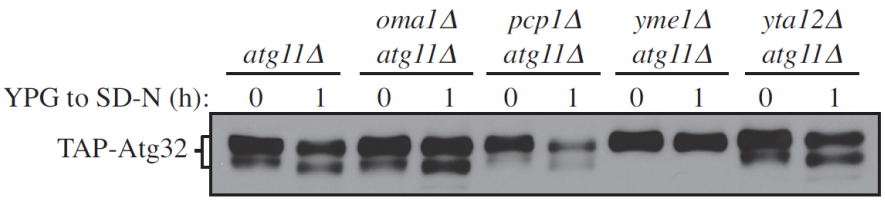

Figure 3.4 Screen for the protease that mediates Atg32 processing
Cells expressing *GAL1* promoter-driven TAP-Atg32 in *atg11*Δ (KWY104), *atg11*Δ *oma1*Δ (KWY113), *atg11*Δ *pcp1*Δ (KWY115), *atg11*Δ *yme1*Δ (KWY114) and *atg11*Δ *yta12*Δ (KWY117) backgrounds were cultured in YPG to mid-log phase and shifted to SD-N for 1 h. TAP-Atg32 was monitored by immunobloting with an antibody that binds to PA.

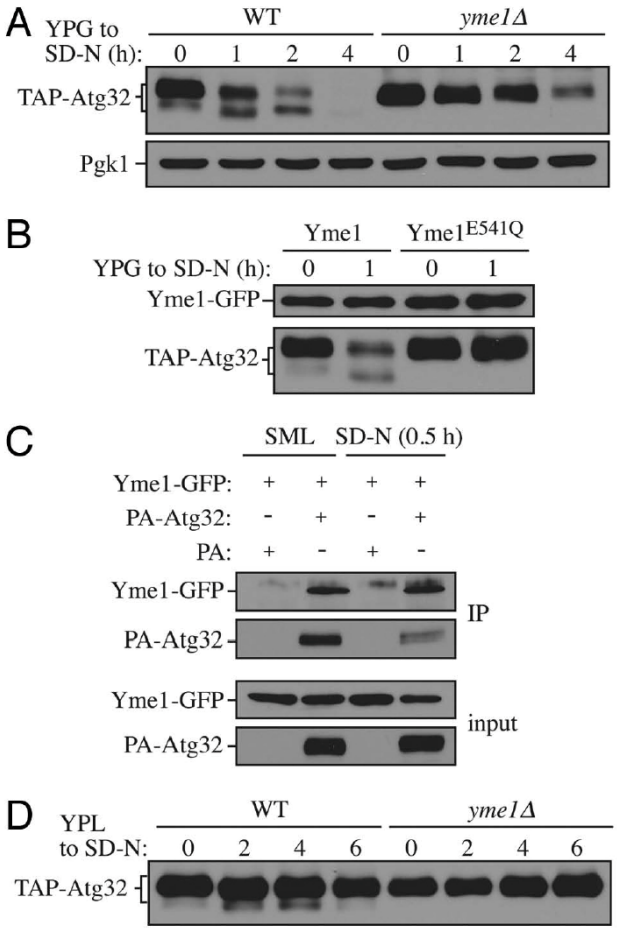

Figure 3.5 Yme1 mediates Atg32 processing
(A) Cells expressing *GAL1* promoter-driven TAP-Atg32 in wild-type (WT; KWY100) and *yme1*Δ (KWY118) strains were cultured as in Figure 1A. TAP-Atg32 was monitored by immunobloting with an antibody that binds to PA. Pgk1 was monitored by immunobloting with anti-Pgk1 antibody as a loading control.
(B) Cells expressing *GAL1* promoter-driven TAP-Atg32 and Yme1-GFP (KWY134) or Yme1^{E541Q}-GFP (KWY141) were cultured as in Figure 1A. TAP-Atg32 was monitored by immunobloting with anti-Atg32 antiserum. Yme1-GFP was monitored by immunobloting with anti-YFP antibody.
(C) A strain expressing Yme1-GFP (KWY133) was transformed with a plasmid expressing protein A only, or PA-Atg32 under the control of the *CUP1* promoter, and cultured in SML medium to mid-log phase or starved in SD-N for 0.5 h. IgG-Sepharose was used to precipitate PA-Atg32 from cell lysates. The bottom two panels show the immunoblot of total cell lysates (input) and the upper two panels show the IgG precipitates (IP), which were probed with anti-YFP antibody and an antibody that recognizes PA.
(D) Cells expressing endogenous promoter-driven TAP-Atg32 in WT (KWY139) and *yme1*Δ (KWY140) strains were cultured as in Figure 1C. TAP-Atg32 was monitored by immunobloting with anti-Atg32 antiserum.

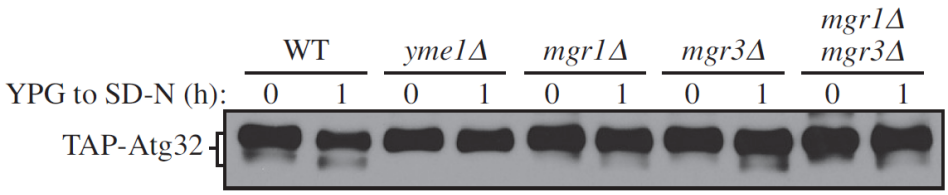

Figure 3.6 Mgr1 and Mgr3 are not critical for Atg32 processing
Cells expressing *GAL1* promoter-driven TAP-Atg32 in wild-type (WT; KWY100), *yme1*Δ (KWY118), *mgr1*Δ (KWY146), *mgr3*Δ (KWY147) and *mgr1*Δ *mgr3*Δ (KWY148) backgrounds were cultured in YPG to mid-log phase and shifted to SD-N for 1 h. TAP-Atg32 was monitored by immunobloting with an antibody that binds to PA.

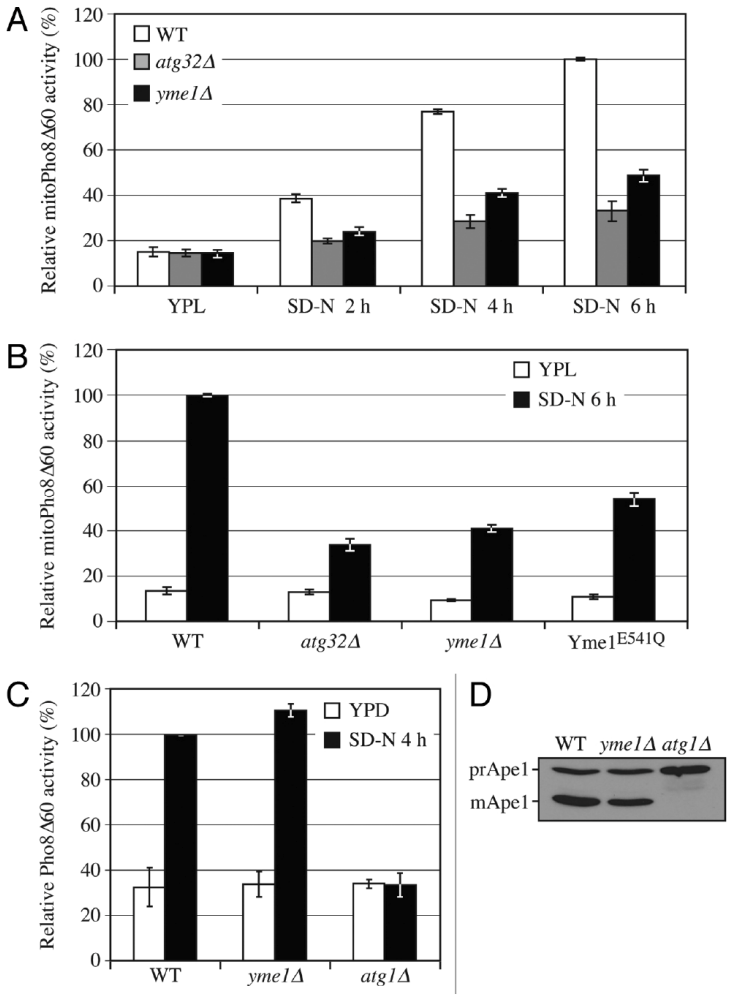

Figure 3.7 Yme1 is specifically required for mitophagy

(A) Wild-type (WT; KWY20), *yme1*Δ (KWY136) and *atg32*Δ (KWY22) strains expressing mitoPho8Δ60 were grown in YPL and shifted to SD-N for the indicated times. Samples were collected and protein extracts were assayed for mitoPho8Δ60 activity. The results represent the mean and standard deviation (SD) of three independent experiments.

(B) Wild-type (KWY20), *yme1*Δ (KWY136), *atg32*Δ (KWY22) and Yme1^{E541Q}-GFP (KWY138) strains expressing mitoPho8Δ60 were grown in YPL and shifted to SD-N for 6 h. Samples were collected and protein extracts were assayed for mitoPho8Δ60 activity. The results represent the mean and standard deviation (SD) of three independent experiments.

(C) Wild-type (WLY176), *yme1*Δ (KWY143) and *atg1*Δ (WLY192) strains expressing Pho8Δ60 were cultured in YPD to mid-log phase and shifted to SD-N for 4 h. Samples were collected and protein extracts were assayed for Pho8Δ60 activity. The results represent the mean and standard deviation (SD) of three independent experiments.

(D) Wild-type (WLY176), *yme1*Δ (KWY143) and *atg1*Δ (WLY192) strains were cultured in YPD medium and analyzed for prApe1 maturation by immunoblotting to monitor the Cvt pathway during vegetative growth. The positions of precursor and mature Ape1 are indicated.

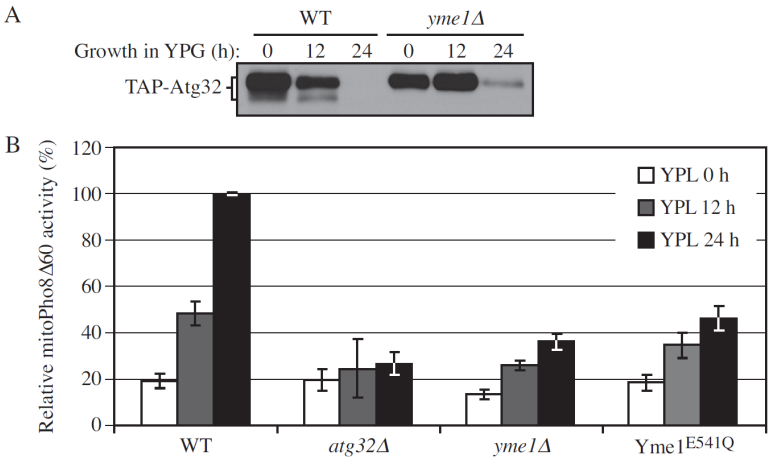

Figure 3.8 Yme1 is required for Atg32 processing and mitophagy during post-log phase growth

(A) Cells expressing *GAL1* promoter-driven TAP-Atg32 in wild-type (WT; KWY100) and *yme1*Δ (KWY118) backgrounds were cultured in YPG to mid-log (0 h) and post-log (12, 24 h) phases. TAP-Atg32 was monitored by immunobloting with an antibody that binds to PA.

(B) Wild-type (KWY20), *yme1*Δ (KWY136) and *atg32*Δ (KWY22) strains expressing mitoPho8Δ60 were grown in YPL to mid-log (0 h) and post-log (12, 24 h) phases. Samples were collected and protein extracts were assayed for mitoPho8Δ60 activity. The results represent the mean and standard deviation (SD) of three independent experiments.

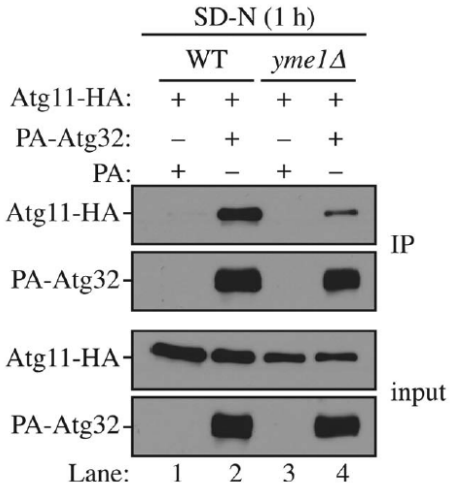

Figure 3.9 Yme1 regulates the interaction between Atg32 and Atg11. Wild-type (WT; SEY6210) and *yme1*Δ (KWY142) strains transformed with a plasmid expressing HA-tagged Atg11 together with a plasmid expressing protein A only or PA-Atg32 were cultured in SMD medium to mid-log phase or starved in SD-N for 1 h. IgG-Sepharose was used to precipitate PA-Atg32 from cell lysates. The bottom two panels show the immunoblot of total cell lysates (input) and the upper two panels show the IgG precipitates (IP), which were probed with anti-YFP antibody and an antibody that binds PA. All plasmids are under the control of the *CUP1* promoter.

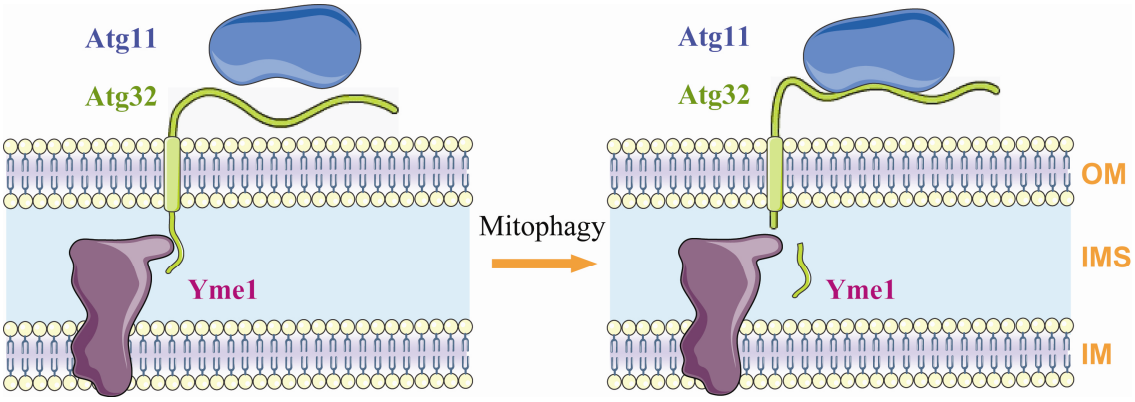

Figure 3.10 Model of Yme1 mediated mitophagy.

Chapter IV
PHOSPHATATIDYLINOSITOL 4-KINASES ARE REQUIRED FOR AUTOPHAGIC MEMBRANE TRAFFICKING

This chapter is reprinted from The Journal of Biological Chemistry, Volume 287, Number 45, Ke Wang*, ZhifenYang*, Xu Liu, Kai Mao, Usha Nair and Daniel J. Klionsky, Phosphatidylinositol 4-Kinases Are Required for Autophagic Membrane Trafficking, pg. 37964-37972, 2012. I was the co-first author with Dr. Zhifen Yang in this publication and I contributed to Figures 4.3, 4.5, 4.6 and 4.7.

4.1 Abstract

Macroautophagy (hereafter autophagy) is a degradative cellular pathway that protects eukaryotic cells from stress, starvation and microbial infection. This process must be tightly controlled because too little or too much autophagy can be deleterious to cellular physiology. The phosphatidylinositol (PtdIns) 3-kinase Vps34 is a lipid kinase that regulates autophagy, but the role of other PtdIns kinases has not been examined. Here, we demonstrate a role for PtdIns 4-kinases and PtdIns4P 5-kinases in selective and nonselective types of autophagy in yeast. The PtdIns 4-kinase Pik1 is involved in Atg9 trafficking through the Golgi, and is involved in both nonselective and selective types of autophagy, whereas the PtdIns4P 5-kinase Mss4 is specifically involved in mitophagy but not nonselective autophagy. Our data indicate that phosphoinositide kinases have multiple roles in the regulation of autophagic pathways.

4.2 Introduction

Selective and nonselective autophagy play essential physiological roles in all eukaryotic cells by controlling the rapid degradation of long-lived proteins, unnecessary or

damaged organelles and/or bulk cytoplasm in response to various types of stress in their intracellular and extracellular environment (Levine and Klionsky, 2004). As our knowledge of the core machinery of autophagy expands (Xie and Klionsky, 2007), we find that there is much more to explore regarding autophagy regulation. Phosphoinositides are important regulators in cellular membrane dynamics (Di Paolo and De Camilli, 2006). In yeast, cellular phosphatidylinositol can be phosphorylated by the PtdIns 3-kinase Vps34 to generate phosphatidylinositol 3-phosphate (PtdIns3P), and further phosphorylation by the PtdIns3P 5-kinase Fab1 converts PtdIns3P into PtdIns(3,5)P_2. The other route for PtdIns metabolism is phosphorylation by PtdIns 4-kinases to generate PtdIns4P, and further phosphorylation by Mss4 generates PtdIns(4,5)P_2 (Strahl and Thorner, 2007). The PtdIns3P signaling pathway is important for autophagy. Yeast Vps34 forms an autophagy-specific complex containing Atg14, Vps30/Atg6 and Vps15, and is important for the organization of the phagophore assembly site (PAS) (Kihara et al., 2001). The corresponding complex that generates PtdIns3P in mammals is also critical for autophagy. Furthermore, PtdIns(3,5)P_2 plays a role in autophagy in mammalian cells (Ferguson et al., 2009). However, the potential roles of the second PtdIns metabolic route involving PtdIns 4-kinases in the autophagic pathway remain largely unexplored.

The *Saccharomyces cerevisiae* genome contains three PtdIns 4-kinases: the Golgi- and nucleus-localized Pik1, the plasma membrane-localized Stt4, and the nonessential Lsb6 (Audhya and Emr, 2002; Han et al., 2002; Strahl et al., 2005). Pik1 and Stt4 are responsible for the synthesis of the majority of cellular PtdIns4P. Whereas the function of the nuclear population of Pik1 remains unclear, the Golgi-localized Pik1 is essential for secretory vesicle exit from the *trans*-Golgi network. Plasma membrane-localized Stt4 is involved in the Slt2 MAP kinase cascade (Audhya and Emr, 2002); the PtdIns4P generated by Stt4 is converted into PtdIns(4,5)P_2 by Mss4, which acts as an upstream regulator of this signaling pathway.

A previous study reported that PtdIns4P is required for peroxisome degradation by selective autophagy in the yeast *Pichia pastoris* (Yamashita et al., 2006). In this regard, PtdIns4P is generated by PpPik1 and is thought to participate in the formation of a pexophagy-specific membrane structure, termed the micropexophagic apparatus. The key autophagy-related (Atg) protein that binds this phosphoinositide in *P. pastoris* is PpAtg26; however, the homologous protein in *S. cerevisiae* does not have a role in autophagy (Cao and Klionsky, 2007). These findings raise several important questions. For example, is PtdIns4P involved in other types of autophagy aside from pexophagy? *P. pastoris*, which is a methylotrophic yeast, has a Golgi complex that, in contrast to that of *S. cerevisiae*, is morphologically organized in a manner similar to the Golgi complex of mammalian cells. Accordingly, it is not clear whether PtdIns 4-kinases would play an equivalent role in budding yeast. In this report, we analyzed the role of PtdIns 4-kinases in both selective and non-selective autophagic pathways and examined their mechanistic roles. Our data suggest that PtdIns 4-kinases have a conserved function in autophagy regulation. In yeast, defects in PtdIns 4-kinase activity affect trafficking of Atg9 and cause blocks both in nonselective autophagy and mitophagy.

4.3 Materials and methods

Media and growth conditions

Yeast cells were grown in YPD (rich medium; 1% yeast extract, 2% peptone, 2% glucose), SMD (synthetic minimal medium; 0.67% yeast nitrogen base without amino acids, 2% glucose, supplemented with vitamins and auxotrophic amino acids as needed), YPL (1% yeast extract, 2% peptone, and 2% lactate) or SML (0.67% yeast nitrogen base, 2% lactate, and auxotrophic amino acids and vitamins as needed). Starvation experiments were performed in SD-N (synthetic medium lacking nitrogen; 0.17% yeast nitrogen base without

ammonium sulfate or amino acids, and 2% glucose). For temperature-sensitive mutants, cells were grown at 24ºC to midlog phase and shifted to 37ºC for 30 min to inactivate the mutants. If not otherwise indicated, cells were grown at 30ºC.

Strains and plasmids

Plasmids used in this study are listed in Table 4.1. pCu416 and pCuGFP-Aut7(416) have been reported previously (Kim et al., 2001; Labbe and Thiele, 1999). To construct pCu3HA-Pik1(416) and pCuGFP-Pik1(416), 3HA or GFP was first cloned into the SpeI/XmaI sites of pCu416 to generate pCu3HA(416) or pCuGFP(416), and then the open reading frame (ORF) of *PIK1* was amplified from genomic DNA and cloned into the XmaI/SalI sites of pCu3HA(416) or pCuGFP(416). To make pCu3HA-Pik1(405), the Cu3HA-Pik1 coding sequence from pCu3HA-Pik1(416) was amplified and cloned into the SacII/BamHI sites of pRS405. pCuGFP-pik1-11(416), and pCuGFP-pik1-104(416) were generated by amplifying *pik1-11*, or *pik1-104* from genomic DNA of the corresponding strains and then cloning into the XmaI/SalI sites of pCuGFP(416). To construct pCuRFP-Atg8(405), RFP was first cloned into the SpeI/XmaI sites of pCu416 to generate pCuRFP(416), followed by cloning of *ATG8* into the XmaI/SalI sites of pCuRFP(416), and then the CuRFP-Atg8 coding sequence from pCuRFP-Atg8(416) was amplified and cloned into the SacII/BamHI sites of pRS405. To construct pCu3HA-Pik1(416) (pZY084) and pCuGFP-Pik1(416) (pZY087), 3HA or GFP was first cloned into the SpeI/XmaI sites of pCu416 to generate pCu3HA(416) or pCuGFP(416), and then the ORF of *PIK1* was amplified from genomic DNA and cloned into the XmaI/SalI sites of pCu3HA(416) or pCuGFP(416).

Yeast strains used in this study are listed in Table 4.2. Gene disruption and C-terminal tagging were carried out using a PCR-based method as described previously (Gueldener et al.,

2002; Longtine et al., 1998). For integration of Cu3HA-Pik1, pCu3HA-Pik1(405) was linearized with BglII and integrated into the *PIK1* locus. To integrate Atg9-3GFP, the pAtg9-3GFP(306) plasmid was linearized with BglII and integrated into the *ATG9* genomic locus (Monastyrska et al., 2008). RFP-Ape1 was incorporated into the chromosome by integrating AvrII-digested pRFP-Ape1(305) into the *APE1* locus (Stromhaug et al., 2004). To integrate GFP-Atg8 and RFP-Atg8, pGFP-Atg8(405) and pRFP-Atg8(405) were linearized with AflII and integrated into the *LEU2* locus. The integration of GFP-PH^{FAPP} has been described previously (Roy and Levine, 2004).

To generate the *pik1-11*, and *pik1-104* strains, the endogenous copy of *PIK1* was replaced with mutant alleles by homologous recombination. First, the 333-base pair genomic region downstream of the *PIK1* ORF including its terminator was cloned and ligated into the SacI/SacII sites of pFA6a-KAN or pFA6a-TRP1, which are downstream of the *KAN* or *TRP1* genes. Next, the *pik1-11*, and *pik1-104* sequences plus the *CYC1* terminator were amplified by PCR from pCuGFP-pik1-11(416), and pCuGFP-pik1-104(416), respectively, and inserted into the XmaI/BglII sites of pFA6a-KAN or pFA6a-TRP1, which are upstream of the *KAN* or *TRP1* genes, to complete the pFA6a-pik1-11-KAN, pFA6a-pik1-104-KAN, pFA6a-pik1-11-TRP1, and pFA6a-pik1-104-TRP1 plasmids. Then, these plasmids were digested with XmaI/SacII, and the resulting fragments were transformed into yeast cells to replace the endogenous copy of *PIK1*. Incorporation of the mutations was confirmed by DNA sequencing.

Table 4.1 Yeast plasmids used in this study

Plasmid	Vector; Insert	Source
pATG9-3×GFP(306)	pRS306; *ATG9-3×GFP*	(Monastyrska et al., 2008)
pCU-GFP-AUT7(416)	pCU-GFP(416); *ATG8*	(Kim et al., 2001)
pRFP-APE1(305)	pRS305; *RFP-APE1*	(Stromhaug et al., 2004)
pCU-GFP-Atg32(416)	pRS416; Atg32	(Kanki et al., 2009b)
pTL334	pPHO5^{prom}(406); *GFP-myc-PH^{FAPP1}*	(Roy and Levine, 2004)
pZY054	pCU(416); *3HA*	This study

pZY084	pCU-3HA(416); *PIK1*	This study
pZY085	pCU-3HA(405); *PIK1*	This study
pZY086	pCU-RFP(405); *ATG8*	This study
pZY087	pCU-GFP(416); *PIK1*	This study
pZY088	pCU-GFP(416); *PIK1-11*	This study
pZY089	pCU-GFP(416); *PIK1-83*	This study
pZY090	pCU-GFP(416); *PIK1-104*	This study
pZY094	pFA6a-KAN1; *PIK1-11*	This study
pZY095	pFA6a-KAN1; *PIK1-83*	This study
pZY096	pFA6a-KAN1; *PIK1-104*	This study
pZY097	pFA6a-TRP1; *PIK1-11*	This study
pZY098	pFA6a-TRP1; *PIK1-83*	This study
pZY099	pFA6a-TRP1; *PIK1-104*	This study

Table 4.2 Yeast strains used in this study

Strain	Genotype	Source or reference
BY4742	*MATa leu2-Δ0 his3-Δ1 lys2-Δ0 ura3-Δ0*	ResGen/Invitrogen
frq1-1	BY4742 *frq1-1*	This study
JGY169	SEY6210 *GFP-ATG8::LEU2 vam3^{ts}::TRP1*	(Geng et al., 2010)
JK9-3da	*MATa leu2-3,112 ura3-52 rme1, trp1 his4 GAL HMLa*	(Heitman et al., 1991)
KWY20	SEY6210 *pho8Δ::TRP1 pho13Δ::LEU2* pRS406-*ADH1-COX4-pho8Δ60*	(Kanki et al., 2009a)
KWY22	SEY6210 *pho8Δ::TRP1 pho13Δ::LEU2* pRS406-*ADH1-COX4-pho8Δ60 atg32Δ::KAN*	(Kanki et al., 2009a)
KWY79	KWY20, *pik1-104::KAN*	This study
TKYM107	BY4742, *OM45-GFP:: HIS3*	(Kanki et al., 2009a)
TKYM137	BY4742, *OM45-GFP:: HIS3 atg32Δ::KAN*	(Kanki et al., 2009a)
KWY80	*stt4-4 OM45-GFP::His3*	This study
KWY81	*pik1-104 OM45-GFP:: HIS3*	This study
KWY82	*mss4-103 OM45-GFP:: HIS3*	This study
KWY83	*mss4-103 pho8Δ60::URA3 pho13Δ::LEU2*	This study
KWY84	BY4742 *pho8Δ::HIS3 pho13Δ::LEU2* pRS406-*ADH1-COX4-pho8Δ60*	This study
KWY85	*stt4-4 pho8Δ::HIS3 pho13Δ::LEU2* pRS406-*ADH1-COX4-pho8Δ60*	This study
KWY86	*mss4-103 pho8Δ::HIS3 pho13Δ::LEU2* pRS406-*ADH1-COX4-pho8Δ60*	This study
KWY87	KWY83 *atg32Δ::KAN*	This study
pik1-104 SEC7-6DsRed	BY4742 *pik1-104* JK9-3da *SEC7-6xDsRed::TRP1*	This study Benjamin Glick
sec14-3	BY4742 *sec14-3*	This study
SEY6210	*MATα ura3-52 leu2-3,112 his3-Δ200 trp1-Δ901 lys2-801 suc2-Δ9 mel GAL*	(Robinson et al., 1988)
stt4-4	BY4742 *stt4-4*	This study
TYY127	YTS158 *atg1Δ::URA3*	(He et al., 2006)
YES47	YPH499 *pik1-11::TRP1*	(Hendricks et al., 1999)

YES102	YPH499 *pik1-83::TRP1*	(Hendricks et al., 1999)
YPH499	*MATa ade2-101^{oc} his3-Δ200 leu2-Δ1 lys2-801^{am} trp1-Δ1 ura3-52*	(Sikorski and Hieter, 1989)
YTS158	BY4742 *pho8Δ60::HIS3 pho13Δ::LEU2*	(He et al., 2006)
ZFY070	SEY6210 *atg1Δ::URA3 ATG27-GFP::HIS3 RFP-APE1::LEU2*	This study
ZFY073	SEY6210 *GFP-ATG8::LEU2*	This study
ZFY202	W303-1B *pho13Δ pho8Δ60::HIS3*	(Yang et al., 2010)
ZFY270	BY4742 *atg1Δ::KAN ATG9-3×GFP::URA3 RFP-APE1::LEU2*	This study
ZFY273	*pik1-104 atg1Δ::KAN ATG9-3×GFP::URA3 RFP-APE1::LEU2*	This study
ZFY276	*frq1-1 atg1Δ::KAN ATG9-3×GFP::URA3 RFP-APE1::LEU2*	This study
ZFY280	*frq1-1 pho8Δ60::URA3 pho13Δ::LEU2*	This study
ZFY281	*pik1-104 pho8Δ60::URA3 pho13Δ::LEU2*	This study
ZFY282	*stt4-4 pho8Δ60: URA3: pho13Δ::LEU2*	This study
ZFY283	YPH499 *pho8Δ60::HIS3 pho13Δ::LEU2*	This study
ZFY284	*pik1-11 pho8Δ60::HIS3 pho13Δ::LEU2*	This study
ZFY285	*frq1-1 Cu3HA-PIK1 ::LEU2*	This study
ZFY286	*pik1-11 Cu3HA-PIK1 ::LEU2*	This study
ZFY287	*pik1-83 Cu3HA-PIK1 ::LEU2*	This study
ZFY288	*pik1-104 Cu3HA-PIK1 ::LEU2*	This study
ZFY290	*sec14-3 Cu3HA-PIK1 ::LEU2*	This study
ZFY293	ZFY202 *pik1-83::TRP1*	This study
ZFY299	SEY6210 *atg1Δ::URA3 ATG27-GFP::HIS3 RFP-APE1::LEU2 pik1-11::TRP1*	This study
ZFY301	SEY6210 *atg1Δ::URA3 ATG27-GFP::HIS3 RFP-APE1::LEU2 pik1-104::TRP1*	This study
ZFY305	SEY6210 *GFP-ATG8::LEU2 pik1-104::TRP1*	This study
ZFY306	JGY169 *pik1-104::KAN*	This study
ZFY312	ZFY202 *pik1-83::TRP1 kes1Δ::LEU2*	This study
ZFY314	*sec14-3^{ts} kes1Δ::LEU2*	This study
ZFY326	*SEC7-6×DsRed::TRP1 ATG9-3×GFP::URA3*	This study
ZFY328	*SEC7-6×DsRed::TRP1 ATG9-3×GFP::URA3 pik1-104::KAN*	This study
ZFY331	BY4742 *CuRFP-ATG8::LEU2 atg1Δ::TRP1*	This study

Fluorescence microscopy

Cells were cultured in YPD or SMD selective media to mid-log phase, and then shifted to SD-N medium as indicated in the corresponding figure legends. Cells were pelleted by centrifugation and resuspended in fresh SMD to reflect growing conditions or in SD-N for starvation conditions. Cells were visualized with a microscope (DeltaVision Spectris; Applied

Precision, Issaquah, WA) fitted with differential interference contrast (DIC) optics and Olympus camera IX-HLSH100. For each microscopy picture, twelve Z-section images were captured. The distance between two neighboring sections was 0.5 μm and the total depth of each stack was 5.5 μm, which is the approximate diameter of a normal yeast cell. The images were deconvolved using softWoRx software (Applied Precision).

Autophagy assays

To monitor bulk autophagy, the Pho8Δ60 assay and the GFP-Atg8 processing assay were performed as previously described (Noda et al., 1995; Shintani and Klionsky, 2004).

Mitophagy assays

Om45-GFP processing and mitoPho8Δ60 assays were performed as described previously (Kanki et al., 2010).

4.4 Results

Golgi-localized Pik1 is required for autophagy

To determine the role of the PtdIns kinases in autophagy, we first examined the autophagic phenotype of a *pik1* mutant using a well-established procedure, the GFP-Atg8 processing assay. The ubiquitin-like protein Atg8 is conjugated to phosphatidylethanolamine and remains associated with the completed autophagosome. When transported into the vacuole during autophagy, GFP-tagged Atg8 is hydrolyzed to yield free GFP. Thus, the relatively stable GFP moiety reflects the level of autophagy (Shintani and Klionsky, 2004).

Using this method, we observed a strong autophagic defect in the temperature sensitive *pik1-104* mutant (Figure 4.1.A). In nutrient-rich conditions at both the permissive temperature (PT) and non-permissive temperature (NPT), there was essentially no detectable

free GFP as expected. After 2-h nitrogen starvation at 24°C there was a clear appearance of the free GFP band in wild-type and *pik1* mutant cells. However, at 37°C, significantly reduced free GFP was detected in the *pik1-104* strain compared to the wild-type cells (Figure 4.1.A). To rule out the possibility that the observed autophagic defect might be due to cell death caused by inactivation of Pik1, which is an essential protein, we shifted the cells back to the PT for another 2-h starvation (recovery period, R); we observed a clear induction of GFP-Atg8 processing during the recovery period, demonstrating that autophagy induction was restored and that the cells were still viable (Figure 4.1.A). The autophagy defect was rescued by a plasmid expressing the *PIK1* gene chromosomally integrated into the *pik1* mutant, suggesting the autophagic defect was indeed due to the functional impairment of Pik1 (data not shown).

To further confirm our observations, we used the Pho8Δ60 assay to quantitatively analyze the autophagic defect in the *pik1* muant. *PHO8* encodes a vacuolar alkaline phosphatase, and its delivery into the vacuole through the secretory pathway is dependent on its N-terminal transmembrane domain (Klionsky and Emr, 1989). Pho8Δ60 is a truncated form that lacks the 60 N-terminal amino acid residues including the transmembrane domain; this altered protein is unable to enter the endoplasmic reticulum, remains in the cytosol and is delivered into the vacuole only through bulk autophagy (Noda et al., 1995). In this way, the magnitude of bulk autophagy is quantified by measuring the activity of alkaline phosphatase in nitrogen starvation conditions. After 4-h nitrogen starvation, wild-type cells showed a strong increase in Pho8Δ60 activity at both 24°C and 37°C, whereas the *atg1*Δ strain that is defective in autophagy showed only background levels of activity (Figure 4.1.B). In *pik1-104*, although the induction of the Pho8Δ60 activity was normal at the PT, there was essentially no increase at the NPT. Similar to the results from the GFP-Atg8 processing assay, the Pho8Δ60 activity of *pik1-104* was partially recovered when the cells were shifted back to the PT

(recovery) or upon the introduction of plasmid-expressed *PIK1* (Figure 4.1.B and data not shown).

Consistent with a previous publication (Hendricks et al., 1999), our sequence analysis showed that the temperature-sensitive *pik1-104* allele contains mutations (S412P, A455T, Y517H, D529G, Q731R, R802G) that are located within the carboxyl-terminal catalytic kinase domain of Pik1. This suggests that the PtdIns 4-kinase activity of Pik1 could be essential for autophagy. However, we also considered the possibility that these point mutations may affect the stability of the Pik1 protein at NPT. To test this, we examined Pik1 in temperature sensitive mutant strains. When shifted to the NPT for 2 h, three Pik1 temperature sensitive alleles, *pik1-11*, *pik1-83* and *pik1-104*, all showed a decreased protein level (data not shown), suggesting that these point mutations destabilized Pik1 at the NPT.

To extend our analysis on the requirement of Pik1 activity (i.e., the generation of PtdIns4P) for autophagy, we decided to examine an additional mutant strain that affects Pik1 function, and the levels of PtdIns4P at the Golgi complex. The phosphatidylcholine (PC)/phosphatidylinositol (PI) transfer protein Sec14 is required for the transport of vesicles from the *trans*-Golgi (Bankaitis et al., 1990; Bankaitis et al., 1989), and the *sec14-3* mutant displays a major reduction in PtdIns4P, generating ~50% of the wild-type level (Hama et al., 1999). Therefore, we examined whether autophagy is affected in the *sec14-3* mutant using the GFP-Atg8 processing assay. The *sec14-3* mutant cells displayed a clear absence of free GFP after 2-h starvation at the NPT, indicating an autophagic defect, and this defect was recovered after the cells were shifted back to the PT (Figure 4.2), indicating that the generation of PtdIns4P, dependent on Sec14 and Pik1 is essential for autophagy.

Pik1 localizes to both the Golgi and the nucleus (Strahl et al., 2005). To test which population of Pik1 is involved in autophagy, we analyzed a regulatory subunit of Pik1, Frq1, which is targeted to the Golgi and is required for the recruitment of Pik1 to this organelle

(Hendricks et al., 1999; Strahl et al., 2005). As shown by the GFP-Atg8 processing assay, the *frq1-1* mutant displayed a clear temperature-sensitive autophagy phenotype (Figure 4.1.A). At the NPT, the absence of free GFP after 2-h starvation indicated a defect of autophagy induction, and this defect was partially recovered after the cells were shifted back to the PT. As with the *pik1-104* mutant, the autophagy impairment in the *frq1-1* mutant was also observed using the Pho8Δ60 assay (Figure 4.1.B). This result suggested that the Golgi localization of Pik1 was essential for autophagy induction.

Pik1 is involved in mitophagy

PpPik1 was previously reported to play a role in pexophagy in *P. pastoris* (Yamashita et al., 2006). Thus, we speculated that Pik1 may also play roles in selective autophagy in *S. cerevisiae*. Therefore, we extended our analysis of Pik1 to examine its role in mitophagy, the selective autophagic degradation of mitochondria. To detect mitophagy, we first utilized the Om45-GFP processing assay. *OM45* encodes a mitochondrial outer membrane protein, and a chromosomally tagged version with the green fluorescent protein (GFP) at the C terminus is correctly localized on this organelle. Similar to the GFP-Atg8 processing assay, when mitophagy is induced, Om45-GFP, as part of the mitochondria, is delivered into the vacuole for degradation. Om45 is proteolytically removed or degraded, whereas the GFP moiety is relatively stable and accumulates in the vacuole. Therefore, mitophagy can be monitored based on the appearance of free GFP by immunoblot (Kanki and Klionsky, 2008). When growing in rich medium containing lactate as the sole carbon source plus nitrogen (YPL), no free GFP band was detected at either 24°C or 37°C (Figure 4.3.A). After nitrogen starvation at 24°C there was a clear appearance of the free GFP band in wild-type and *pik1-104* mutant cells. At 37°C, significantly reduced free GFP was detected in *pik1-104* compared to the wild type (Figure 4.3.A), indicating a strong mitophagy block in the *pik1-104* mutant. An *atg32*Δ

mutant, which is completely defective in mitophagy, showed a complete block in Om45-GFP processing at either temperature, as expected (Kanki et al., 2009).

We also used the mitoPho8Δ60 assay to quantitatively examine the mitophagy defect in the *pik1* mutant (Kanki et al., 2010). The mitoPho8Δ60 construct is a modified version of Pho8Δ60 that allows the quantitative measurement of mitophagy activity. If *PHO8Δ60* is fused with a mitochondrial targeting sequence, the encoded protein is specifically localized to mitochondria, and the ensuing alkaline phosphatase activity becomes an indicator of mitophagy (Kanki et al., 2010). When mitophagy was induced by nitrogen starvation, wild-type cells showed a dramatic increase in mitoPho8Δ60 activity at both 24°C and 37°C (Figure 4.3.B). In the *pik1-104* mutant, mitophagy induction at the PT was comparable to wild-type cells. In contrast, at the NPT there was a clear decrease of mitoPho8Δ60 activity (Figure 4.3.B), although not as strong as that seen with the Om45-GFP assay (Figure 4.3.A). This difference may reflect the different sensitivities of these two assays. Nonetheless, together, these results demonstrate that Pik1 is also involved in selective autophagy, in particular mitophagy.

Pik1 affects the anterograde movement of Atg9

To further extend our analysis we explored the mechanism through which Pik1 participates in the regulation of selective and nonselective autophagy. Inactivation of Sec7, which is indispensable for post-Golgi transport, affects Atg9 trafficking to the PAS (van der Vaart et al., 2010). Atg9 is the only known conserved transmembrane protein of the yeast autophagy core machinery. Atg9 cycles between the PAS and other peripheral cytoplasmic sites (termed Atg9 reservoirs) and is important for the recruitment of additional Atg proteins (He and Klionsky, 2007). Since Pik1 is also critical for secretion at the Golgi, we hypothesized that the anterograde movement of Atg9 to the PAS would also be affected in the

pik1 mutant.

To test this, we used the TAKA (Transport of Atg9 after Knocking out *ATG1*) assay (Klionsky et al., 2011; Shintani and Klionsky, 2004). In brief, this assay is based on previous findings that Atg9 is retrieved from the PAS back to peripheral sites, and this retrieval process requires the Atg1-Atg13 complex (Reggiori et al., 2004); *atg1*Δ cells accumulate Atg9 almost exclusively at the PAS as a single dot unless the introduction of a second mutation causes its impaired anterograde transport. To check Atg9 localization, we made a functional C-terminal triple GFP fusion protein (Atg9-3GFP); this triple GFP chimera appears stable and does not interfere with the normal function and proper localization of Atg9 (He et al., 2008; Monastyrska et al., 2008). As reported previously, in *atg1*Δ cells, under both growing (data not shown) and starvation conditions, Atg9-3GFP displayed exclusively one single dot at the PAS (marked by RFP-Ape1), irrespective of the temperature (Figure 4.4.A). At 24°C, *atg1*Δ *pik1-104* cells showed the same pattern as the *atg1*Δ cells, whereas at the NPT, Atg9 was present in multiple puncta under both growing (data not shown) and starvation conditions (Figure 4.4.A). In some cells, one of these dots colocalized with the PAS. These data indicated that there was a substantial reduction, but not a complete block, in the anterograde movement of Atg9 to the PAS in the *pik1-104* mutant. A similar trafficking defect was also observed for Atg27, which is another transmembrane protein that also shuttles among the PAS, Golgi complex and other peripheral sites, in the *pik1-104* (Figure 4.4.B) and *pik1-11* (data not shown) mutants.

Because Pik1 functions at the late Golgi, we hypothesized that the defect in Atg9-3GFP localization to the PAS detected in the TAKA assay reflected accumulation of this protein in the *trans*-Golgi network. Accordingly, we further investigated the subcellular localization of Atg9-3GFP in the *pik1* mutant. Newly synthesized Atg9 is transported into the ER and reaches its destination at the Atg9 reservoirs after passing through the Golgi complex,

based on the observation that there is a partial colocalization between Atg9 and the late Golgi protein marker Sec7 (van der Vaart et al., 2010). Therefore, we examined the colocalization of Atg9-3GFP with Sec7-6DsRed in a strain having the mutant *pik1-104* allele. In wild-type cells, Atg9-3GFP was present in multiple puncta, partially colocalized with Sec7. When cultured at the PT and NPT for 30 min, the frequencies of colocalization (quantified by the percentage of cells that showed at least one colocalizing dot) in wild-type cells were 42.9 ± 1.7% and 42.9 ± 0.5% at 24°C and 37°C, respectively (Figure 4.5.A and B, data not shown). In the *pik1-104* mutant, the frequency of Atg9 and Sec7 colocalization was 36.2 ± 6.3% at the PT. In contrast, at the NPT when Pik1 was inactivated, the frequency increased to 64.0% ± 2.5% (Figure 4.5.B). An additional 30-min incubation at the NPT increased the frequency of colocalization in the *pik1-104* mutant to 77.5% ± 4.3% (Figure 4.5.B), whereas the wild-type strain showed only a minor increase in colocalization of 49.6% ± 1.5%. These data underscore the requirement of Pik1 in the exit of Atg9 from the Golgi complex or a post-Golgi compartment, and hence provide an explanation for the failure of additional Atg9 to reach the PAS in the *pik1* mutant. Taken together, our results indicate that Golgi-localized Pik1 is required for normal Atg9 trafficking through the secretory pathway and transport to the PAS, and this defect in Atg9 movement may be the cause of the autophagy defect seen in the *pik1* mutants.

The plasma membrane-localized Stt4 is required for autophagy and mitophagy

Next, we explored the role of the plasma membrane-localized PtdIns 4-kinase Stt4 in autophagy using the GFP-Atg8 processing assay. Similar to the *pik1* mutant, significantly reduced free GFP was detected in a *stt4-4* mutant at 37°C compared to wild-type cells, suggesting a strong defect in autophagy (Figure 4.6.A). Again, a subsequent 2-h starvation at 24°C (R, recovery) restored the autophagy phenotype. This result was also confirmed by the

Pho8Δ60 assay (Figure 4.6.B), although in this case the recovery was clearly less robust; the *stt4-4* mutant showed a quite severe growth phenotype at the NPT, which may have compromised the ability of the mutant strain to recover when shifted back to the PT. To test whether a similar mechanism may apply for Stt4, we also examined Atg9 movement in the *stt4-4* mutant by the TAKA assay; however, normal Atg9 trafficking to the PAS was observed in the *stt4* mutant, as Atg9 accumulated as a single dot in the *atg1*Δ *stt4-4* strain in growing conditions and after starvation at both PT and NPT (Figure 4.6.C). Therefore, the plasma membrane-localized Stt4 is required for autophagy by a mechanism distinct from that of Pik1.

Next, we tested the role of Stt4 in mitophagy using both the Om45-GFP processing and mitoPho8Δ60 assays. After a 6-h starvation at 37°C in the *stt4-4* mutant, a significantly reduced level of free GFP or mitoPho8Δ60 activity was observed compared to the wild type, indicating a strong mitophagy block in this mutant (Figure 4.6.D E). Taken together, these results demonstrated that Stt4 is required for both selective and nonselective autophagy.

The PtdIns4P 5-kinase Mss4 is required primarily for selective autophagy

Stt4 has been previously reported to function upstream of the Pkc1-mediated MAP kinase cascade (Yoshida et al., 1994). Mss4, the only identified PtdIns4P 5-kinase in yeast converts PtdIns4P generated by Stt4 at the plasma membrane into PtdIns(4,5)P_2, which is required for efficient Pkc1-dependent signaling in the cell wall integrity pathway (Audhya and Emr, 2002). Pkc1 is involved in nonselective autophagy regulation (Shahnazari et al., 2010), whereas the downstream MAP kinase of this pathway, Slt2, is involved only in selective types of autophagy (Manjithaya et al., 2010; Mao et al., 2011). Therefore, we tested the role of Mss4 in both autophagy and mitophagy.

First we used the GFP-Atg8 processing assay to test the autophagy phenotype in a

temperature sensitive *mss4-103* mutant strain. A comparable free GFP band was observed after 2-h starvation at 37°C in this mutant relative to the wild type, suggesting that there was not a major autophagy defect in the *mss4-103* mutant (Figure 4.7.A). We further confirmed this result by the quantitative Pho8Δ60 assay; a slightly decreased, but still comparable Pho8Δ60 activity was observed in the *mss4-103* mutant at 37°C (Figure 4.7.B). Therefore, these results demonstrated that Mss4 was not required for nonselective autophagy. This finding agrees with the observation that Stt4 appears to have an Mss4-independent function in the regulation of cell wall maintenance, as the *stt4-4* mutant cannot be rescued by overexpression of Mss4 (Audhya et al., 2000).

Next, we tested the role of Mss4 in mitophagy by both the Om45-GFP processing and mitoPho8Δ60 assays. After 6-h starvation at 37°C in the *mss4-103* mutant, a significantly reduced level of free GFP or mitoPho8Δ60 activity was observed compared to the wild type, indicating a strong mitophagy block in this mutant almost as severe as seen in the *atg32*Δ strain (Figure 4.7.C and Figure 4.6.E). Taken together, these results demonstrated that Mss4 is specifically involved in selective, but not nonselective autophagy.

4.5 Discussion

The importance of phosphoinositides in autophagy regulation has been demonstrated by the study of the Vps34-containing PtdIns 3-kinase complex in yeast (Kihara et al., 2001), and both the PtdIns 3-kinase and PtdIns3P 5-kinase in mammalian cells (Ho et al., 2012; Lindmo and Stenmark, 2006). However, relatively little attention has been paid to the role of PtdIns 4-kinases in autophagy (Yamashita et al., 2006), and, to our knowledge, there is no information regarding the function of such enzymes in autophagy in *S. cerevisiae*. Here, we reported the involvement of two other enzymes, a PtdIns 4-kinase and PtdIns4P 5-kinase, in selective and nonselective autophagy. We demonstrated that two major yeast PtdIns 4-kinases,

Pik1 and Stt4, are both required for autophagy. In addition, we also showed that the PtdIns4P 5-kinase Mss4 is specifically involved in mitophagy.

While the mechanism through which plasma membrane-localized Stt4 affects autophagy is still under study, we showed that Golgi-localized Pik1, which plays an essential role in vesicle exit from this organelle, may be involved in autophagy by affecting normal Atg9 trafficking to the PAS. This conclusion is consistent with several recent studies that demonstrate Atg9 traffics through part of the secretory pathway to the peripheral Atg9 reservoirs (Mari et al., 2010; Nair et al., 2011), and exit from the Golgi complex is required for normal Atg9 trafficking (Geng et al., 2010; van der Vaart et al.). However, little is known about Atg9 trafficking beyond Golgi exit. Atg9 does not colocalize with any known organelle markers after leaving the Golgi, and electron microscopy data suggest that Atg9 becomes part of a structure called the tubulovesicular cluster (TVC) (Mari et al., 2010; Nair et al., 2011). Atg27 and Atg23 are two other proteins found at the TVC; however, except for these morphological studies, we do not know anything more about this structure. As Pik1-generated PtdIns4P is also important for vesicle transport after exit from the Golgi, we speculated that Pik1 might play a role(s) in directing Atg9-containing vesicles from the Golgi to their next destination. This function could be achieved by the recruitment of a PtdIns4P effector protein(s) that is involved in autophagy. Unfortunately, even though we tested several potential PtdIns4P effectors (Mdr1, Ysp2, Yfl042C, Yhr080C and Ylr072W) that have a GRAM domain with the capacity to bind PtdIns4P (Yamashita et al., 2006), we did not observe an autophagy defect (data not shown). Therefore, a still unknown effector(s) might participate in PtdIns4P-mediated Atg9 trafficking to the TVC. Identifying the potential effector(s) may provide critical insight into the formation of the TVC, and thus would be helpful in adding to our understanding of the organization of the PAS.

We also reported that Pik1 plays an important role in mitophagy. The observation that

PtdIns4P participates in the formation of the micropexophagic apparatus provided the initial insight into the connection between PtdIns4P and selective autophagy (Yamashita et al., 2006). Our results that Pik1 is required for mitophagy extended this finding. For further exploration, we also tested possible colocalization of a PtdIns4P marker (GFP-Osh2-PH) with the mitophagy marker protein Atg32, but we did not observe a significant level of colocalization (data not shown). This result could reflect the inability of this PtdIns4P probe to mark all cellular PtdIns4P, or the possibility that the population of PtdIns4P that participates in mitophagy may not be sufficient to be detectably marked by GFP-Osh2-PH.

In the meantime, it remains unclear as to how the plasma membrane-localized Stt4 participates in autophagy. Our results excluded the possibility that Stt4 acts solely as an upstream factor of Mss4 for autophagy, because the PtdIns4P 5-kinase Mss4 that functions at the plasma membrane is dispensable for nonselective autophagy, although Mss4 is required for mitophagy. PtdIns(4,5)P_2 is important for the organization of the actin cytoskeleton (Desrivieres et al., 1998), which is involved in selective autophagy (Reggiori et al., 2005). The actin cytoskeleton may facilitate cargo transport to the PAS. However, we found that Atg32 trafficking to the mitochondria-specific PAS is essentially normal in the *mss4-103* mutant (data not shown). Further study is thus required to understand the role of Mss4 in mitophagy.

In summary, our study established a role of PtdIns 4-kinases and PtdIns4P 5-kinases in selective and nonselective autophagy pathways, and provides the first information on the mechanism by which the PtdIns 4-kinase may regulate these processes. Continued studies should provide additional insight into how these enzymes control autophagy.

4.6 Figures

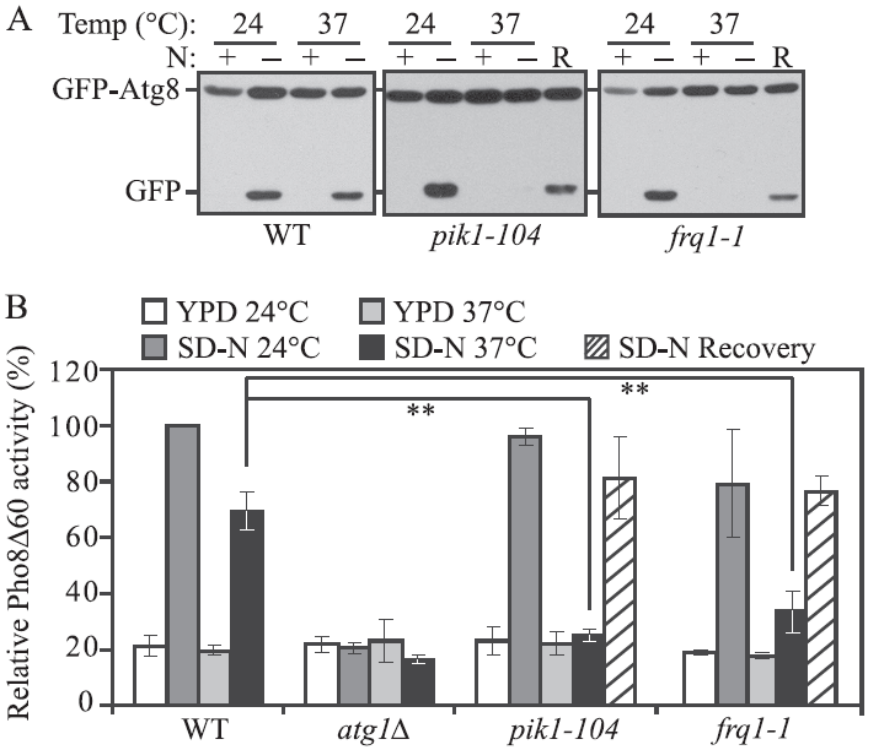

Figure 4.1 Pik1 is required for autophagy.
(A) GFP-Atg8 processing is blocked in the *pik1-104* and *frq1-1* mutants. Wild-type (WT; BY4742), *pik1-104* (BY4742), and *frq1-1* (BY4742) strains transformed with a plasmid expressing GFP-Atg8 under the control of the *CUP1* promoter were grown in SMD-Ura medium at 24°C to mid-log phase. For each strain, the culture was divided into two aliquots. One aliquot was preincubated at 37°C for 30 min and shifted to SD-N for 2 h at 37°C, then (for the mutants) shifted back to 24°C for another 2 h (R, recovery). The other aliquot was kept at 24°C for 30 min and then shifted to SD-N for 2 h at 24°C. For each aliquot, samples were taken before (N+) and after (N-) starvation and at the recovery stage. Immunoblotting was done with anti-YFP antibody and the position of full-length GFP-Atg8 and free GFP are indicated.
(B) Nonspecific autophagy is blocked in the *pik1-104* and *frq1-1* mutants. WT (YTS158), *atg1*Δ (TYY127), *pik1-104* (ZFY281) and *frq1-1* (ZFY280) strains were cultured as in A, but the incubation time in SD-N was increased to 4 h; recovery was carried out as in A. The Pho8Δ60 activity was measured as described in Experimental Procedures. Error bars represent the standard deviations (SD), which were obtained from at least three independent repeats. **, $p<0.005$.

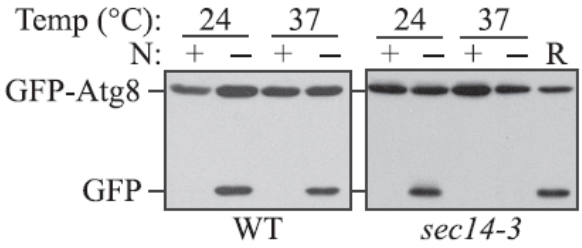

Figure 4.2 Sec14 is required for autophagy.
GFP-Atg8 processing is blocked in the *sec14-3* mutant. Wild-type (WT; BY4742) and *sec14-3* (BY4742) strains transformed with a plasmid expressing GFP-Atg8 under the control of the *CUP1* promoter were cultured as in Figure 1A. Samples were taken before (N+) and after (N-) starvation and at the recovery stage (R). Immunoblotting was done with anti-YFP antibody and the positions of full-length GFP-Atg8 and free GFP are indicated.

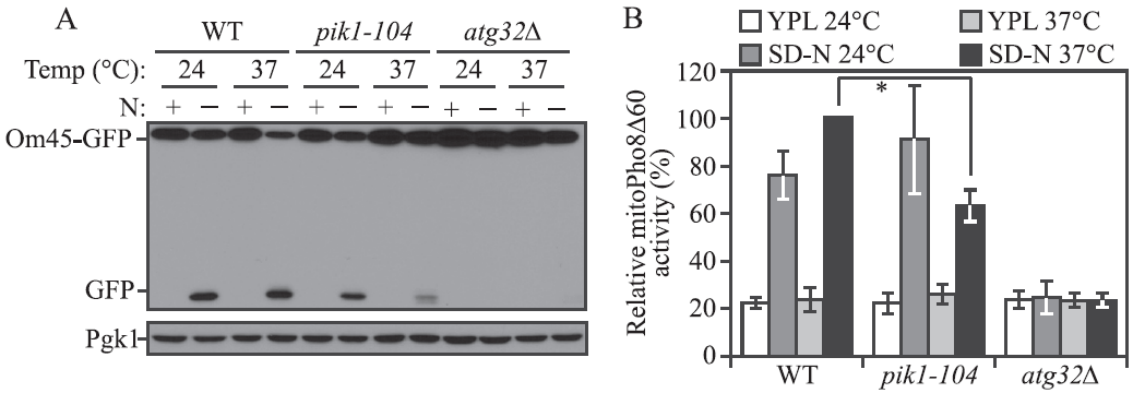

Figure 4.3 Mitophagy is defective in the absence of Pik1 activity.
(A) Om45-GFP processing is blocked in the *pik1-104* mutant. *OM45* was chromosomally tagged with *GFP* in the wild-type (WT; TKYM107), *atg32*Δ (TKYM137) and *pik1-104* (KWY81) strains. Cells were cultured in YPL to mid-log phase at 24°C, and then the culture was divided into two aliquots. One aliquot was kept at 24°C for 30 min and then shifted to SD-N for 6 h at 24°C. The other aliquot was preincubated at 37°C for 30 min and then shifted to SD-N for 6 h at 37°C. For each aliquot, samples were taken before (N+) and after (N-) starvation. Protein extractes were probed with anti-YFP antibody and anti-Pgk1 antibody (the latter as a loading control).
(B) The mitoPho8Δ60 activity is reduced in the *pik1-104* mutant. WT (KWY20), *atg32*Δ (KWY22), and *pik1-104* (KWY79) strains were cultured as in *C*. The mitoPho8Δ60 activity was measured as described in Experimental Procedures. Error bars correspond to the SD from at least three independent repeats. *, $p<0.01$.

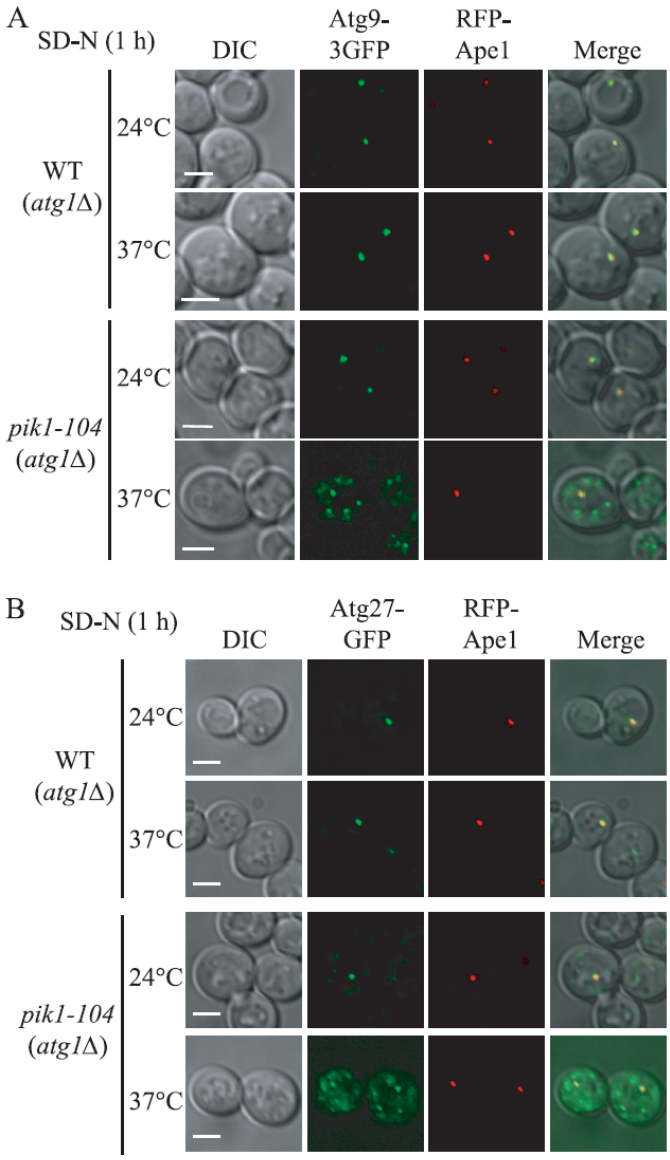

Figure 4.4 Atg9 and Atg27 trafficking is defective in the *pik1* mutant.
(A) Atg9 anterograde movement to the PAS is defective in the *pik1* mutant. Wild-type (WT; ZFY270) and *pik1-104* (ZFY273) strains in an *atg1*Δ background were cultured as in Figure 1, and shifted to SD-N for 1 h. The localization of Atg9-3GFP and RFP-Ape1 was observed for samples cultured at the indicated temperature.
(B) Atg27 trafficking to the PAS is defective in the *pik1* mutant. Wild-type (WT; ZFY070), *pik1-11* (ZFY299) and *pik1-104* (ZFY301) strains were cultured as in *A*. The localization of Atg27-GFP and RFP-Ape1 was observed for samples cultured at the indicated temperature. Representative pictures from single Z-section images are shown. DIC, differential interference contrast. Scale bars, 5 μm.

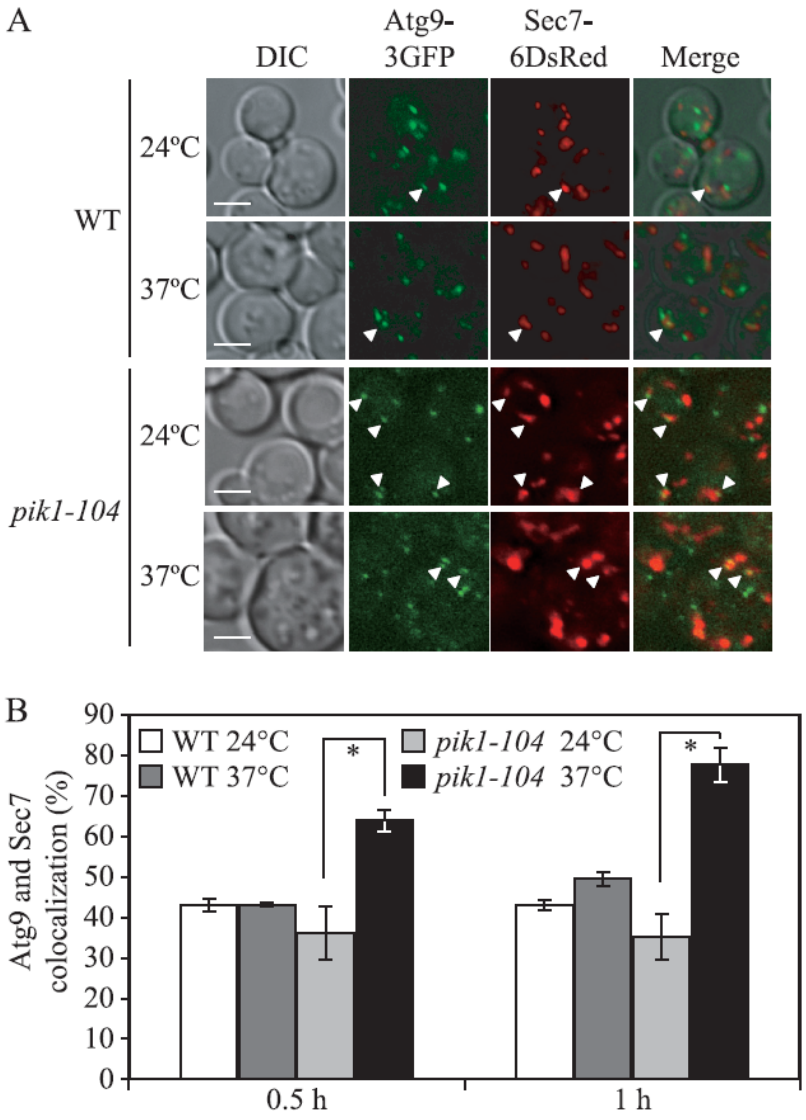

Figure 4.5 Atg9 exit from the Golgi is defective in the *pik1* mutant.
(A) WT (ZFY326) and *pik1-104* (ZFY328) strains were cultured in SMD medium at 24°C to mid-log phase and then divided into two aliquots. One aliquot was kept at 24°C and the other aliquot was shifted to 37°C for 0.5 h. The localization of Atg9-3GFP and Sec7-6DsRed was observed for samples cultured at the indicated temperature. Representative pictures from single Z-section images are shown. DIC, differential interference contrast. Scale bars, 5 μm.
(B) Quantification of the colocalization of Atg9-3GFP and Sec7-6DsRed from the data in *A* and after an additional 30 min at the indicated temperatures. Error bars represent the SD from at least three independent repeats. *, $p<0.05$.

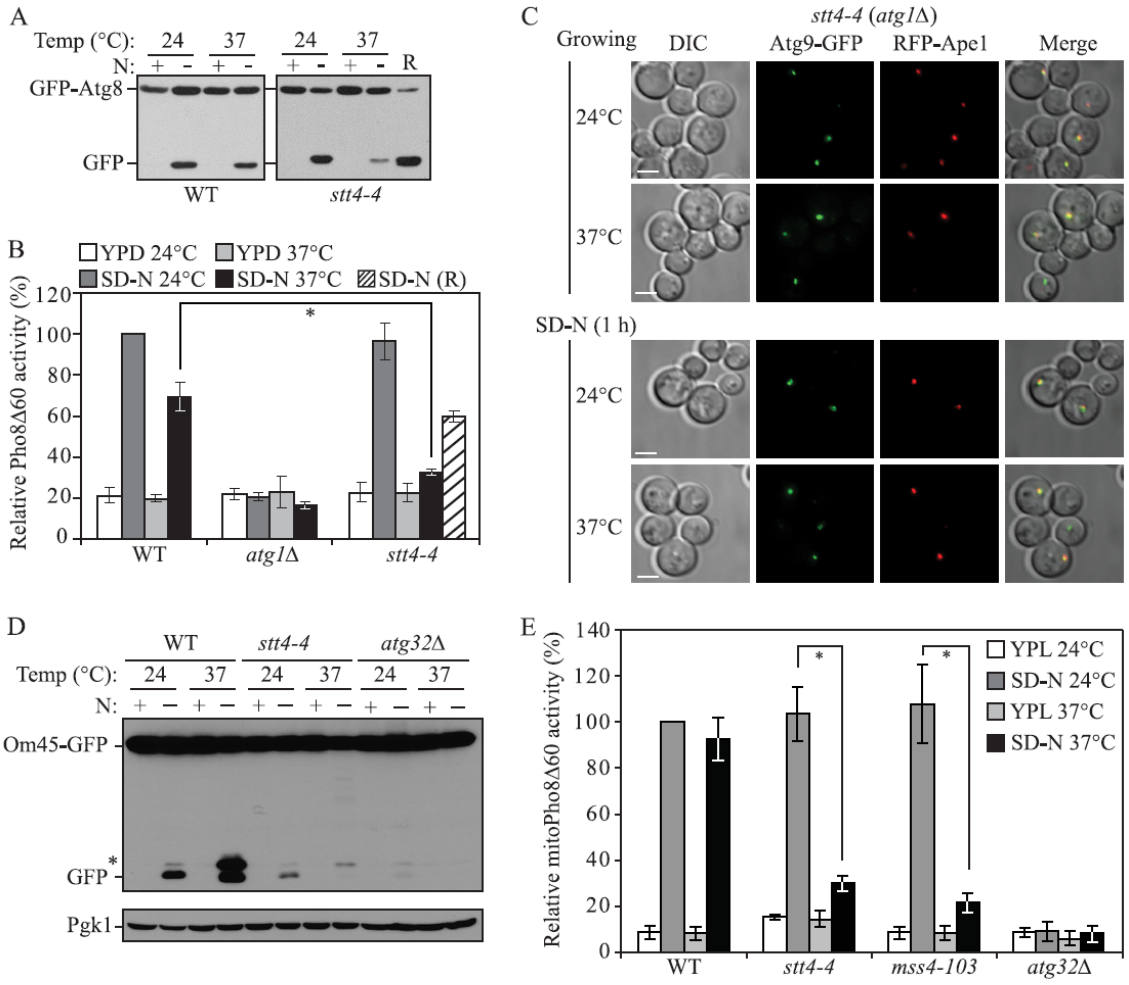

Figure 4.6 Stt4 is required for autophagy.

(A) GFP-Atg8 processing is blocked in the *stt4-4* mutant. Wild-type (WT; BY4742) and *stt4-4* (BY4742) strains transformed with a plasmid expressing GFP-Atg8 under the control of the *CUP1* promoter were cultured as in Figure 1A. Samples were taken before (N+) and after (N-) starvation and at the recovery stage (R). Immunoblotting was done with anti-YFP antibody and the positions of full-length GFP-Atg8 and free GFP are indicated.

(B) Pho8Δ60 activity is blocked in the *stt4-4* mutant. WT (YTS158), *atg1*Δ (TYY127), and *stt4-4* (ZFY282) strains were cultured as in Figure 1B. The Pho8Δ60 activity was measured as described in Experimental Procedures. Error bars represent the SD, which were obtained from at least three independent repeats.

(C) Atg9 anterograde movement to the PAS is normal in the *stt4-4* mutant. The *stt4-4* strain was cultured as in Figure 4A. The localization of Atg9-GFP and RFP-Ape1 was observed for samples cultured at the indicated temperature in growing or starvation conditions. Representative pictures from single Z-section images are shown. DIC, differential interference contrast. Scale bars, 5 μm.

(D) Om45-GFP processing is blocked in the *stt4-4* mutant. *OM45* was chromosomally tagged with *GFP* in the wild-type (WT; TKYM107), *atg32*Δ (TKYM137) and *stt4-4* (KWY80) strains. Cells were cultured as in Figure 3A. Samples were taken before (N+) and after (N-) starvation. Protein extractes were probed with anti-YFP antibody and anti-Pgk1 antibody (the latter as a loading control). The asterisk marks a nonspecific band. *E*, The mitoPho8Δ60

activity is reduced in the *stt4-4* and *mss4-103* mutants. Wild-type (KWY84), *atg32*Δ (KWY87), *stt4-4* (KWY85) and *mss4-103* (KWY86) strains were cultured as in *D*. The mitoPho8Δ60 activity was measured as described in Experimental Procedures. Error bars correspond to the SD from at least three independent repeats. *, $p<0.01$.

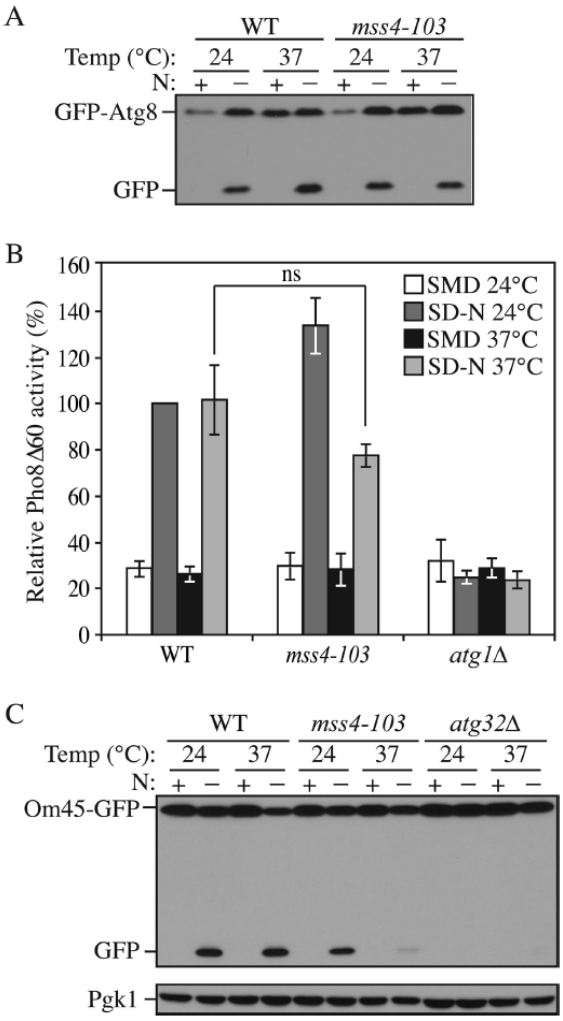

Figure 4.7 Mss4 is required for mitophagy, but not nonselective autophagy.
(A) GFP-Atg8 processing is normal in the *mss4-103* mutant. Wild-type (WT; BY4742) and *mss4-103* (BY4742) strains transformed with a plasmid expressing GFP-Atg8 under the control of the *CUP1* promoter were cultured as in Figure 1A, but without the recovery stage. Samples were taken before (N+) and after (N-) starvation. Immunoblotting was done with anti-YFP antibody and the positions of full-length GFP-Atg8 and free GFP are indicated.
(B) The Pho8Δ60 activity is normal in the *mss4-103* mutant. WT (YTS158), *atg1*Δ (TYY127) and *mss4-103* (KWY83) strains were cultured as in Figure 1B. The Pho8Δ60 activity was measured as described in Experimental Procedures. Error bars represent the SD, which were obtained from at least three independent repeats.
(C) Om45-GFP processing is blocked in the *mss4-103* mutant. Wild-type (TKYM107), *atg32*Δ (TKYM137) and *mss4-103* (KWY82) strains were cultured as in Figure 3A. Samples were taken before (N+) and after (N-) starvation. Protein extractes were probed with anti-YFP antibody and anti-Pgk1 antibody (the latter as a loading control). ns (not significant), $p>0.05$.

Chapter V
CONLUSION AND DISCUSSION

This chapter is reprinted from the book Autophagy: Cancer, Other Pathologies, Inflammation, Immunity, Infection, and Aging, Volume 4, Chapter 2, Ke Wang and Daniel Klionsky, Molecular Process and Physiological Significance of Mitophagy, in press, with minor modifications.

The past decades have seen great advancement of our knowledge in both the molecular mechanism and physiological significance of autophagy. Mitochondria have also been clearly demonstrated to be a substrate selectively recognized by the autophagic machinery for degradation. The process of mitophagy has attracted great attention during recent years for it may serve as a defense mechanism against mitochondria-dysfunction related diseases. Here, I am going to summarize our current understanding of the molecular mechanism and physiological relevance of mitophagy from knowledge generated by both this thesis and other related research.

5.1 Mitophagy in Yeast

As previously discussed in Chapter II, when yeast cells are cultured in media with a nonfermentable carbon source, such as lactate or glycerol, they shift from anaerobic fermentation to aerobic respiration resulting in mitochondria proliferation. When these cells are transferred to nitrogen-starvation medium supplemented with glucose as the carbon source, mitophagy occurs primarily as a mechanism to eliminate superfluous mitochondria. In addition, mitophagy can also be induced when cells grow under aerobic respiration

conditions into the post-log phase (Kanki and Klionsky, 2008). In this case, mitophagy may be induced as a quality control mechanism to eliminate damaged mitochondria caused by oxidative stress during post-log phase growth (Okamoto et al., 2009).

Core autophagy machinery proteins and Atg11 are required for mitophagy, demonstrating that this is a selective form of autophagy (Kanki and Klionsky, 2008). Two genetic screens targeted to identify mitophagy-related genes led to the discovery of Atg32 as the receptor protein that confers selectivity for mitochondrial recognition and sequestration (Figure 5.1.A) (Kanki et al., 2009; Okamoto et al., 2009).

As discussed above, Atg32 is a mitochondrial outer membrane protein that contains a single transmembrane domain with its N terminus facing the cytosol and the C terminus in the intermembrane space (Kanki et al., 2009; Okamoto et al., 2009). As a mitochondrial resident protein, Atg32 bridges the degrading fragment of mitochondria with the autophagic machinery through its interactions with the scaffolding protein Atg11 and Atg8; however, the interaction between Atg32 and Atg8 appears to not be essential for mitophagy, because disruption of this interaction only causes a partial block of mitophagy activity (Kondo-Okamoto et al., 2012). The mitochondrial reticulum is large and is not a good target for sequestration. Accordingly, fission is a critical step in the process that generates mitochondria fragments that are amenable to inclusion within an autophagosome. Cytosolic Atg11 interacts with the fission protein Dnm1, which is subsequently recruited to mitochondria via the interaction of Atg11 with Atg32 (Mao et al., 2013).

Considering the essential roles of mitochondria in the cell, the process of mitophagy needs to be tightly controlled. Several recent studies have established at least some of the regulatory mechanisms of mitophagy. First, Atg32 undergoes starvation-dependent phosphorylation (Aoki et al., 2011). When mitophagy is induced, S114 and S119 on the N terminus of Atg32 are phosphorylated. These phosphorylation events are important for

Atg32-Atg11 interaction and subsequent mitophagy induction. Hog1 and Pbs2, kinases of the mitogen-activated protein kinase pathway, are important for mitophagy activity, although these kinases are not directly involved in Atg32 phsophorylation (Aoki et al., 2011). Instead, casein kinase 2 directly phosphorylates Atg32 on these two sites and regulates mitophagy activity (Kanki et al., 2013).

In addition to phosphorylation, recent work has demonstrated that Atg32 also undergoes another level of regulation through the proteolytic processing of its intermembrane space region at the C terminus (Wang et al., 2013). In this case, the mitochondrial i-AAA protease Yme1 mediates Atg32 processing and is required for efficient Atg32 and Atg11 interaction and subsequent mitophagy activity. Since Yme1 is an important component of the proteolysis level mitochondrial quality control system and is responsible for the degradation of unfolded or misfolded mitochondrial proteins (Weber et al., 1996), this study suggests a crosstalk between different mitochondria quality control mechanisms.

Physiologically, mitophagy occurs in yeast as a system that acts to prevent the damaging effect of functionally compromised mitochondria (Kurihara et al., 2012). When mitophagy-deficient (*atg11*Δ or *atg32*Δ) cells are challenged with nutrient starvation, mitochondria cannot be degraded and are vulnerable to damage resulting from exposure to ROS. These damaged mitochondria gradually lose their mitochondrial DNA, and cells bearing these mitochondria exhibit a 'petite' phenotype, being unable to grow on non-fermentable carbon sources. Therefore, mitophagy in yeast plays an essential role in maintaining mitochondria quality.

5.2 Mitophagy in Mammalian Cells

Autophagy also plays a critical role in mitochondria degradation in higher eukaryotes. In fact, mitochondria were detected inside an autophagosome in the kidney cells of mice as

early as the 1950s (Clark, 1957). Multiple stress conditions can induce mitophagy in mammalian cells such as starvation (Egan et al., 2011), CCCP-induced disruption of mitochondria membrane potential (Narendra et al., 2008a), and hypoxia (Liu et al., 2012). In addition, mitophagy can also be observed during normal development such as occurs during the maturation of erythrocytes (Sandoval et al., 2008) and in the process of spermatogenesis in some organisms (Al Rawi et al., 2011). Our knowledge of the molecular process of mitophagy in mammalian cells has greatly expanded during recent years. As mentioned above, there is no clear counterpart of Atg11 that acts as a scaffold in mammalian cells so that the molecular machinery involved in mammalian mitophagy is more diverse. In fact, in contrast to yeast cells, most mammalian cells need to constantly undergo aerobic respiration, so it is possible that mammalian cells may face a more stringent and complicated situation with regard to the regulation of mitochondria quantity and quality. During recent years, different proteins have been discovered to mediate mitophagy, either in different cellular processes or in response to different stimuli. Despite the differences in the particular mechanisms, the association of mitochondria with the molecular machinery of autophagy typically involves LC3.

BNIP3L and BNIP3

One of the very first studies in mammalian cells in regard to the molecular mechanism of mitophagy is the discovery of BNIP3L in the selective elimination of mitochondria during the maturation of erythrocytes (Sandoval et al., 2008). During terminal differentiation, erythroid cells undergo autophagic elimination of organelles including mitochondria. BNIP3L, a BH3-only member of the BCL2 family, is a mitochondrial outer membrane protein essential for this process (Schweers et al., 2007). *bnip3l*$^{-/-}$ mice display a reduced number of mature erythrocytes, and exhibit mitochondrial retention and defective entry of

mitochondria into autophagosomes (Sandoval et al., 2008). This study also established the primary link between the loss of mitochondrial membrane potential and mitophagy. More recent studies revealed that BNIP3L has a WXXL motif in its N terminus and can bind to Atg8 homologs, especially LC3A and the GABARAP sub-family. The interaction of BNIP3L with Atg8 homologs is upregulated upon mitochondrial stress such as occurs following treatment with rotenone or the mitochondrial uncoupler CCCP, which potently induce mitophagy. Mutation of the WXXL motif reduces the interaction and causes a defect in mitochondria clearance (Novak et al., 2010). Therefore, BNIP3L plays a role in mitophagy through linking the degrading mitochondria with LC3. The BNIP3L-LC3 model is reminiscent of the Atg32-Atg11 model in yeast cells, and thus BNIP3L is also considered to function as a mammalian mitophagy receptor (Figure 5.1.B).

More recently, BNIP3, a protein homologous to BNIP3L, has been reported to be involved in mitophagy (Zhu et al., 2013). BNIP3 shares high sequence similarity with BNIP3L including the LIR motif, and BNIP3 also interacts with LC3. Both proteins also have a similar mitochondrial localization pattern. Interestingly, Serine residues 17 and 24 flanking the BNIP3 LIR region are phosphorylated, and this phosphorylation is important for binding to the LC3 family proteins LC3B and GABARAPL2/GATE-16 (Zhu et al., 2013). This result suggests that a similar regulatory mechanism of receptor phosphorylation as with Atg32 may also occur with mitophagy receptor proteins in mammalian cells (Figure 5.1.C). However, whether BNIP3L undergoes a similar type of regulation through phosphorylation remains to be discovered.

FUNDC1

Another mitochondrial outer membrane protein, FUNDC1, functions as a mitophagy receptor and plays an important role in hypoxia-induced mitophagy (Liu et al., 2012).

FUNDC1 interacts with LC3 through a LIR consisting of the residues YXXL (equivalent to WXXL), and mutation of this region abolishes its interaction with LC3 and subsequent mitophagy. FUNDC1 overexpression induces mitophagy in multiple cell lines and knockdown of endogenous FUNDC1 causes a defect in hypoxia-induced mitophagy. Interestingly, FUNDC1 seems to play a less important role in starvation-induced mitophagy or CCCP-induced mitophagy, suggesting different mechanisms may be responsible for mitophagy that occurs in response to different stress conditions.

Similar to the case of Atg32 and BNIP3L, FUNDC1-mediated mitophagy is also regulated by its phosphorylation. SRC kinase phosphorylates FUNDC1 at Tyr18 in the LIR motif under normal physiological conditions. In contrast to the regulation of BNIP3L and Atg32, SRC is inactivated upon hypoxia, and FUNDC1 is subsequently dephosphorylated, leading to its enhanced association with LC3, which in turn results in the selective incorporation of the degrading mitochondria into the phagophore. The phosphatases that are predicted to be involved in the dephosphorylation of Tyr8 on FUNDC1 have not been identified, but this would add another level of regulation (Figure 5.1.D).

In conclusion, the LIR-containing motif in BNIP3L and FUNDC1, functionally similar to the Atg8-family interacting motif in Atg32, acts as a central mitophagy signaling transduction domain and is thus highly regulated in response to different cellular signals.

PARK2 and PINK1

The discovery of the involvement of PARK2 in mitophagy is another milestone in mammalian mitophagy studies. PARK2 is a cytosolic E3-ubiquitin ligase that mediates proteasomal protein degradation (Kitada et al., 1998). Mutations in *PARK2* are associated with the familial autosomal recessive juvenile form of Parkinson disease (Kitada et al., 1998), and the association of PARK2 with mitophagy provides an intriguing possibility to explain

the pathogenesis of PD. Upon treatment with the mitochondrial uncoupler CCCP, PARK2 rapidly translocates from the cytosol to mitochondria, followed by substantial mitochondria degradation. PARK2 is selectively recruited to the mitochondrial fragments with reduced membrane potential, suggesting that the cell has a mechanism to distinguish between healthy and damaged mitochondria; recruitment of PARK2 specifically promotes the elimination of dysfunctional mitochondria fragments. The degradation of damaged mitochondria is dependent on autophagy proteins such as ATG5, demonstrating that the process is mediated through autophagy. Indeed, these PARK2-marked mitochondrial fragments are LC3-positive, providing direct evidence that the clearance of these fragments occurs through autophagy. In addition, similar PARK2 translocation is also observed following treatment with paraquat, a herbicide frequently used in the study of PD.

The translocation of PARK2 to the damaged mitochondria requires another PD-related protein, PINK1 (PTEN induced putative kinase 1). PINK1 is a mitochondrial membrane-arnchored protein kinase. Genetic studies in *Drosophila* suggested that Pink1 and Park function in the same pathway. Several studies reported that PINK1 plays a role in the recruitment of PARK2 (Matsuda et al., 2010; Narendra et al., 2010b; Vives-Bauza et al., 2010), and overexpression of PINK1 is sufficient to induce PARK2 translocation to mitochondria even without mitochondrial membrane depolarization via uncouplers. In healthy mitochondria, PINK1 is constitutively expressed and imported via the TOMM-TIMM complex, to the mitochondrial inner membrane, where it is rapidly degraded through proteolysis by the inner membrane rhomboid protease PARL (presenilin associated, rhomboid-like) (Zhu et al., 2013). However, when mitochondria depolarize, PINK1 import into the inner membrane is impaired and subsequent proteolysis is inhibited, leading to a rapid accumulation of PINK1 on the outer membrane of damaged mitochondria, and the subsequent recruitment of PARK2. While PINK1 has been reported to be able to bind and

phosphorylate PARK2, and PINK1 kinase activity is also required for PARK2 recruitment (Kim et al., 2008), how PINK1 phosphorylation of PARK2 affects the latter's recruitment and subsequently drives mitophagy is still under investigation.

As an E3 ubiquitin ligase, PARK2 ubiquitinates a subset of mitochondrial substrates(Chan et al., 2011). As with PINK1 function, however, how PARK2-mediated ubiquitination initiates the onset of mitophagy remains unclear. Multiple mitochondrial outer membrane proteins are rapidly degraded following PARK2-mediated polyubiquitination, suggesting the activation of the ubiquitin-proteasome system is an important step prior to PARK2-mediated mitophagy (Chan et al., 2011). VDAC1 is a substrate for PARK2 and may be required for PARK2-mediated mitophagy (Geisler et al., 2010), but this conclusion is not fully supported by other studies (Narendra et al., 2010a). MFN1 and MFN2 are also ubiquitinated by PARK2 upon mitophagy induction and are subsequently degraded in the proteasome (Tanaka et al., 2010). MFN1 and MFN2 are large GTPases that mediates mitochondrial fusion. Therefore, the degradation of MFN1 and MFN2 results in mitochondria fragmentation, which promotes subsequent mitophagy; this process may be functionally equivalent to Dnm1-dependent fission and mitophagy in yeast. However, PARK2 is also able to ubiquitinate the mitochondrial fission protein DNM1L/DRP1, leading to its degradation (Wang et al., 2011b). Furthermore, what mediates the association of degrading mitochondria marked by PARK2 with the autophagic machinery remains unclear. The ubiquitin binding adaptor protein SQSTM1 may play such role due to its ability to bind to both ubiquitin and LC3; and SQSTM1 accumulates on mitochondria following PARK2-mediated ubiquitination (Geisler et al., 2010). However, whether SQSTM1 is essential for PARK2-mediated mitophagy remains controversial (Narendra et al., 2010a). Nonetheless, these lines of research provided important insights into how mitochondria dysfunction may be associated with the pathogenesis of PD. Indeed, several studies showed that disease-associated *PARK2*

and *PINK1* mutations result in defective mitophagy, thereby implicating the involvement of mitophagy defects in the development of PD (Lee et al., 2010; Matsuda et al., 2010; Narendra et al., 2010) (Figure 5.1.E).

5.3 Discussion and Perspectives

Although our understanding of the molecular process and physiological significance of mitophagy has greatly advanced during the last few years, further questions remain to be addressed. First, despite the well-established model of PARK2-mediated mitophagy, the research has primarily been carried out using mammalian cell lines. Gaps are apparent in our understanding of the activity of mitophagy and the pathogenesis of age-related diseases such as PD, AD and HD. Although PARK2 and PINK1 mutation seen in PD patients result in extensive mitophagy defects in cultured cells, *in vivo* evidence is still lacking in regard to the connection between defective mitophagy and the onset of PD. It will therefore be very helpful to generate knockout or knockdown mouse models of the mitophagy-related proteins to study their relationship with distinct diseases.

Second, the list of mitophagy-related proteins is expanding; however, we are still largely ignorant of the upstream signaling events that regulate mitophagy. Unidentified kinases, phosphatases and other signaling molecules play important roles in the regulation of mitophagy through modification of the relevant receptor proteins. How these signaling molecules are associated with the bigger picture of mitochondria metabolism, such as ROS production and energy generation, is a question that needs to be further addressed.

Third, the discovery of different mechanisms of mitophagy provokes the intriguing question of the possible cross-talk between these mitophagy pathways. Evidence suggests that these pathways are not totally independent of each other. For example, BNIP3L was initially identified in the process of erythrocyte maturation; however, later studies

demonstrated that it is also involved in CCCP-induced mitophagy (Novak et al., 2010), where PARK2 is known to play a key role. How cells coordinate these different mitophagy pathways remains an interesting topic for future study.

Fourth, the discrepancy between yeast mitophagy and mammalian mitophagy needs more attention. Mitochondria dysfunction caused by a loss of mitochondria membrane potential has been clearly shown to be a potential inducing signal for mitophagy in mammalian cells; however, the same signal does not induce mitophagy efficiently in yeast (our unpublished data). Nonetheless, mitophagy is important for yeast to survive extensive oxidative stress. Intriguingly, the yeast *Saccharomyces cerevisiae* is adapted to carry out fermentation, instead of respiration, during normal growth conditions in the presence of glucose regardless of the availability of oxygen, which is reminiscent of the metabolic pattern of tumors. Therefore, a deeper understanding and characterization of the regulation of mitophagy in yeast may provide insight into the connection between mitophagy and cancer.

While mitochondrial activity and quality are highly regulated through mitophagy-dependent degradation, recent studies in yeast demonstrated that the maintenance of a healthy population of mitochondria is in return required for proper autophagy activity (Graef and Nunnari, 2011). Defects in mitochondrial respiration cause the activation of cAMP-dependent protein kinase A and lead to autophagy inhibition. Therefore, this observation adds another level of interplay between mitochondrial function and autophagy, and suggests a possible link between mitochondrial dysfunction and disease through the deregulation of autophagy. Since this study was carried out in yeast cells, it will be intriguing to see whether the same mechanism is also present in higher eukaryotes.

5.4 Figures

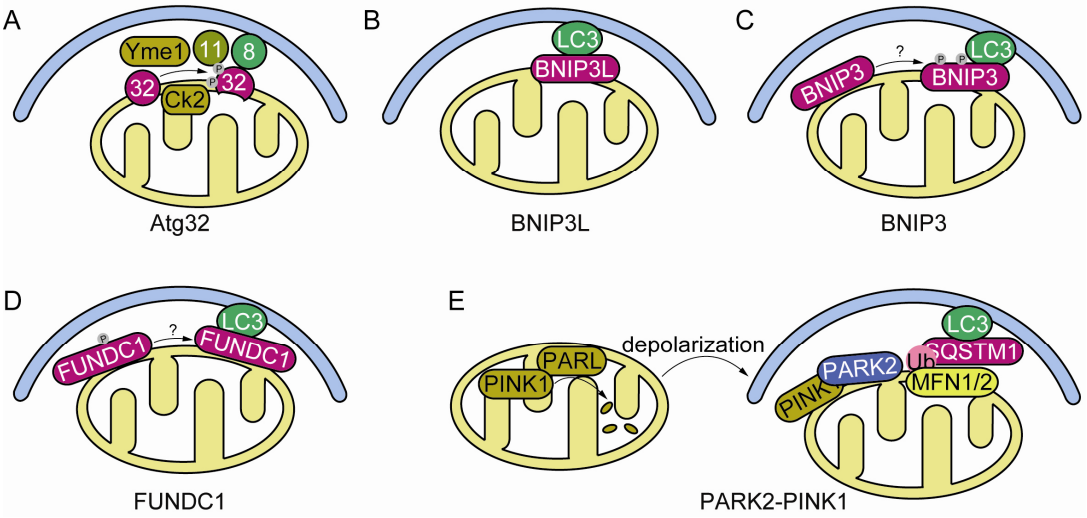

Figure 5.1 Different mechanisms of mitophagy are illustrated schematically
(A) Atg32-mediated mitophagy. Atg32 is phosphorylated by casein kinase 2 (Ck2), and processed by Yme1. The modified Atg32 interacts with Atg11 and brings mitochondria to the autophagic machinery for degradation.
(B) BNIP3L-mediated mitophagy. BNIP3L interacts with LC3 through its LIR domain.
(C) BNIP3-mediated mitophagy. BNIP3 is phosphorylated by an unknown kinase. Phosphorylated BNIP3 interacts with LC3.
(D) FUNDC1-mediated mitophagy. FUNDC1 is constitutively phosphorylated by SRC kinase (not shown). Hypoxia leads to the inactivation of SRC and dephosphorylation of FUNDC1 by an unknown phosphatase. Dephosphorylated FUNDC1 interacts with LC3.
(E)PARK2-PINK1-mediated mitophagy. PINK1 is steadily imported into mitochondria, where the PARL protease mediates its degradation. Mitochondria depolarization inhibits PARL activity and PINK1 import, which leads to the accumulation of PINK1 on the outer membrane, and the subsequent recruitment of PARK2. PARK2 then ubiquitinates several mitochondrial proteins including MFN1/2. The ubiquitinated MFN1/2 may be recognized by SQSTM1, which interacts with LC3 and directs the mitochondria to the autophagic machinery for degradation.

REFERENCES

Abeliovich, H., and Klionsky, D.J. (2001). Autophagy in yeast: mechanistic insights and physiological function. Microbiol Mol Biol Rev *65*, 463-479, table of contents.

Al Rawi, S., Louvet-Vallee, S., Djeddi, A., Sachse, M., Culetto, E., Hajjar, C., Boyd, L., Legouis, R., and Galy, V. (2011). Postfertilization autophagy of sperm organelles prevents paternal mitochondrial DNA transmission. Science *334*, 1144-1147.

Aoki, Y., Kanki, T., Hirota, Y., Kurihara, Y., Saigusa, T., Uchiumi, T., and Kang, D. (2011). Phosphorylation of Serine 114 on Atg32 mediates mitophagy. Mol Biol Cell *22*, 3206-3217.

Arai, M., Imai, H., Koumura, T., Yoshida, M., Emoto, K., Umeda, M., Chiba, N., and Nakagawa, Y. (1999). Mitochondrial phospholipid hydroperoxide glutathione peroxidase plays a major role in preventing oxidative injury to cells. J Biol Chem *274*, 4924-4933.

Ashrafi, G., and Schwarz, T.L. (2013). The pathways of mitophagy for quality control and clearance of mitochondria. Cell Death Differ *20*, 31-42.

Audhya, A., and Emr, S.D. (2002). Stt4 PI 4-kinase localizes to the plasma membrane and functions in the Pkc1-mediated MAP kinase cascade. Dev Cell *2*, 593-605.

Audhya, A., Foti, M., and Emr, S.D. (2000). Distinct roles for the yeast phosphatidylinositol 4-kinases, Stt4p and Pik1p, in secretion, cell growth, and organelle membrane dynamics. Mol Biol Cell *11*, 2673-2689.

Baba, M. (2008). Electron microscopy in yeast. Methods Enzymol *451*, 133-149.

Baba, M., Osumi, M., Scott, S.V., Klionsky, D.J., and Ohsumi, Y. (1997). Two distinct pathways for targeting proteins from the cytoplasm to the vacuole/lysosome. J Cell Biol *139*, 1687-1695.

Bankaitis, V.A., Aitken, J.R., Cleves, A.E., and Dowhan, W. (1990). An essential role for a phospholipid transfer protein in yeast Golgi function. Nature *347*, 561-562.

Bankaitis, V.A., Malehorn, D.E., Emr, S.D., and Greene, R. (1989). The *Saccharomyces cerevisiae SEC14* gene encodes a cytosolic factor that is required for transport of secretory proteins from the yeast Golgi complex. The Journal of cell biology *108*, 1271-1281.

Bossy-Wetzel, E., Petrilli, A., and Knott, A.B. (2008). Mutant huntingtin and mitochondrial dysfunction. Trends Neurosci *31*, 609-616.

Campbell, C.L., and Thorsness, P.E. (1998). Escape of mitochondrial DNA to the nucleus in yme1 yeast is mediated by vacuolar-dependent turnover of abnormal mitochondrial compartments. J Cell Sci *111* 2455-2464.

Cao, Y., and Klionsky, D.J. (2007). Atg26 is not involved in autophagy-related pathways in *Saccharomyces cerevisiae*. Autophagy *3*, 17-20.

Chan, N.C., Salazar, A.M., Pham, A.H., Sweredoski, M.J., Kolawa, N.J., Graham, R.L., Hess, S., and Chan, D.C. (2011). Broad activation of the ubiquitin-proteasome system by Parkin is critical for mitophagy. Hum Mol Genet *20*, 1726-1737.

Clark, S.L., Jr. (1957). Cellular differentiation in the kidneys of newborn mice studies with the electron microscope. J Biophys Biochem Cytol *3*, 349-362.

Dauer, W., and Przedborski, S. (2003). Parkinson's disease: mechanisms and models. Neuron *39*, 889-909.

Desrivieres, S., Cooke, F.T., Parker, P.J., and Hall, M.N. (1998). MSS4, a phosphatidylinositol-4-phosphate 5-kinase required for organization of the actin cytoskeleton in *Saccharomyces cerevisiae*. J Biol Chem *273*, 15787-15793.

Di Paolo, G., and De Camilli, P. (2006). Phosphoinositides in cell regulation and membrane dynamics. Nature *443*, 651-657.
Dodson, M.W., and Guo, M. (2007). Pink1, Parkin, DJ-1 and mitochondrial dysfunction in Parkinson's disease. Current opinion in neurobiology *17*, 331-337.
Dunn, C.D., Tamura, Y., Sesaki, H., and Jensen, R.E. (2008). Mgr3p and Mgr1p are adaptors for the mitochondrial i-AAA protease complex. Mol Biol Cell *19*, 5387-5397.
Farre, J.C., Manjithaya, R., Mathewson, R.D., and Subramani, S. (2008). PpAtg30 Tags Peroxisomes for Turnover by Selective Autophagy. Dev Cell *14*, 365-376.
Ferguson, C.J., Lenk, G.M., and Meisler, M.H. (2009). Defective autophagy in neurons and astrocytes from mice deficient in PI(3,5)P2. Hum Mol Genet *18*, 4868-4878.
Geisler, S., Holmstrom, K.M., Skujat, D., Fiesel, F.C., Rothfuss, O.C., Kahle, P.J., and Springer, W. (2010). PINK1/Parkin-mediated mitophagy is dependent on VDAC1 and p62/SQSTM1. Nat Cell Biol *12*, 119-131.
Geng, J., Nair, U., Yasumura-Yorimitsu, K., and Klionsky, D.J. (2010). Post-Golgi Sec proteins are required for autophagy in *Saccharomyces cerevisiae*. Mol Biol Cell *21*, 2257-2269.
Gerdes, F., Tatsuta, T., and Langer, T. (2012). Mitochondrial AAA proteases--towards a molecular understanding of membrane-bound proteolytic machines. Biochim Biophys Acta *1823*, 49-55.
Graef, M., and Nunnari, J. (2011). Mitochondria regulate autophagy by conserved signalling pathways. Embo J *30*, 2101-2114.
Graef, M., Seewald, G., and Langer, T. (2007). Substrate recognition by AAA+ ATPases: distinct substrate binding modes in ATP-dependent protease Yme1 of the mitochondrial intermembrane space. Molecular and cellular biology *27*, 2476-2485.
Gueldener, U., Heinisch, J., Koehler, G.J., Voss, D., and Hegemann, J.H. (2002). A second set of loxP marker cassettes for Cre-mediated multiple gene knockouts in budding yeast. Nucleic Acids Res *30*, e23.
Hama, H., Schnieders, E.A., Thorner, J., Takemoto, J.Y., and DeWald, D.B. (1999). Direct involvement of phosphatidylinositol 4-phosphate in secretion in the yeast *Saccharomyces cerevisiae*. The Journal of biological chemistry *274*, 34294-34300.
Han, G.S., Audhya, A., Markley, D.J., Emr, S.D., and Carman, G.M. (2002). The Saccharomyces cerevisiae LSB6 gene encodes phosphatidylinositol 4-kinase activity. J Biol Chem *277*, 47709-47718.
Harding, T.M., Morano, K.A., Scott, S.V., and Klionsky, D.J. (1995). Isolation and characterization of yeast mutants in the cytoplasm to vacuole protein targeting pathway. J Cell Biol *131*, 591-602.
He, C., Baba, M., Cao, Y., and Klionsky, D.J. (2008). Self-interaction is critical for Atg9 transport and function at the phagophore assembly site during autophagy. Mol Biol Cell *19*, 5506-5516.
He, C., and Klionsky, D.J. (2007). Atg9 trafficking in autophagy-related pathways. Autophagy *3*, 271-274.
Hendricks, K.B., Wang, B.Q., Schnieders, E.A., and Thorner, J. (1999). Yeast homologue of neuronal frequenin is a regulator of phosphatidylinositol-4-OH kinase. Nat Cell Biol *1*, 234-241.
Heo, J.M., Livnat-Levanon, N., Taylor, E.B., Jones, K.T., Dephoure, N., Ring, J., Xie, J., Brodsky, J.L., Madeo, F., Gygi, S.P*., et al.* (2010). A stress-responsive system for mitochondrial protein degradation. Mol Cell *40*, 465-480.
Ho, C.Y., Alghamdi, T.A., and Botelho, R.J. (2012). Phosphatidylinositol-3,5-*Bis*phosphate: No Longer the Poor PIP(2). Traffic *13*, 1-8.
Jin, S.M., Lazarou, M., Wang, C., Kane, L.A., Narendra, D.P., and Youle, R.J. (2010).

Mitochondrial membrane potential regulates PINK1 import and proteolytic destabilization by PARL. The Journal of cell biology *191*, 933-942.
Kanki, T., and Klionsky, D.J. (2008). Mitophagy in yeast occurs through a selective mechanism. J Biol Chem *283*, 32386-32393.
Kanki, T., Kurihara, Y., Jin, X., Goda, T., Ono, Y., Aihara, M., Hirota, Y., Saigusa, T., Aoki, Y., Uchiumi, T.*, et al.* (2013). Casein kinase 2 is essential for mitophagy. EMBO Rep *14*, 788-794.
Kanki, T., Wang, K., Cao, Y., Baba, M., and Klionsky, D.J. (2009). Atg32 is a mitochondrial protein that confers selectivity during mitophagy. Dev Cell *17*, 98-109.
Kanki, T., Wang, K., and Klionsky, D.J. (2010). A genomic screen for yeast mutants defective in mitophagy. Autophagy *6*, 278-280.
Kihara, A., Noda, T., Ishihara, N., and Ohsumi, Y. (2001). Two distinct Vps34 phosphatidylinositol 3-kinase complexes function in autophagy and carboxypeptidase Y sorting in *Saccharomyces cerevisiae*. J Cell Biol *152*, 519-530.
Kim, J., Huang, W.P., and Klionsky, D.J. (2001). Membrane recruitment of Aut7p in the autophagy and cytoplasm to vacuole targeting pathways requires Aut1p, Aut2p, and the autophagy conjugation complex. J Cell Biol *152*, 51-64.
Kim, J., Scott, S.V., Oda, M.N., and Klionsky, D.J. (1997). Transport of a large oligomeric protein by the cytoplasm to vacuole protein targeting pathway. J Cell Biol *137*, 609-618.
Kim, Y., Park, J., Kim, S., Song, S., Kwon, S.K., Lee, S.H., Kitada, T., Kim, J.M., and Chung, J. (2008). PINK1 controls mitochondrial localization of Parkin through direct phosphorylation. Biochem Biophys Res Commun *377*, 975-980.
Kissova, I., Salin, B., Schaeffer, J., Bhatia, S., Manon, S., and Camougrand, N. (2007). Selective and non-selective autophagic degradation of mitochondria in yeast. Autophagy *3*, 329-336. Epub 2007 Jul 2021.
Klionsky, D.J. (2007). Monitoring autophagy in yeast: the Pho8Δ60 assay. Methods Mol Biol *390*, 363-371.
Klionsky, D.J., Baehrecke, E.H., Brumell, J.H., Chu, C.T., Codogno, P., Cuervo, A.M., Debnath, J., Deretic, V., Elazar, Z., Eskelinen, E.-L.*, et al.* (2011). A comprehensive glossary of autophagy-related molecules and processes (2nd edition). Autophagy *7*, 1273-1294.
Klionsky, D.J., Cueva, R., and Yaver, D.S. (1992). Aminopeptidase I of *Saccharomyces cerevisiae* is localized to the vacuole independent of the secretory pathway. J Cell Biol *119*, 287-299.
Klionsky, D.J., and Emr, S.D. (1989). Membrane protein sorting: biosynthesis, transport and processing of yeast vacuolar alkaline phosphatase. EMBO J *8*, 2241-2250.
Klionsky, D.J., and Emr, S.D. (2000). Autophagy as a regulated pathway of cellular degradation. Science *290*, 1717-1721.
Kondo-Okamoto, N., Noda, N.N., Suzuki, S.W., Nakatogawa, H., Takahashi, I., Matsunami, M., Hashimoto, A., Inagaki, F., Ohsumi, Y., and Okamoto, K. (2012). Autophagy-related protein 32 acts as autophagic degron and directly initiates mitophagy. J Biol Chem *287*, 10631-10638.
Koppen, M., and Langer, T. (2007). Protein degradation within mitochondria: versatile activities of AAA proteases and other peptidases. Crit Rev Biochem Mol Biol *42*, 221-242.
Kraft, C., Deplazes, A., Sohrmann, M., and Peter, M. (2008). Mature ribosomes are selectively degraded upon starvation by an autophagy pathway requiring the Ubp3p/Bre5p ubiquitin protease. Nat Cell Biol *10*, 602-610.
Kurihara, Y., Kanki, T., Aoki, Y., Hirota, Y., Saigusa, T., Uchiumi, T., and Kang, D. (2012). Mitophagy plays an essential role in reducing mitochondrial production of reactive oxygen species and mutation of mitochondrial DNA by maintaining mitochondrial quantity and quality in yeast. J Biol Chem *287*, 3265-3272.

Labbé, S., and Thiele, D.J. (1999). Copper ion inducible and repressible promoter systems in yeast. Methods in enzymology *306*, 145-153.
Larsson, N.G., and Clayton, D.A. (1995). Molecular genetic aspects of human mitochondrial disorders. Annu Rev Genet *29*, 151-178.
Lee, J.Y., Nagano, Y., Taylor, J.P., Lim, K.L., and Yao, T.P. (2010). Disease-causing mutations in parkin impair mitochondrial ubiquitination, aggregation, and HDAC6-dependent mitophagy. J Cell Biol *189*, 671-679.
Lemmon, M.A., and Schlessinger, J. (2010). Cell signaling by receptor tyrosine kinases. Cell *141*, 1117-1134.
Leonhard, K., Stiegler, A., Neupert, W., and Langer, T. (1999). Chaperone-like activity of the AAA domain of the yeast Yme1 AAA protease. Nature *398*, 348-351.
Levine, B., and Klionsky, D.J. (2004). Development by self-digestion: molecular mechanisms and biological functions of autophagy. Dev Cell *6*, 463-477.
Lindmo, K., and Stenmark, H. (2006). Regulation of membrane traffic by phosphoinositide 3-kinases. J Cell Sci *119*, 605-614.
Longtine, M.S., McKenzie, A., III, Demarini, D.J., Shah, N.G., Wach, A., Brachat, A., Philippsen, P., and Pringle, J.R. (1998a). Additional modules for versatile and economical PCR-based gene deletion and modification in *Saccharomyces cerevisiae*. Yeast *14*, 953-961.
Lynch-Day, M.A., and Klionsky, D.J. (2010). The Cvt pathway as a model for selective autophagy. FEBS Lett *584*, 1359-1366.
Manjithaya, R., Jain, S., Farre, J.C., and Subramani, S. (2010). A yeast MAPK cascade regulates pexophagy but not other autophagy pathways. J Cell Biol *189*, 303-310.
Mann, V.M., Cooper, J.M., Daniel, S.E., Srai, K., Jenner, P., Marsden, C.D., and Schapira, A.H. (1994). Complex I, iron, and ferritin in Parkinson's disease substantia nigra. Annals Neurol *36*, 876-881.
Mao, K., Wang, K., Zhao, M., Xu, T., and Klionsky, D.J. (2011). Two MAPK-signaling pathways are required for mitophagy in *Saccharomyces cerevisiae*. J Cell Biol *193*, 755-767.
Mari, M., Griffith, J., Rieter, E., Krishnappa, L., Klionsky, D.J., and Reggiori, F. (2010). An Atg9-containing compartment that functions in the early steps of autophagosome biogenesis. J Cell Biol *190*, 1005-1022.
Matsuda, N., Sato, S., Shiba, K., Okatsu, K., Saisho, K., Gautier, C.A., Sou, Y.S., Saiki, S., Kawajiri, S., Sato, F.*, et al.* (2010). PINK1 stabilized by mitochondrial depolarization recruits Parkin to damaged mitochondria and activates latent Parkin for mitophagy. J Cell Biol *189*, 211-221.
Mijaljica, D., Nazarko, T.Y., Brumell, J.H., Huang, W.P., Komatsu, M., Prescott, M., Simonsen, A., Yamamoto, A., Zhang, H., Klionsky, D.J.*, et al.* (2012). Receptor protein complexes are in control of autophagy. Autophagy *8*. 1701-1705
Miquel, J., Economos, A.C., Fleming, J., and Johnson, J.E., Jr. (1980). Mitochondrial role in cell aging. Exp Gerontol *15*, 575-591.
Monastyrska, I., He, C., Geng, J., Hoppe, A.D., Li, Z., and Klionsky, D.J. (2008). Arp2 links autophagic machinery with the actin cytoskeleton. Mol Biol Cell *19*, 1962-1975.
Motley, A.M., Nuttall, J.M., and Hettema, E.H. (2012). Pex3-anchored Atg36 tags peroxisomes for degradation in Saccharomyces cerevisiae. Embo J *31*, 2852-2868.
Nair, U., Jotwani, A., Geng, J., Gammoh, N., Richerson, D., Yen, W.-L., Griffith, J., Nag, S., Wang, K., Moss, T.*, et al.* (2011). SNARE proteins are required for macroautophagy. Cell *146*, 290-302.
Narendra, D., Tanaka, A., Suen, D.F., and Youle, R.J. (2008). Parkin is recruited selectively to impaired mitochondria and promotes their autophagy. J Cell Biol *183*, 795-803.
Narendra, D.P., Jin, S.M., Tanaka, A., Suen, D.F., Gautier, C.A., Shen, J., Cookson, M.R., and Youle, R.J. (2010). PINK1 is selectively stabilized on impaired mitochondria to activate

Parkin. PLoS Biol *8*, e1000298.
Noda, T., and Klionsky, D.J. (2008). The quantitative Pho8Δ60 assay of nonspecific autophagy. Methods Enzymol *451*, 33-42.
Noda, T., Matsuura, A., Wada, Y., and Ohsumi, Y. (1995). Novel system for monitoring autophagy in the yeast *Saccharomyces cerevisiae*. Biochem Biophys Res Commun *210*, 126-132.
Okamoto, K., Kondo-Okamoto, N., and Ohsumi, Y. (2009). Mitochondria-anchored receptor Atg32 mediates degradation of mitochondria via selective autophagy. Dev Cell *17*, 87-97.
Onodera, J., and Ohsumi, Y. (2004). Ald6p is a preferred target for autophagy in yeast, Saccharomyces cerevisiae. J Biol Chem *279*, 16071-16076.
Pankiv, S., Clausen, T.H., Lamark, T., Brech, A., Bruun, J.A., Outzen, H., Overvatn, A., Bjorkoy, G., and Johansen, T. (2007). p62/SQSTM1 binds directly to Atg8/LC3 to facilitate degradation of ubiquitinated protein aggregates by autophagy. J Biol Chem *282*, 24131-24145.
Puig, O., Caspary, F., Rigaut, G., Rutz, B., Bouveret, E., Bragado-Nilsson, E., Wilm, M., and Seraphin, B. (2001). The tandem affinity purification (TAP) method: a general procedure of protein complex purification. Methods *24*, 218-229.
Reggiori, F., Monastyrska, I., Shintani, T., and Klionsky, D.J. (2005). The actin cytoskeleton is required for selective types of autophagy, but not nonspecific autophagy, in the yeast *Saccharomyces cerevisiae*. Mol Biol Cell *16*, 5843-5856. Epub 2005 Oct 5812.
Reggiori, F., Tucker, K.A., Stromhaug, P.E., and Klionsky, D.J. (2004). The Atg1-Atg13 complex regulates Atg9 and Atg23 retrieval transport from the pre-autophagosomal structure. Dev Cell *6*, 79-90.
Roy, A., and Levine, T.P. (2004). Multiple pools of phosphatidylinositol 4-phosphate detected using the pleckstrin homology domain of Osh2p. J Biol Chem *279*, 44683-44689.
Sandoval, H., Thiagarajan, P., Dasgupta, S.K., Schumacher, A., Prchal, J.T., Chen, M., and Wang, J. (2008). Essential role for Nix in autophagic maturation of erythroid cells. Nature *454*, 232-235.
Shahnazari, S., Yen, W.L., Birmingham, C.L., Shiu, J., Namolovan, A., Zheng, Y.T., Nakayama, K., Klionsky, D.J., and Brumell, J.H. (2010). A diacylglycerol-dependent signaling pathway contributes to regulation of antibacterial autophagy. Cell Host Microbe *8*, 137-146.
Shintani, T., and Klionsky, D.J. (2004). Cargo proteins facilitate the formation of transport vesicles in the cytoplasm to vacuole targeting pathway. J Biol Chem *279*, 29889-29894.
Soubannier, V., McLelland, G.L., Zunino, R., Braschi, E., Rippstein, P., Fon, E.A., and McBride, H.M. (2012). A vesicular transport pathway shuttles cargo from mitochondria to lysosomes. Curr Biol *22*, 135-141.
Strahl, T., Hama, H., DeWald, D.B., and Thorner, J. (2005). Yeast phosphatidylinositol 4-kinase, Pik1, has essential roles at the Golgi and in the nucleus. J Cell Biol *171*, 967-979.
Strahl, T., and Thorner, J. (2007). Synthesis and function of membrane phosphoinositides in budding yeast, Saccharomyces cerevisiae. Biochim Biophys Acta *1771*, 353-404.
Stromhaug, P.E., Reggiori, F., Guan, J., Wang, C.-W., and Klionsky, D.J. (2004). Atg21 is a phosphoinositide binding protein required for efficient lipidation and localization of Atg8 during uptake of aminopeptidase I by selective autophagy. Mol Biol Cell *15*, 3553-3566.
Takeshige, K., Baba, M., Tsuboi, S., Noda, T., and Ohsumi, Y. (1992). Autophagy in yeast demonstrated with proteinase-deficient mutants and conditions for its induction. J Cell Biol *119*, 301-311.
Tatsuta, T., and Langer, T. (2008). Quality control of mitochondria: protection against neurodegeneration and ageing. Embo J *27*, 306-314.
Thorsness, P.E., White, K.H., and Fox, T.D. (1993). Inactivation of YME1, a member of the

ftsH-SEC18-PAS1-CDC48 family of putative ATPase-encoding genes, causes increased escape of DNA from mitochondria in *Saccharomyces cerevisiae*. Molecular and cellular biology *13*, 5418-5426.
van der Vaart, A., Griffith, J., and Reggiori, F. (2010). Exit from the Golgi is required for the expansion of the autophagosomal phagophore in yeast *Saccharomyces cerevisiae*. Molecular biology of the cell *21*, 2270-2284.
Wallace, D.C. (2005). A mitochondrial paradigm of metabolic and degenerative diseases, aging, and cancer: a dawn for evolutionary medicine. Annu Rev Genet *39*, 359-407.
Wang, H., Song, P., Du, L., Tian, W., Yue, W., Liu, M., Li, D., Wang, B., Zhu, Y., Cao, C.*, et al.* (2011). Parkin Ubiquitinates Drp1 for Proteasome-dependent Degradation: Implication of dysregulated mitochondrial dynamics in Parkinson disease. The Journal of biological chemistry *286*, 11649-11658.
Wang, K., Jin, M., Liu, X., and Klionsky, D.J. (2013). Proteolytic processing of Atg32 by the mitochondrial i-AAA protease Yme1 regulates mitophagy. Autophagy *9*, 1828-1836.
Weber, E.R., Hanekamp, T., and Thorsness, P.E. (1996). Biochemical and functional analysis of the *YME1* gene product, an ATP and zinc-dependent mitochondrial protease from *S. cerevisiae*. Mol Biol Cell *7*, 307-317.
Xie, Z., and Klionsky, D.J. (2007). Autophagosome formation: core machinery and adaptations. Nat Cell Biol *9*, 1102-1109.
Yamashita, S., Oku, M., Wasada, Y., Ano, Y., and Sakai, Y. (2006). PI4P-signaling pathway for the synthesis of a nascent membrane structure in selective autophagy. J Cell Biol *173*, 709-717.
Yang, Z., Huang, J., Geng, J., Nair, U., and Klionsky, D.J. (2006). Atg22 recycles amino acids to link the degradative and recycling functions of autophagy. Mol Biol Cell *17*, 5094-5104.
Yang, Z., and Klionsky, D.J. (2010). Eaten alive: a history of macroautophagy. Nat Cell Biol *12*, 814-822.
Yen, W.L., and Klionsky, D.J. (2008). How to live long and prosper: autophagy, mitochondria, and aging. Physiology *23*, 248-262.
Yorimitsu, T., and Klionsky, D.J. (2005). Atg11 links cargo to the vesicle-forming machinery in the cytoplasm to vacuole targeting pathway. Mol Biol Cell *16*, 1593-1605. Epub 2005 Jan 1519.
Yorimitsu, T., and Klionsky, D.J. (2005c). Autophagy: molecular machinery for self-eating. Cell Death Differ *12*, 1542-1552.
Yoshida, S., Ohya, Y., Goebl, M., Nakano, A., and Anraku, Y. (1994). A novel gene, *STT4*, encodes a phosphatidylinositol 4-kinase in the *PKC1* protein kinase pathway of *Saccharomyces cerevisiae*. J Biol Chem*269*, 1166-1172.